

POLITECNICO DI TORINO

Corso di Laurea Magistrale in Ingegneria per l'Ambiente e il Territorio

A.a. 2021/2022

Sessione di Laurea luglio 2022

TESI MAGISTRALE

Technical aspects related to the Brenner Base Tunnel jobsite: disassembly of a
Double Shield TBM and back analysis on the cutter discs wear



**Politecnico
di Torino**

Relatore: prof. Daniele Martinelli

Candidato: Nicolò Alfero

Correlatore: Ing. Alessandro Cresto

1 TABLE OF CONTENTS

2	Abstract.....	9
3	General Introduction	11
3.1	Geography	11
3.2	Environmental improvements	13
3.3	Project design	14
3.3.1	Lot H61 Mules 2-3:.....	16
3.4	Geological context.....	18
3.4.1	Structural order.....	20
3.5	Hydrogeological context	22
3.6	General overview on the TBM types.....	24
3.6.1	EPB Shield.....	24
3.6.2	Hydroshield TBM.....	25
3.6.3	Gripper TBM.....	26
3.6.4	Single Shield TBM.....	27
3.6.5	Double Shield TBM.....	28
3.7	TBM used in Brenner Basistunnel	29
4	PART ONE: disassembly of the tbm Herrenknecht S-1054	31
4.1	TBM S-1054: General description	31
4.1.1	Back-up system	31
4.1.2	Shield Area	37
4.2	Disassembly project: general features.....	39
4.3	Project description	41
4.3.1	Back Up and tunnel components disassembly	41
4.3.2	Shield components disassembly	41
4.3.3	Disassembly bridges and gantry 1	43
4.3.4	Erector disassembly	45
4.3.5	Main Drive disassembly	46
4.3.6	Shield dismantling.....	49
4.4	Disassembly actually done	50

4.4.1	Dismantle of the cutterhead	50
4.4.2	Dismantle of tunnel and TBM services	51
4.4.3	Pull out of the Back-Up system (from gantries 25 to gantry 3)	51
4.4.4	Disassembly of bridges and gantries 1-2	53
4.4.5	Disassembly of the Erector	54
4.4.6	Disassembly of the shield area	55
4.4.7	Main drive disassembly	59
4.4.8	Dismantling of the shield	60
4.5	Comparison between the disassembly project and the work actually done	61
5	PART TWO: back analysis on cutter discs wear	63
5.1	Introduction part one	63
5.2	Geological areas analyzed	63
5.2.2	Lithologies analyzed	68
5.3	Cutterhead design	69
5.3.1	Design analysis TBM S-1054	72
5.3.2	Design analysis TBM S-1071 and TBM S-1072	73
5.4	Machine parameters	74
5.5	Cutter discs description	76
5.5.1	Failure mechanism	76
5.5.2	Main parts of cutter discs	77
5.5.3	Theoretical overview on wear mechanism of cutter ring and HRC influence:	78
5.6	Wear and Damage of disc cutters	81
5.7	Cutter discs refurbishment	85
5.8	Back analysis: general features	86
5.8.1	Mechanical Parameters analysis	86
5.8.2	Wear analysis – dependance on the machine parameters	93
5.8.3	Analysis on the cutter ring specific wear per each track	100
5.8.4	Analysis on the type of wear and damage	102
5.9	NTNU prediction model for the cutter discs wear analysis	109
5.9.1	Determination of the penetration rate	109
5.9.2	Wear prognosis	118

5.9.3	Model computation for the different geologies analyzed:	121
5.9.4	Summary of the results obtained by the NTNU prediction model.....	128
6	Conclusions.....	130
7	Bibliography.....	133

Figure 1 – map of the Brenner Base Tunnel (blue, under construction) and Innsbruck bypass (green), side by side with the Brenner railway (OpenStreetMap, Eigenes Werk).....	11
Figure 2 - Trans-European Transport Networks (https://transport.ec.europa.eu/transport-themes/infrastructure-and-investment/trans-european-transport-network-ten-t_it)	13
Figure 3 - Emergency stops of Innsbruck, Steinach am Brenner and Prati/Wiesen (BBT_Progetto Generale Brenner Basis Tunnel, 2008)	14
Figure 4 - Emergency stop design	15
Figure 5 - Frontal view of the two main pipes and explorative tunnel (BBT_Progetto Generale Brenner Basis Tunnel, 2008)	17
Figure 6 - Lot Mules 2-3 (https://www.bbt-se.com/it/galleria/avanzamento-lavori/)	17
Figure 7 - General geological order (Mancktelow, 1980)	19
Figure 8 - Hydraulic head along the tunnels (BBT_Relazione geomeccanica generale Brenner Basis Tunnel, 2015)	23
Figure 9 - EPB Shield (Herrenknecht, 2022)	24
Figure 10 - Earth Pressure Balance system (Herrenknecht, 2022)	25
Figure 11 - Hydroschild TBM (Herrenknecht, 2022)	25
Figure 12 - Gripper TBM (Herrenknecht, 2022)	26
Figure 13 - Single Shield TBM (Herrenknecht, 2022)	27
Figure 14 - Double Shield TBM (Herrenknecht, 2022)	28
Figure 15 - Thrust cylinders retracted	29
Figure 16 - Thrust cylinders extended	29
Figure 17 - Schematic path from the Tunnel Face to the Storage Area (red arrow) (Planimetria schematica ingombri smontaggio TBM S-1054, 2022)	40
Figure 18 - Most critical cross-section of the tunnel (Planimetria schematica ingombri smontaggio TBM S-1054, 2022)	40
Figure 19 - Starting conditions for the shield disassembly (Herrenknecht, 2022)	41
Figure 20 - Installation thrust cylinders extensions (“HK 5102-091-001-01 Shield Disassembly”, Herrenknecht, 2022).....	42
Figure 21 - Cutting and rotation of the cutterhead (“HK 5102-091-001-01 Shield Disassembly”, Herrenknecht, 2022).....	42
Figure 22 - Crane runway installation (“HK 5102-091-001-01 Shield Disassembly”, Herrenknecht, 2022).....	43
Figure 23 - Disassembly gantry 1 (“HK 5102-091-001-01 Shield Disassembly”, Herrenknecht, 2022)	44
Figure 24 - Bridge 1 dismantling (“HK 5102-091-001-01 Shield Disassembly”, Herrenknecht, 2022)	45
Figure 25 - Lengthen of the crane runway (“HK 5102-091-001-01 Shield Disassembly”, Herrenknecht, 2022)	45
Figure 26 - Gripper shoes and advance cylinders disassembly (“HK 5102-091-001-01 Shield Disassembly”, Herrenknecht, 2022).....	46
Figure 27 - Main drive pulled backwards by means of pushing cylinders (“HK 5102-091-001-01 Shield Disassembly”, Herrenknecht, 2022)	47
Figure 28 - Swivel Lug device connected to the main drive (Herrenknecht, 2022)	47
Figure 29 - Tilt maneuver for the main drive (“Investigation Main Drive Disassembly”, Herrenknecht, 2022)	48
Figure 30 - Shield components completely disassembled (“HK 5102-091-001-01 Shield Disassembly”, Herrenknecht, 2022).....	49

Figure 31 - Installation of "double T beam" on the shield (Herrenknecht, 2022)	49
Figure 32 - Cut of shield roof ("Shield disassembly concept", Herrenknecht, 2022)	50
Figure 33 - Cutterhead divided into three portions. The photo was taken after the main drive disassembly.....	51
Figure 34 - example of gantry transportation (gantry 24)	52
Figure 35 - train crane used during the disassembly	52
Figure 36 - disassembly of the shield area: removal of thrust cylinders	56
Figure 37 - disassembly of the shield area: removal of main thrust cylinders, gripper cylinders, torque cylinders and electromotors with gearboxes	57
Figure 38 - gripper shoe safe to the TBM shield by means of a steel beam.....	58
Figure 39 - gripper shoes dismantling.....	58
Figure 40 - separation of the main drive from the cutterhead flange.....	59
Figure 41- main drive lying on the shield floor, trolley and easel devices.....	60
Figure 42 - CAI test equipment (Thuro, 2010)	65
Figure 43 - Geological Strength Index table (Hoek, 1997)	67
Figure 44 - chainage relative to each geology	68
Figure 45 - Cutterhead lateral view TBM S-1054 – cutter position (Herrenknecht , 2017).....	70
Figure 46 - Cutterhead lateral view TBM S-1071 & TBM S-1072 – cutter position (Herrenknecht, 2017). ..	71
Figure 47 - Circumference per each track number (TBM S-1054)	72
Figure 48 - Influence area per each track number (TBM S-1054).....	72
Figure 49 - Circumference per each track number (TBM S-1071 & TBM S-1072)	73
Figure 50 - Circumference per each track number (TBM S-1071 & TBM S-1072)	73
Figure 51 - Failure mechanism for disc cutters ("Boreability Testing", Blindeheim and Bruland)	77
Figure 52 - Section of a cutter disc (Herrenknecht, 2021).....	77
Figure 53 - Double ring cutter	78
Figure 54 - Abrasive wear mechanism: a) Micro cutting; b) Furrow deformation; c) Brittle fracture. ("Experimental study on wear of TBM disc cutter rings with different kinds of hardness", Zhang et al., 2018)	79
Figure 55 - Hardness of cutter ring ("Experimental study on wear of TBM disc cutter rings with different kinds of hardness", Zhang et al., 2018).....	80
Figure 56 - Wear gauge template for cutter ring wear measurement	81
Figure 57 - Cutter normal wear (Herrenknecht, S-1054 TBM GL Brenner Basis Tunnel Lot 2-3 Mauls/Mules, 2017).....	82
Figure 58 - Cutter clogging bearing (Herrenknecht, S-1054 TBM GL Brenner Basis Tunnel Lot 2-3 Mauls/Mules, 2017).....	82
Figure 59 - Cutting ring breakage.....	83
Figure 60 - Cutting ring chipping.....	83
Figure 61 - Cutting ring mushrooming	84
Figure 62 - Defective roller casing	84
Figure 63 - Circlipping	85
Figure 64 - Machine parameter recorded during the tunnelling in Paragneiss.....	88
Figure 65 - Machine parameter recorded during the tunnelling in Amphibolite	89
Figure 66 - Machine parameter recorded during the tunnelling in Metabasalts	90
Figure 67 - Machine parameter recorded during the tunnelling in Calcschist	91

Figure 68 - machine parameter recorded during the tunnelling in Gneiss.....	93
Figure 69 - Cutter ring wear [mm/m] vs torque [MNm] depending on the TBM and the geology	94
Figure 70 - Cutter ring wear [mm/m] vs total thrust force [kN] depending on the TBM and the geology	95
Figure 71 - Cutter ring wear [mm/m] vs cutting wheel rotational speed [rpm] depending on the TBM and the geology	97
Figure 72 - Cutter ring wear [mm/m] vs penetration [mm/rot] depending on the TBM and the geology	98
Figure 73 - Cutter ring wear [mm/m] vs advance speed [mm/min] depending on the TBM and the geology	99
Figure 74 - Cutter ring wear [mm/m] depending on the track for each TBM and each geology	102
Figure 75 – Disc replacement causes during the tunnelling in the Paragneiss.....	103
Figure 76 - Different frequencies of cutter tools substitution related to the excavation in Paragneiss ..	104
Figure 77 – Disc replacement causes during the tunnelling in the Amphibolite	104
Figure 78 - Different frequencies of cutter tools substitution related to the excavation in Amphibolite	105
Figure 79 – Disc replacement causes during the tunnelling in the Metabasalts	106
Figure 80 - Different frequencies of cutter tools substitution related to the excavation in Metabasalts	106
Figure 81 – Disc replacement causes during the tunnelling in the Calcschists	107
Figure 82 - Different frequencies of cutter tools substitution related to the excavation in Calcschists ..	108
Figure 83 – Disc replacement causes during the tunnelling in the Gneiss	108
Figure 84 - Different frequencies of cutter tools substitution related to the excavation in Gneiss.....	109
Figure 85 - Recorded Drilling Rate Index (DRI) for some rock types (Bruland, 1998).....	110
Figure 86 - Determination of fracture class (NTNU Method)	111
Figure 87 - examples of inclination of weakness planes.....	112
Figure 88 – Chart for the determination of Ks parameter	112
Figure 89 - Determination of the K_DRI value	113
Figure 90 - Determination of Kd coefficient	114
Figure 91 - Determination of cutter spacing coefficient (Ka)	115
Figure 92 - Determination of the porosity coefficient (Kpor)	115
Figure 93 - Determination of the critical thrust M1	116
Figure 94 - General progress of a penetration curve (Bruland , 1998).....	117
Figure 95 - Correlation between CLI (Cutter Life Index) and geology.....	118
Figure 96 - Determination of the Base cutter life (Hc)	119
Figure 97 - Correction due to the quartz content.....	119
Figure 98 - Correction for cutterhead diameter (Kd).....	120
Figure 99 - Determination of the parameter N ₀	121

2 ABSTRACT

Questo elaborato è inerente a due tematiche dello scavo meccanizzato con TBM (Tunnel Boring Machine), con particolare riferimento al Progetto “Brenner Basis Tunnel”, la galleria ferroviaria in costruzione più lunga al mondo che collegherà gli abitati di Fortezza e Innsbruck. I lavori di tesi si sono concentrati nel cantiere Mules 2-3, presso Mules (BZ). Il primo argomento trattato si riferisce allo smontaggio in caverna della TBM Herrenknecht S-1054, il cui diametro è di 6800 mm, effettuato al termine dello scavo del cunicolo esplorativo dal versante italiano. La maggiore particolarità di questo smontaggio risiede nel fatto che non è stato eseguito un sovra-scavo e perciò tutte le operazioni si sono dovute effettuare nello spazio delimitato dal perimetro tunnel scavato. Infatti, questo tipo di smontaggio viene svolto molto raramente e richiede una preparazione specifica ed accurata. Nello specifico, è stata svolta una descrizione del progetto proposto per lo smontaggio e delle attività effettivamente svolte durante lo smontaggio. È stato dunque possibile confrontare il progetto con il lavoro eseguito ed evidenziare le principali differenze dell’uno dall’altro, per poterne usufruire, qualora necessario, per il futuro smontaggio in assenza di caverna di altre TBM. La seconda parte della tesi, invece, si concentra su una componente fondamentale dello scavo con TBM in roccia dura: gli utensili di taglio, più comunemente noti come “cutter discs”. In particolare, è stata effettuata una analisi sull’usura riscontrata nelle diverse zone geologicamente omogenee che sono state attraversate durante lo scavo con le TBM Herrenknecht S-1054, S-1071, S-1072: Paragneiss, Anfibolite, Metabasalti, Calcescisti e Gneiss. Per ciascuna di queste geologie è stato svolto uno studio sull’usura dei cutter, analizzando i dati di usura ottenuti con il procedere dello scavo, in relazione ai seguenti parametri macchina: coppia, forza di spinta, velocità di rotazione della testa, penetrazione e velocità di avanzamento. Inoltre, sempre con riferimento alle geologie sopraelencate, sono state catalogate le principali cause per cui i cutter sono stati sostituiti. Anche in questo caso, il principale obiettivo dello studio è di carattere pratico e consiste nel miglioramento della scelta dei parametri di scavo per ottenere il miglior rendimento degli utensili di taglio e nel poter prevenire, in anticipo, il numero di sostituzioni che probabilmente si dovranno effettuare in futuri scavi, in geologie affini a quelle analizzate, al fine di ottenere vantaggi logistici ed economici.

This paper focuses on two main themes of the mechanized excavation with TBM (Tunnel Boring Machine), with reference to the “Brenner Basis Tunnel” Project, which is the longest railway tunnel under construction that will connect the towns of Fortezza (Italy) and Innsbruck (Austria). The thesis work has been carried out in the Mules 2-3 jobsite, near to Mules (Bolzano, Italy). The first topic deals with the disassembly inside the tunnel of the TBM Herrenknecht S-1054, whose diameter is 6800 mm, carried out at the end of the excavation of the exploratory tunnel from the Italian side. The main peculiarity of this disassembly is that no over-excavation has been realized and therefore, the only space available for the disassembly purpose is the delimited by the perimeter of the tunnel excavated. In particular, it has been made a description of the proposed disassembly project and of the work actually perform during the disassembly. It was thus possible to compare the project with the operations executed and highlight the main differences between the two, in order to collect information on how to proceed in some other disassembly of TBM inside the tunnel. The second part of the thesis, on the other hand, focuses on one of the most important components of the mechanized excavation in hard rock: the cutter discs. In particular, has been carried out an analysis on the wear rate depending on the different geological areas that were crossed during the excavation by the three TBM Herrenknecht S-1054, S-1071 and S-1072. The lithologies are: Paragneiss, Amphibolite, Metabasalts, Calchschists and Gneiss. For each of these geologies has been performed a study on the cutter disc wear, thanks to the analysis of the wear data collected with the progress of the excavation, in relation to the following machine parameters: torque, thrust force, cutterhead rotation speed, penetration and advance speed. Furthermore, it is presented a discussion on the amount of disc substitutions and their relative causes of replacement; even in this case it is referred to the geologies above-mentioned. The objective of the study is again of a practical nature, and it is linked with the improvement of the selection of the best machine parameters during the tunnelling and to forecast, in advance, the number of replacements that they probably must do in future excavations in similar geologies. In this way should be possible to obtain logistical and economic advantages.

3 GENERAL INTRODUCTION

Passenger and freight traffic across the Alps has increased significantly in recent years and a further growth is expected. Austria is a key country in movement of goods between Eastern and Western Europe and around three-quarters of traffic across the Brenner Pass is currently carried by road transport; for this reason, local residents have long been fighting for the relief from associated pollution.

This chapter describes the main works concerning the construction of the Brenner Base Tunnel (BBT), in particular those relating to the construction lot Mules 2-3 on the Italian Side.

to raramenteto raramente

3.1 GEOGRAPHY



Figure 1 – map of the Brenner Base Tunnel (blue, under construction) and Innsbruck bypass (green), side by side with the Brenner railway (OpenStreetMap, Eigenes Werk)

The Brenner Base Tunnel BBT-SE is a straight and flat railway tunnel that will connect two countries. The project involves the construction of a railway tunnel that will link Innsbruck (Austria) and Fortezza (Italy), with a length of 56 km for each pipe. Near Innsbruck the railway will be joined underground with the already existing Innsbruck ring road, reaching a total length of 64 km. Once completed, this line will become the longest underground railway connection in the world.

The slope in the base tunnel is in the range 4-7 ‰ and the highest point is 790m above sea level, lying 580 m below the Brenner Pass itself (1370 m a.s.l.). (BBT SE - Brenner Basis Tunnel Società Economica, 2008)

This tunnel represents an important infrastructure because it will be the heart of the European TEN SCAN-MED (Scandinavia-Mediterranean) corridor from Helsinki to Valletta; this set of infrastructures will play an important role from a commercial point of view because it will connect the major urban centers of Italy, Austria and Germany and their harbors, as shown in the figure below (Figure 2). (Transport, n.d.)

The main function of the tunnel under construction is to move heavy traffic from the highway to the railway, reducing the environmental impact and travel time in favor of sustainable and faster mobility. Based on the forecast data, there will be a reduction of 69% in overall travel times compared to the existing railway from Bolzano to Innsbruck and, thanks to the elimination of the steep slopes present on the current railway line, it will be possible to use longer and faster trains. The new line will thus make it possible to fully exploit the Verona intermodal terminal “Quadrante Europa”, which plays an important role in intermodal transport on the Munich-Verona axis.

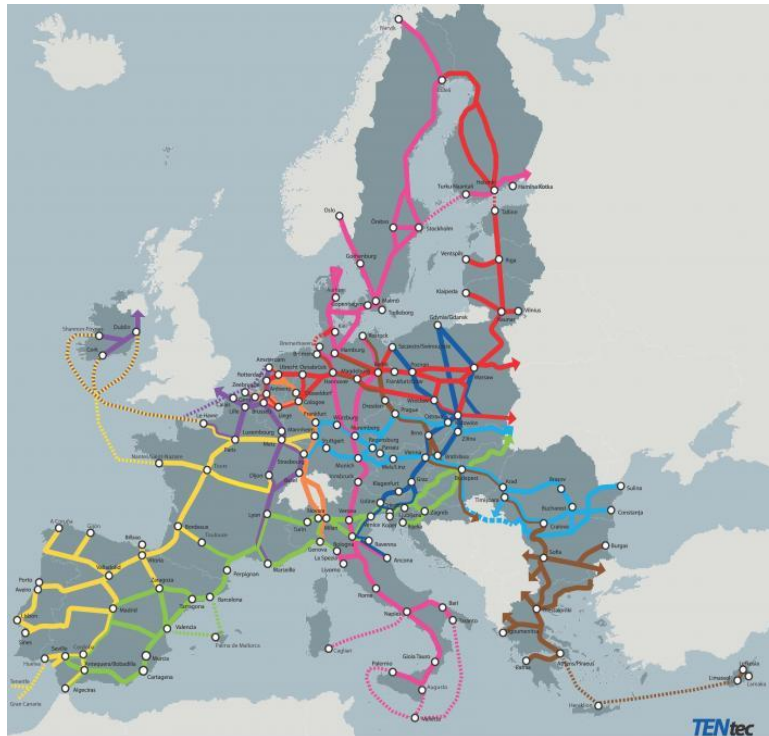


Figure 2 - Trans-European Transport Networks (https://transport.ec.europa.eu/transport-themes/infrastructure-and-investment/trans-european-transport-network-ten-t_it)

3.2 ENVIRONMENTAL IMPROVEMENTS

For a respectful approach to nature Austria and Italy verified the environmental compatibility of the project on the basis of the environmental applicable national laws, bringing about the improvements for people and nature. To minimize the impact on the environment, the tunnel portals are carefully embedded in the landscape and the disposal sites are located near the lateral access tunnel. Additionally, nesting and feeding places for wild animals have been located around the constructions area and the nature and environment monitoring is carried out. According to the forecast data, once the entire infrastructure will be finished, 171,500 tons of CO₂ emissions per year should be avoided. (WeBuild, 2022) (BBT SE , 2022)

3.3 PROJECT DESIGN

The Brenner Base Tunnel consists of two twin single-track tunnels running parallel with a distance ranging from 40 to 70 meters. The two tubes are connected every 333 m by connection side tunnels, to be used in emergencies as escape routes. Furthermore, given the considerable length of the tunnels and to ensure the safety of the trains that will pass through the tunnels, three emergency stops are built: the main goal of those stops is to allow travelers to evacuate safely in case of need.

The three emergency stops will be placed at:

- Innsbruck
- Steinach am Brenner
- Prati/Wiesen

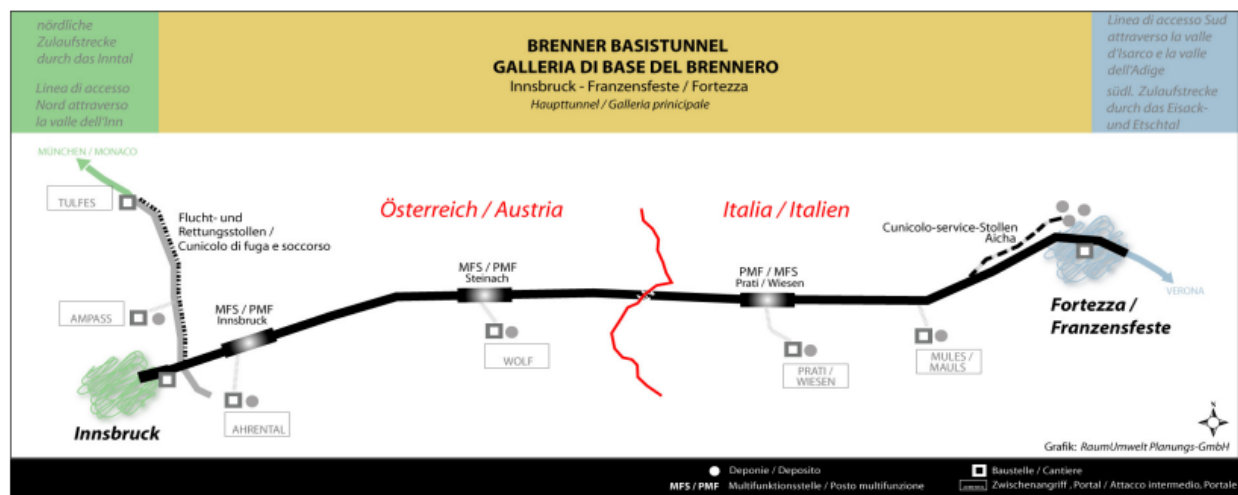


Figure 3 - Emergency stops of Innsbruck, Steinach am Brenner and Prati/Wiesen (BBT_Progetto Generale Brenner Basis Tunnel, 2008)

Each emergency stop consists of two chambers, one for each pipe. Each chamber is 470 meters long and it is connected via escape ways located perpendicular to the main tunnels at a distance of 90 meters (Figure 4). The inflow of fresh air is also provided by means of small tunnel placed at 90 meters and staggered of 45 meters with respect to the escape routes.

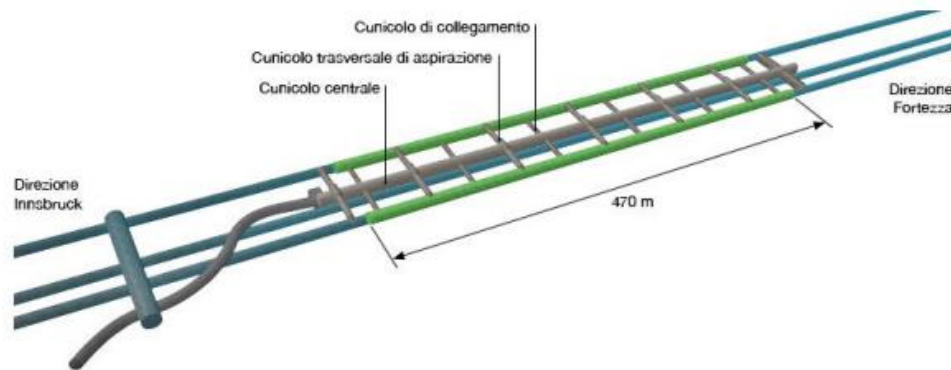


Figure 4 - Emergency stop design

The complete project also includes the construction of an exploratory tunnel, running from one end to the other in the Italian side and which represents the uniqueness of this project. This tube is located approximately 12m below the two main tubes and it has a diameter of almost 6m, hence smaller than the two railway tunnels. In this way, the tunnel is nearly close to the twin tubes, but it doesn't interfere with the emergency transverse tunnels. From the planimetric point of view, the exploratory tunnel is placed between the two main tunnels but from the chainage project 51,000 km it diverts towards the south portal in Aica (Figure 4).

The main functions of this pilot tunnel are related to both the construction phase and the working phase. Those purposes are:

- Geological prospecting during the construction phase
- Design of the support system for the main tunnels
- Drainage and service tunnel during the working phase

However, the main purpose of the excavation of the exploratory tunnel is to reduce construction cost and times during the construction phase of the two main pipes, providing geological and geomechanical information on the rock mass.

The whole project is subdivided into seven construction sites:

- Lot H21 Sill Gorge
- Lot H41 Sill Gorge-Pfons

- Lot H33 Tulfes-Pfons
- Lot H52 Hochstegen
- Lot H53 Pfons Brenner
- Lot H61 Mules 2-3
- Lot H71 Isarco River underpass

Five of the aforementioned construction sites are currently operational: three of them in Austria and two in Italy. (BBT SE , 2022)

3.3.1 Lot H61 Mules 2-3:

The studies carried out during this thesis relate to the lot Mules 2-3; it is placed between Fortezza and Brenner Pass, close to the Mules village.

Work on this lot began in September 2016 and is still ongoing. Geographically, this construction site extends from the lot Isarco River underpass (Lot H71) to the State Border with Austria. During the total construction period will be excavated:

- 39.856 km of main tubes (cross-section 85 m²)
- 14.757 km of exploratory tunnel (cross-section 35 m²)
- 3.805 km of access tunnel to the emergency stop (cross-section 80 m²)
- 6.930 km of safety and logistics tunnels (cross-section 26-56 m²)

Thus, the total excavation is approximately 65 km.

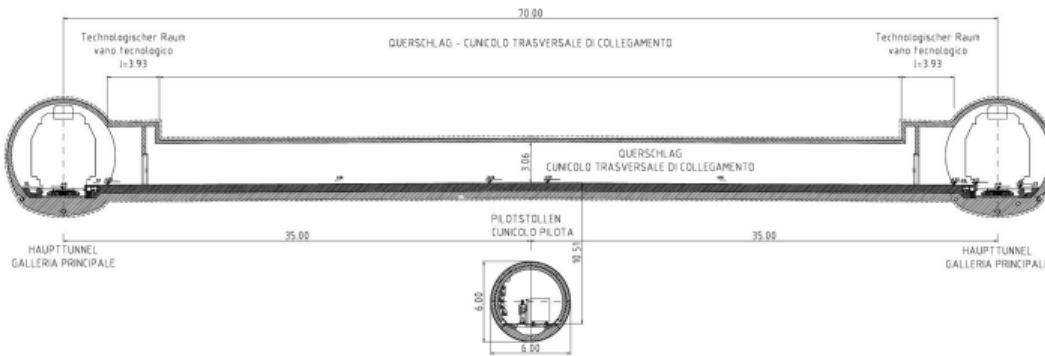


Figure 5 - Frontal view of the two main pipes and explorative tunnel (BBT_Progetto Generale Brenner Basis Tunnel, 2008)

The excavation of the twin main tubes and the exploratory tunnel is performed using the mechanized TBM excavation while the other sections are excavated by traditional Drill & Blast excavation type.

Once the Mules 2-3 lot is finished, all excavation activities in the Italian project area will be complete.

In the Figure 6 the whole area involved in the lot Mules 2-3 is displayed.

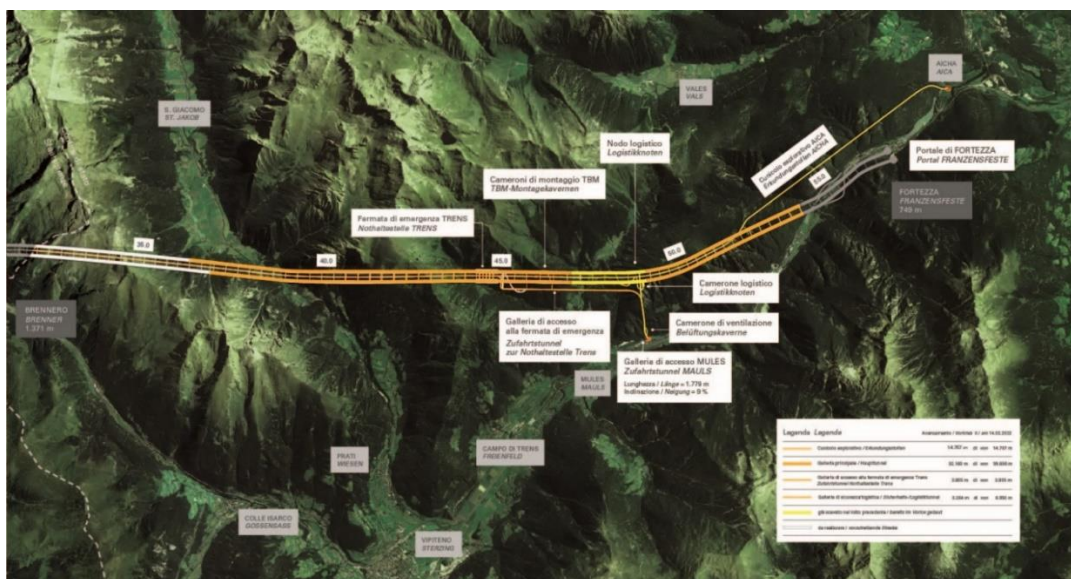


Figure 6 - Lot Mules 2-3 (<https://www.bbt-se.com/it/galleria/avanzamento-lavori/>)

3.4 GEOLOGICAL CONTEXT

From a geological point of view, the Brenner Base Tunnel overcomes the major tectonic units that form the Alpine Chain. The current structure is the result of deformation processes that occurred during the Alpine orogenetic events. These units are a system of overlapping pitches which have been formed as a result of the collision of the European plate and the Adriatic (African) plate. In the project area these two plates shape a dome, at the center of which the Penninic and Sub-penninic units of the Tauern Window emerge. For this reason, the deepest structural sectors of Tauern Window are represented by the central gneiss (nucleus of Tux towards north and nucleus of Zillertal towards south). These European tectonic units are then mantled by the Penninic units of the Oceanic origin (Falda del Vizzo and Glockner complex) and the Oceanic units are further overcome by the African origin Austro-alpine Unit.

Almost all the rock masses involved in the project area are characterized by a ductile deformation, typical of the alpine metamorphism, but the rock mass in the southern part of the South-alpine line shows only a brittle deformation, due to the fact that this area was not involved in the subduction process. (BBT SE , 2015)

In the figure below (Figure 7) is exposed the general geological order related to the area of the entire tunnels system.

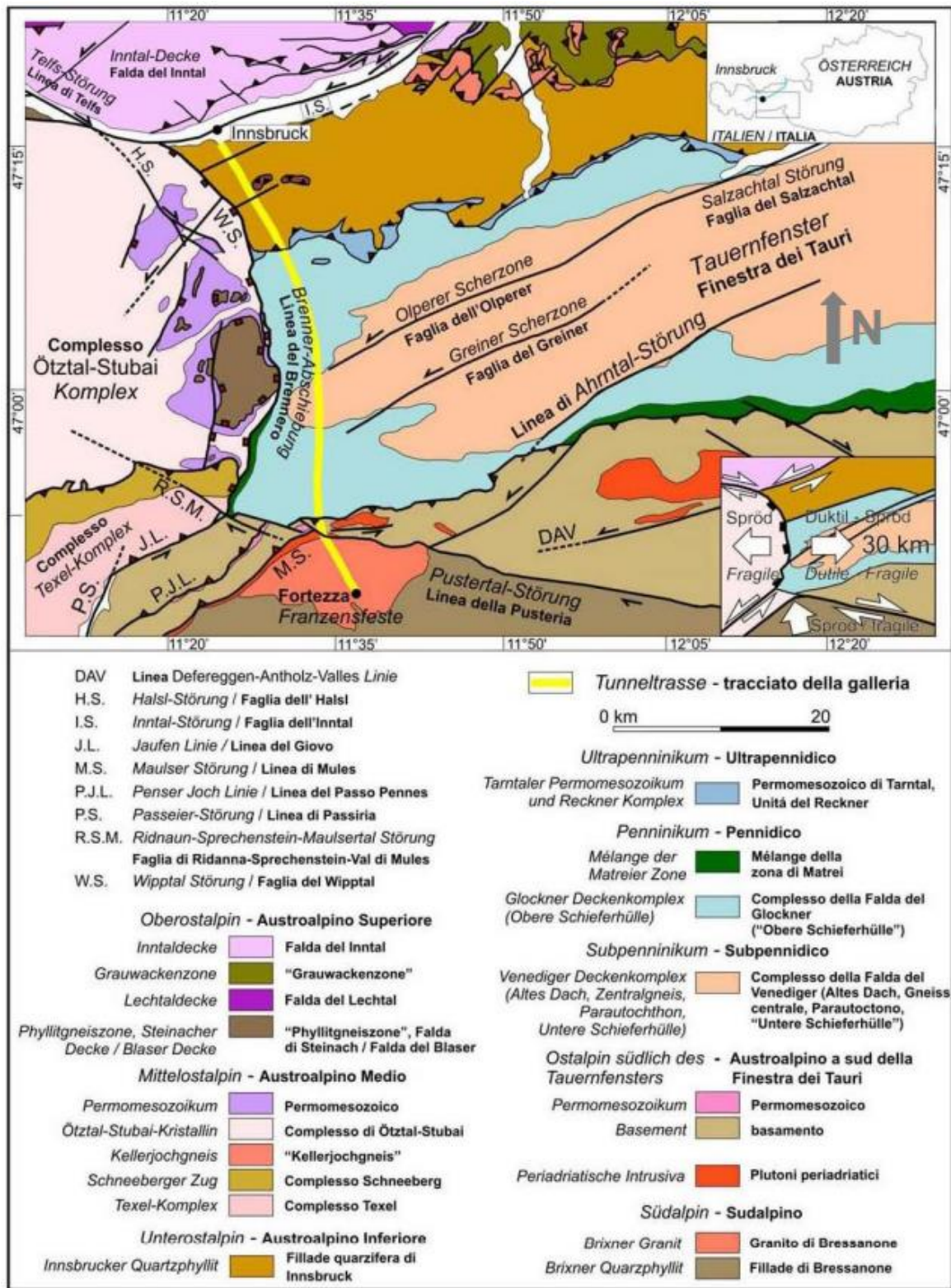


Figure 7 - General geological order (Mancktelow, 1980)

3.4.1 Structural order

The Brenner Base Tunnel path crosses three different tectonic units from south to north:

- Southern-alpine Unit
- Austro-alpine Unit
- Pennidic and Southern-pennidic Units of the Tauern Window

The contact between these tectonic units is mainly linked to a set of faults, which starts from the crust and extends laterally and vertically for long distances. After the cooling process of the Tauern Window, the ductile deformation was overlayed by a brittle deformation.

3.4.1.1 Ductile deformations: folds and ductile shear zones

The tectonic units present along the route of the tunnel are characterized by different deformation styles depending on the geodynamic-tectonic evolution undergone.

In general, the Pennidic unit shows a metamorphism and deformation of alpine type, and the rocks present in this area have undergone several ductile deformative phases.

On the other hand, the Austro-alpine sector, which is located in the south of the Tauern Window, is characterized by a metamorphic basement covered by permotriassic sediments. It is represented by a low-grade metamorphism, and it is heavily deformed in some parts.

3.4.1.2 Brittle deformation: faults and master joints

There are many sets of joints along the path of the twin tubes; the main fault systems are here listed:

- Wipptal fault
- Vizze Valley fault
- Avenes fault
- Tulves Fault
- Southern limit of Tauern fault
- Mules Valley fault

- Pusteria Valley fault
- Sub-vertical Granite Brixen fault with N-S direction
- Sub-vertical master joints of Brixen Granite with direction from E-W to ENE-WSE

3.4.1.3 Geological order

The main geology that was encountered during the excavation with the TBMs 1071, 1072 and 1054 is reported here, from the Italy-Austria border towards the Italian portal of the tunnel:

- Orthogneiss belonging to the Central Gneiss unit which represent, as said before, the Tauern Window. This gneiss was intercalated with the rocks of the granite basement.
- Metasedimentary successions (limestone schists, quartzites and marbles) belonging to the Inner Schieferhülle Unit; these rocks were often folded. This geologic area is also known as “Arcobaleno Sector”.
- Calcschists of the “Falda del Vizzo” consisting of siliciclastic limestone, graphitic schists, and impure marble, with intercalations of green rocks, which were often schists.
- Antiform fold of the Zillertal, consisting of rocks belonging to the Peripheral Schieferhülle Unit. It was mainly represented by chlorite calcschists, micaceous quartzites, quartz / micaschist fillads and anhydrite rich rocks.
- Calcschists with local intercalation of Dolomite, Gypsum, Anhydrites.
- Austro-alpine Crystalline and Mules Faults Area: this zone was characterized by Amphibolites, Paragneiss, Micaschists and local intercalations of Orthogneiss and impure Marbles.
- Tonalite of Mules and Phyllonites placed in an uncertain stratigraphic position. The northern part of the Mules Fault and southern part of Pusteria Valley Fault make up the complex of Periadriatic line.
- Granite of Brixen composed of Granites and Granodiorites with aplitic and pegmatitic, locally disaggregated and altered. (BBT SE , 2015)

3.5 HYDROGEOLOGICAL CONTEXT

Starting from the border between Italy and Austria, the hydrogeology system is quite complex; the geology is characterized, as previously explained, by the dome structure in which nucleus is present the Central Granite.

In the border area, there is the deep system of the Brenner thermal spring, but in the Central Gneiss are not present high flux of water due to the low permeability of the rock mass. The maximum flow is related to the Olperer fault, and it is of the order of 150 l/s, reaching in some cases values of 300 l/s depending on the rainfall.

In the southern part of the Vizze Valley, the hydrogeologic complex is related to a second dome structure known as Tulver-Senges dome. This dome is surrounded by calcschists and hence are not present consistent flows. In this case the main hydrogeologic problems are connected to the set of joints with NNE-SSW orientation which allow fluxes of 100-150 l/s. However, these fluxes, due to the low capacity of this acquifer, are not constant and dependent on the season. Furthermore, the nucleus of the dome is composed of Gneiss overlayed with marble and shists; the permeability of these layers is not constant and therefore high flows occur in some area, mainly due to the presence of chemical dissolution processes.

In the initial zone of excavation there are important fluxes of water related to the Pusteria fault and to the set of joints existing in the Brixen Granite. (BBT SE , 2015) (Herrenknecht, 2022)

HYDROGEOLOGISCHER LÄNGSSCHNITT EKS MAULS-BRENNER [11] / PROFILO IDROGEOLOGICO CE MULES-BRENNERO [11]		
[km Oströhre] [km canna Est]		Wasserdrucke / Carico idraulico
von / da	bis / a	Klasse / Classe
32+085	32+535	1300-1400
32+535	33+750	1400-1500
33+750	33+900	1500-1600
33+900	34+800	1400-1500
34+800	35+000	1300-1400
35+000	35+150	1300-1400
35+150	35+400	1100-1200
35+400	35+600	1000-1100
35+600	36+200	800-1000
36+200	36+450	900-750
36+450	37+340	750-650
37+340	37+700	750-800
37+700	37+950	650-750
37+950	38+500	600-650
38+500	38+650	650-750
38+650	38+915	750-850
38+915	39+100	850-1000
39+100	40+300	1000-1100
40+300	40+590	1100-1200
40+590	43+400	1200-1400
43+400	43+620	1100-1200
43+620	43+780	1000-1100
43+780	44+520	900-1000
44+520	45+515	1000-1100
45+515	46+450	900-1000
46+450	46+630	800-900
46+630	46+780	700-800
46+780	46+900	600-700

Figure 8 - Hydraulic head along the tunnels (BBT_Relazione geomeccanica generale Brenner Basis Tunnel, 2015)

3.6 GENERAL OVERVIEW ON THE TBM TYPES

This paragraph provides a general overview on the main TBM types used for different kind of rocks and soils.

3.6.1 EPB Shield

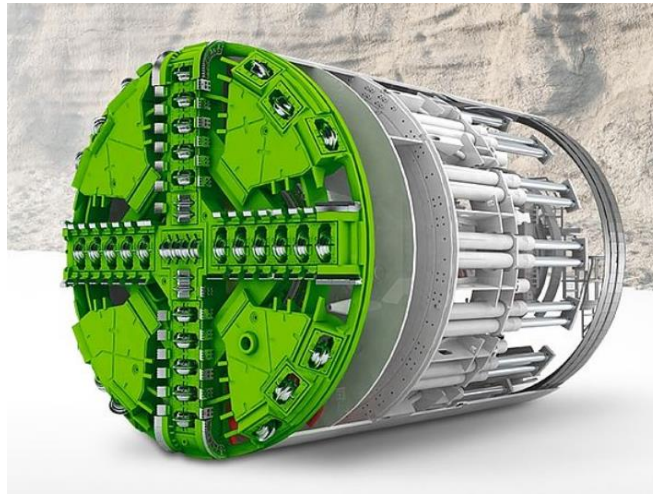


Figure 9 - EPB Shield (Herrenknecht, 2022)

The EPB Shield is mainly used for soft and cohesive soils. The principal characteristic of this TBM type is the ability to turn the excavated material into a soil paste that is used as plastic support medium. A rotating cutting wheel equipped with tools is pressed against the tunnel face and excavates the material. The soil enters the excavation chamber through openings and there is mixed with soil paste already present by means of mixing arms. The bulkhead, placed behind the cutter wheel, transfers the pressure of the thrust cylinders to the soil paste. When the pressure of the soil paste in the excavation chamber is equal to the pressure of the tunnel face (surrounding soil and groundwater), the necessary balance has been achieved. For this purpose, the screw conveyor speed, which aim is to bring the excavated material from the bottom of the excavation chamber to the conveyor belt, is regulated and matched with the advanced speed in order to keep steady equilibrium between the quantity of soil removed by the screw conveyor and the quantity of soil accumulated during the shield tunneling process. In this way there is a pressure acting against the tunnel face and it avoids the uncontrolled inflow of soil into the machine and creates conditions for rapid tunnelling with minimum settlement.

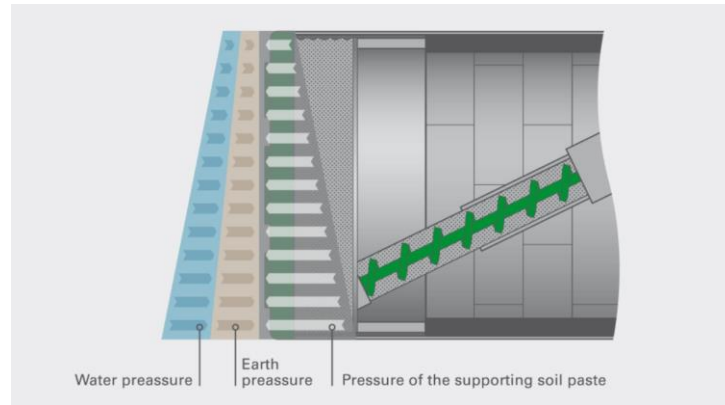


Figure 10 - Earth Pressure Balance system (Herrenknecht, 2022)

The application range for this type of TBM is strictly related to the soil conditioning. Indeed, changing the plasticity, the texture and the water permeability by injecting conditioning materials such as water, bentonite or foam is possible to achieve good advance rates even in heterogeneous soils or in unstable geological conditions.

In this case the diameter varies between 1.7m to 16m and can be reached a very high and consistent advance rates in cohesive soils. (Herrenknecht, 2022)

3.6.2 Hydroschild TBM

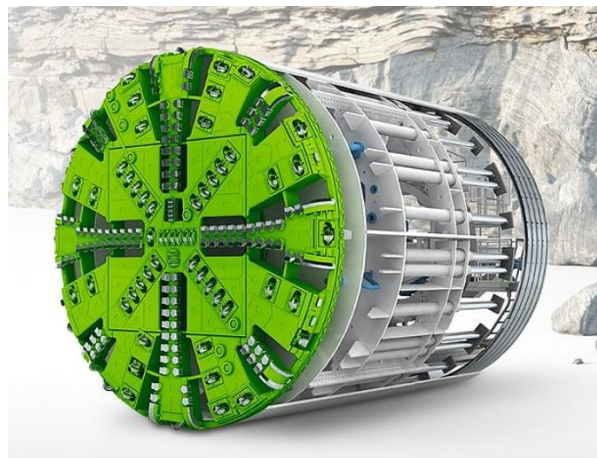


Figure 11 - Hydroschild TBM (Herrenknecht, 2022)

The hydroshield TBM is used in heterogeneous ground which are composed by sand and gravel and that have a high water permeability and a high water pressure. The hydroshield are an evolution of the slurry TBM. Indeed, the support pressure in the excavation chamber is a controlled air cushion. The main representative element of the hydroshield TBM is the excavation chamber that is divided in submerged wall. The front section is filled with suspension for the face support during the tunnelling. The counter-pressure needed at the tunnel face is supplied using a compressible air cushion. In this type of machine is also very important the sealing system between the TBM and the ground to be excavated. For this reason, it is equipped with a multiple sealing system in order to keep out the soil and the groundwater. The excavation is performed by means of cutting knives and disc cutters and the removal of the muck is usually provided by an hydraulic conveyance through a closed slurry circuit. The thrust is given by means of thrust cylinders which push on the already in place segmental lining. (Herrenknecht, 2022)

3.6.3 Gripper TBM

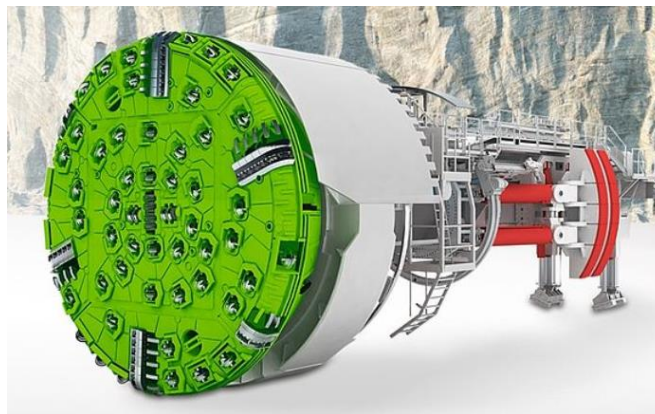


Figure 12 - Gripper TBM (Herrenknecht, 2022)

Gripper TBMs are open-mode TBM and do not have a closed shield skin. This type of TBM is mainly used for fast mechanized tunnelling in hard rock. The typical process is without the use of segments and hence medium to high rock strengths are required for high advance rate. During the excavation process, the cutterhead is pressed against the tunnel face by means of thrust cylinders. Due to the rolling movement of the cutters present on the cutterhead, chips of rock are broken out of the rock. Some buckets installed at the cutterhead take up the excavated

material, which slides to the center of the machine and then falls down in the machine belt; from there the excavated material is then transported by conveyor belts or trucks depending on the project. However, the main characteristic is that the Gripper TBM is braced against the previously excavated tunnel, hence directly in the rock, by means extendible hydraulic cylinders. Indeed, the two so called “grripper shoes” are core elements of this TBM type: they allow the stability of Gripper TBM during the excavation when the thrust cylinders are pushing the cutterhead against the tunnel face. Several telescopic partial shields stabilize the machine, reducing wear and tear. The roof shield offers protection against breaking rocks. After the completion of a stroke, given by the total extension of thrust cylinders, the tunnelling is interrupted, and the gripping unit is moved forward.

The tunnelling performance of Gripper TBMs is strongly dependent on the time requires to secure the rock, which is usually achieved using rock anchors, steel mats and steel arches.

The diameter can vary between 2m and 12.5m and it is suitable for hard and stable rocks, such as granite, gneiss or basalt. (Herrenknecht, 2022)

3.6.4 Single Shield TBM

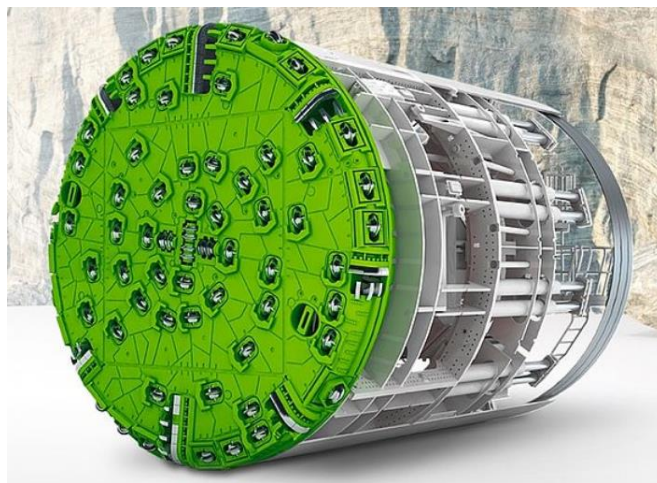


Figure 13 - Single Shield TBM (Herrenknecht , 2022)

Single Shield TBMs are the ideal machine type for tunnelling through rock and other stable, non-groundwater-bearing soils. The rotating cutterhead is pressed against the tunnel face by means of thrust cylinders pushing on the last ring built. In this type of machine, the excavation operation

and the ring construction operation must be performed in two different times. The excavated material is also in this case brought out using a funnel-shaped muck ring. The excavated diameter is larger than the shield skin, to avoid the jamming in the rock and for a better control of the machine.

For this machine type the diameter varies between 1.5 m to 14 m. It is, as said before, mainly used for heterogeneous rock mass, diverging from soft, brittle rock to very hard rock. (Herrenknecht, 2022)

3.6.5 Double Shield TBM

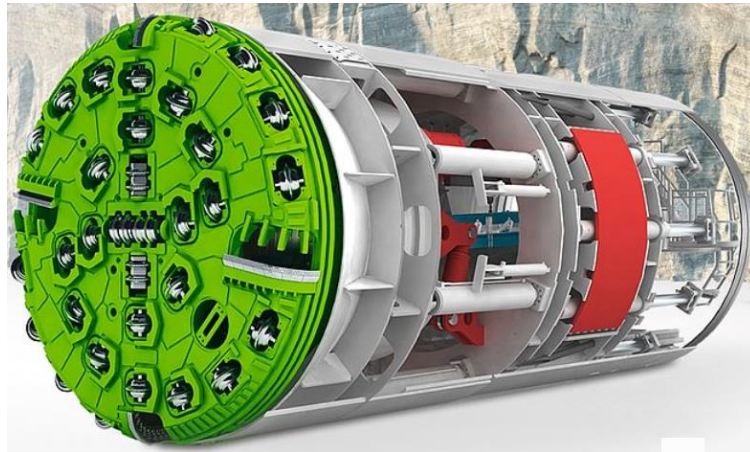


Figure 14 - Double Shield TBM (Herrenknecht, 2022)

The Double Shield TBMs unify the principles of Gripper TBM and Single Shield TBM in one machine. For this reason, this type of TBM can be considered the most technically sophisticated among the TBM machine already presented. In good geological conditions this type of TBM allows the installation of concrete segments during the excavation. Due to this characteristic, this TBM is the best one to use for excavating long tunnels in hard rock. The Double Shield Tunnel Boring Machine consists of two main components: a front shield with the cutterhead and the main drive and a gripper shield with a gripper unit and auxiliary thrust cylinders. Those two shields are connected by the main thrust cylinders which are protected by the telescopic shield where the shield skins of the front and of the gripper shield overlap. In stable rocks, the machine is braced radially against the tunnel with the gripper shoes. In this way the front shield can be advanced independently of the gripper shield using the main thrust cylinders. The reaction forces

are in this case transferred to the rock instead of to the last erected ring as happen in the Single Shield TBM. During the excavation and ring-building phase the auxiliary thrust cylinders are used only to keep the installed ring in place. When the stroke is completed, the gripper shoes are loosened and the gripper shield is pushed behind the front shield using the auxiliary thrust cylinders. The time requested for the regripping is very small with respect to the excavation time: it means that we can assume the excavation almost continuous using this Tunnel Boring Machine. Another key point for this TBM is the tunnelling the geological fault zones. In these sections the use of gripper shoes is not possible, and the thrust forces are applied using the auxiliary thrust cylinders: in this way the tunnelling is the same as explained for the Single Shield TBM. Thanks to this combined method of Gripper and Single Shield TBM, it is often used for long drives in hard rock, especially when the geology is not homogeneous. Additionally, it can be used in all kind of rock, stable and unstable and with a diameter vary between 2.8 m to 12.5 m. (Herrenknecht, 2022)

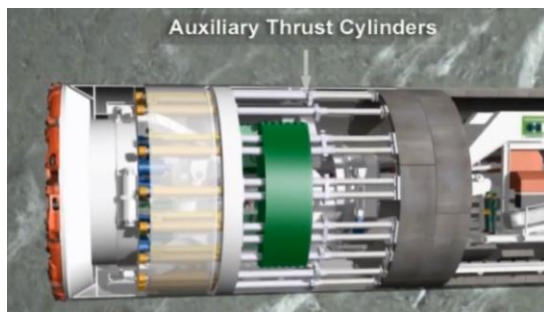


Figure 15 - Thrust cylinders retracted

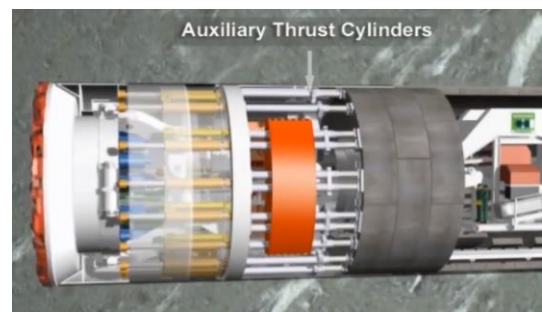


Figure 16 - Thrust cylinders extended

3.7 TBM USED IN BRENNER BASISTUNNEL

In the Mules 2-3 jobsite analyzed in this thesis are used three TBMs: two identic TBMs for the two twin pipes and one smaller diameter TBM for the exploratory tunnel. The main features are listed below:

Double Shield TBM used for exploratory tunnel (TBM S-1054):

Diameter: 6,800 mm

Lining method: Segmental lining

Cutterhead power: 2,800 kW

Double Shield TBMs used for the two main pipes (TBM S-1071 and TBM S-1072):

Diameter: 10,650 mm

Lining method: Segmental lining

Cutterhead power: 4,200 kW

All those three TBMs were manufactured by Herrenknecht company in Schwanau (Germany) factory and then delivered by means of trucks for the smaller parts and ships first and then trucks for the heavier parts, to avoid crossing the Alps.

4 PART ONE: DISASSEMBLY OF THE TBM HERRENKNECHT S-1054

4.1 TBM S-1054: GENERAL DESCRIPTION

The Double Shield TBM S-1054 was made by Herrenknecht in 2017. The total length, considering the shield structure and the back-up, is approximately 310 m and the weight of the shield machine and the back-up are respectively 349.2 tons and 309 tons.

The concrete segments used for the lining have a length of 1500 mm and a thickness of 300 mm which gives an outer ring diameter of 6420 mm and an inner ring diameter of 5820 mm. The ring arrangement is consisting of 5 normal segments and one key segment. Regarding the tunnel characteristics, the total tunnel length is approximately 14 km, with a maximum upward gradient of 0.39% and a minimum curve radius of 10035 m. (Herrenknecht , 2017)

In the following part, the main components present on the TBM will be examined. Starting from the last gantry present on the back up (gantry 25) the description will proceed towards the tunnel face, until to reach the TBM cutterhead. This brief analysis is performed in order to get a wider knowledge and to better understand the disassembly operations.

4.1.1 Back-up system

The back-up system of the TBM is formed by 25 gantries and 2 bridges. In general gantries have a one floor steel construction and are pulled on during the regrip running on rails.

Gantry 25:

The last gantry of the back-up represents the connection between the service devices already installed in the tunnel and the service requested on the TBM. The main components present on this gantry are the high voltage cable drum, which is used to bring the electricity coming from outside to the TBM and the duct storage cassette for the connection between the ventilation system of the tunnel and the ventilation system of the TBM; once the flexible tube inside the cassette is finished, the cassette must be replaced with a new cassette coming from outside by

train. The last device present on this gantry is the emergency generator, used to supply energy in case of a fault in the external electricity system.

Gantry 24:

The only device present on this gantry is the pipe installation crane, which is used to lift the TBM airduct storage.

Gantry 23:

The main goal for this gantry is the development of tunnel services. For this purpose, on the gantry 23 there are four hose reels which aim is to extend the tunnel service tubes during the advancement of the TBM: in particular these tubes connect the fresh water, the dirty water, the dewatering system and the air from outside to the TBM.

Gantry 22:

The key components standing on this gantry are the chiller unit and the extension of tunnel conveyor. The former device is used to make the air colder, while the latter acts as a bridge between the tunnel conveyor belt and the TBM conveyor belt. The TBM conveyor belt has a belt speed of 2.5 m/s, a maximum conveyance rate of 800 t/h and a total length of 210m.

Gantry 21:

On this gantry, the only component present is the material crane conveyor, which goal is to lift and transport the material necessary for maintenance procedures that arrive by train on the TBM. This material is lifted by means of two electric chain hoists placed on a crane runway.

Gantry 20:

This gantry denotes the complete passage of the excavated material from the TBM conveyor belt to the tunnel conveyor belt. The other element placed on this gantry is the air cooler system. This device works together with the air chiller, and it makes the room temperature air coming from

outside the tunnel cooler. This is suitable because on the front of the TBM there is an increase of temperature during the tunnelling and hence the need to cool down the air.

Gantry 18:

On the 18th gantry, the whole available space is occupied by the wastewater tank with a volume of 15 m³. The dirty water coming from the tailskin is pumped in the wastewater tank. Here the water stops for a certain period and the solid parcels have time to settle on the bottom of the tank. At the end of this process the cleaner water is pumped out.

Gantries 16-17:

On these two gantries are installed the Rescue Chambers. They have a capacity of 12 people each one. The rescue chamber offers protection to the workers, when the escape routes are too long or interrupted in the event of an accident, to allow the external rescuers to establish the contact. The available air inside the chamber is regenerated with oxygen regulators.

In each chamber are located some rescue device and the most important are: (mineARC systems, 2020)

- Self-regenerative ELV CO and CO₂ scrubbing
- Medical O₂ regulator and backup
- Positive pressure maintenance system with visual reference
- Fixed Gas Monitor
- Air conditioning and dehumidifying
- Ergonomically designed seating

In general, also some others safety devices are installed along the TBM, such as:

- Measured gases CH₄, CO, CO₂, O₂
- Fire extinguisher
- Smoke and heat detectors
- Water curtains at the end of the last gantry

Gantry 15:

Here is place the staff container which is used by the workers during the shift break time.

Gantry 14:

The cooling water power unit connected with the industrie water tank and an air pressure tank are installed on this gantry. The goal of this cooling water system is to get colder water for the machine circuit. It consists of a heat exchanger where the cold water coming from outside cools down the hot water of the TBM circuit water, which is used for all the devices on the TBM.

In general, there are two water systems: the TBM water system and the external water system. The TBM water circuit is a closed circuit and the used water is cooled down by the above described cooling water system.

Gantry 13:

The whole space is occupied by the five screw type compressors. The aim of these compressors is to ensure the compressed air for the correct use of the pneumatic devices.

Gantries from 9 to 12:

These four gantries can be considered as the electrical heart of the TBM. In fact, almost all the electrical devices placed on the TBM are installed here. There are three main distribution, two sub-distribution and three transformers.

Gantry 6-7-8:

The space between the segment rings and the excavated rock must be filled in other to avoid future settlements in the rock mass. For this purpose, the so-called PEA gravel for the top and the cement for the bottom part of the ring are used. Both materials are transported by train and the containers are unloaded from the trailer to the gantry by means of lifting unit. Once the train is completely unloaded, it can exit the tunnel and carry other useful materials for the next tunnelling. For this reason, on these gantries are located the PEA gravel crane, used for the lifting of the container from the PEA gravel car of the train, the grout injection and the accelerator

power unit. From this area the PEA gravel and the cement are then pumped towards the front to fill the gap between the rock and last ring built. For this last operation, on gantry number 6 is placed the PEA gravel pump system.

Gantry 5:

Starting from the 5th gantry to the 3rd gantry are installed segment quickunloader. The intent of these elements is similar to the PEA gravel crane. In this case, the incoming segments on the train are lifted to allow the segment cars to unloaded and let the train to exit the machine.

Gantry 4:

The steel frame of this gantry is the same of the previous one, but, in this case, is installed the hydraulic power unit instead of the hydraulic tank. The goal of the hydraulic power unit is to pressurize the water needed for hydraulic tools.

Gantry 3:

Here is where the control cabin is placed: this is the location where are taken the decisions about how to proceed with the excavation. From this place is regulated, among other parameters, the thrust force of the thrust cylinders necessary for the advance of the excavation and the rotation speed of the cutter head, which are matched together to obtain the wanted penetration rate. Furthermore, it is possible to start the re-grip and to regulate the pressure of auxiliary cylinders. The drilling power unit is also installed on this gantry, which aim is to supply the necessary power to the drilling unit placed forward towards the face.

Gantry 2:

There are present two grease pumps and one EP2 pump. The EP2 grease is used for the normal lubrication: for example, it greases the bearing parts and the erector. The other type is the tailskin grease compound: it is necessary to sail the tailskin to prevent cement or PEA gravel leakage from the outside part of the ring.

Bridge 2:

The steel frame of the bridge is different from the gantry frame. In this case there is no contact between the structure and the ring floor, so as to leave space for the segments transit. For this purpose, a segment feeder is used, which aim is to deliver the concrete segments from the segment quickunloader to the erector. The segments are grabbed and transported by means of the segment transport crane; it works with a vacuum system to lift the segments in an easy and fast way, from the gantry 5 to the segment feeder on the bridge 1. It is powered by electricity, the longitudinal driveway is about 80 meters and the lifting height, on this machine, is 2.6 m. Another reason for which the bridge needs to be lifted from the floor is because the railway on the ground under the bridge is not yet completely assembled and therefore the gantry could not travel on it.

The main element present on this bridge is the rail placing crane system, which aim is the construction of the railway on the ring floor already in place: there are two rail laying crane because two parallel railway must be built: the first one is for the gantries advance while the second railway is used to access the train on the TBM.

Gantry 1:

The last gantry structure is different from the other gantries because it runs on the concrete segments already in place instead of on the railway. For this reason, it has no steel wheels, but it has got smooth hard plastic wheels that allows it to run on the concrete. The aim of this bridge is to connect the first and the second bridge because the span is too long to be covered by a single bridge.

On this gantry is installed the deduster. It is used to clean the air coming from the cutterhead during the tunnelling. It works with a vacuum system and a set of 7 bag filters, with a flow rate of 500 m³/min. The solid parcels removed from the air are then mixed with water to create a slurry and pumped out.

Bridge 1:

The second bridge connects the last gantry with the shield part of the machine. The main element mounted on this bridge is the drilling unit. The drilling unit is used to perform some core drilling in order to get additional information about the geology that should be found during the next tunnelling. The probe drilling has a working area of 360° and a bore diameter ranging between 82mm and 115 mm.

4.1.2 Shield Area

The heaviest components of the TBM are present in the shield area.

Steel structure shield:

The shield is composed of three main portions: the front shield, the gripper shield and the tailskin. The front shield has a diameter of 6800 mm and a length of 1830 mm, the gripper shield has a diameter of 6650 mm and a length of 4370 mm while the tailskin has a diameter of 6630 mm and a length of 2380 mm. The tailskin slides under the front shield during the re-grip.

The aim of the shield is to protect the machine and the workers from the unpredictable fall of blocks from the rock mass.

Stabilizers:

There are two stabilizers cylinders with a stroke of 200mm which allow the stability of the TBM and the rotation of the cutterhead to follow the right direction.

Gripping:

Gripping and gripper shoes work together to ensure the contact and bracing between the TBM and the rock previously excavated. For this purpose, 2 gripper cylinders with a stroke of 500 mm are used, which ensure a contact force of almost 37000 kN. The re-grip lasts few minutes and during this operation the auxiliary cylinders are completely extended while the thrust cylinders are consequently retracted, as previously explained for the Gripper TBM machine.

Advance:

The advance is usually achieved using the main thrust cylinders. They are 10 cylinders with a stroke of 1700 mm. The last ring is held in place by 16 thrust force auxiliary cylinders. These cylinders have a stroke of 2100 mm.

Erector:

The Erector is used to place the segments in the right position. During this operation the auxiliary cylinders are from time to time retracted to make possible to put into the position the concrete segments. It is driven by hydraulic power and has a rotary angle of $\pm 200^\circ$; segments are grabbed by the vacuum system. This is one of the heaviest parts to handle during the disassembly, as the total weight is around 29 tons.

Main Drive:

The power is supplied by means of 8 electro-motors for a total power of 2800 kW. The total main drive diameter is 3600 mm.

Cutterhead:

The steel construction of the cutterhead is the part of the TBM which is pushed towards the rock to proceed with the excavation. For this TBM, it has a bore diameter of 6850 mm and a total weight of approximately 100 tons. The cutterhead is equipped with 33 single disc cutters and 4 double fold disc cutters with a diameter of 19" and 4 buckets. The wear detection of the cutterhead is guaranteed by 8 sensors.

An important role for the whole good tunnelling process of the TBM is played by the workers, which is the reason why it is possible to include the TBM crew in the description of the TBM. It is a very complex and valuable system of mechanics, electronics, logistics etc. To achieve the best performance and economy of the system as a whole, a skilled and motivated crew is a decisive factor. It is important that the crew has procedures and methods available to handle the ordinary machine and geological problems.

4.2 DISASSEMBLY PROJECT: GENERAL FEATURES

The goal of the disassembly project for the TBM S-1054 is to remove the machine from the tunnel. In this case, the most unusual element for the disassembly is the absence of the chamber. In fact, the space available for the dismantle is only the excavated cross-section of the tunnel and therefore it is not possible to use crane systems larger than the tunnel cross-section. For this project, it has been decided to scrap the entire steel frame of the back up and of the shield structure, while most of the components previously described should be only disassembled, cleaned and used for some other project. This happens because the steel frame is strictly related to the excavation diameter, and usually each TBM project has its own specific diameter. As for the components placed on gantries, most of them are not dependent on diameter and, hence, they can actually be used on other TBMs, even if the excavation diameter does not fit perfectly. The organization of the work is roughly planned as follows:

- Disassembly of the larger components of the machine inside the tunnel to allow the transport by train towards the disassembly cavern; the railway line has a length of almost 15 kilometers.
 - In the disassembly cavern, all disassembled elements coming from the train are loaded onto the track by means of a wheeled crane and are carried to the outside storage area.
 - In the storage area the “buy-back” components are divided from the steel construction. All buy-back items are then cleaned and prepared for delivery to the TBM assembly Factory.
- Instead, the steel frames of gantries and all other unusable parts are scrubbed and delivered to the steel dump.

Basically, each component pulled out from the TBM follows the path depicted by the red arrow in the figure below (Figure 17).

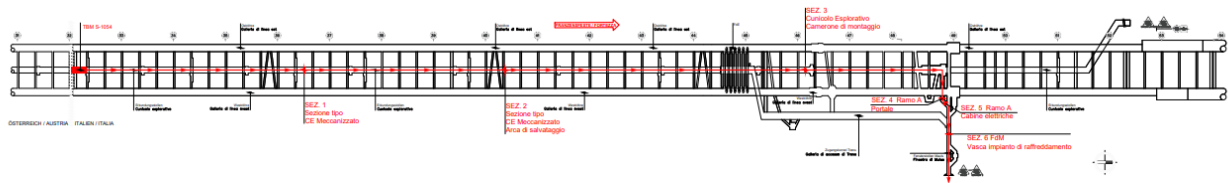


Figure 17 - Schematic path from the Tunnel Face to the Storage Area (red arrow) (Planimetria schematica ingombri smontaggio TBM S-1054, 2022)

The issues related to the confined space must be also considered during the transport on rails. For this purpose, during the project phase was also analyzed the most critical cross section that should be overcome during the conveyance on rails. The boundaries of the free space available for the passage of the train are represented by the refuge chamber and the air duct. A refuge chamber is placed every 2 kilometers along the tunnel that has already been excavated, while the air duct is present along all the pipe. The maximum height available is 2400 mm while the maximum width is 3000 mm. In the following sketch are shown the overall dimensions (Figure 18).

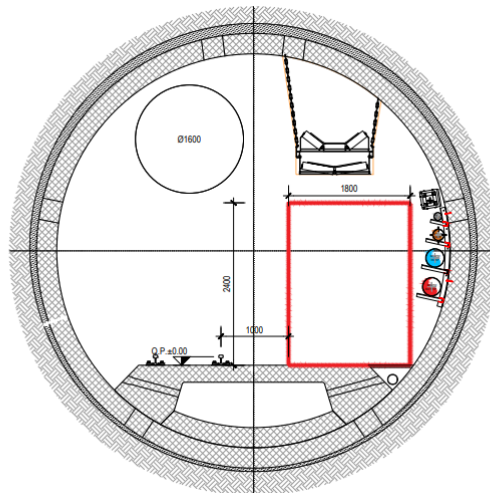


Figure 18 - Most critical cross-section of the tunnel (Planimetria schematica ingombri smontaggio TBM S-1054, 2022)

The last element to take into account regarding the transport is the dimension and the maximum capacity of segment cars used for transport. This consideration about the maximum load is very important for the heavier elements of the machine, which are placed in the shield area.

4.3 PROJECT DESCRIPTION

4.3.1 Back Up and tunnel components disassembly

Firstly, once the excavation is complete, all the service pipes and the conveyor belt used during the tunnelling and no longer suitable for the disassembly of the machine, must be disassembled. Instead, the ventilation duct and the refuge chamber must be left in place in order to keep the required safe work conditions.

The disassembly of the machine inside the tunnel, according to the disassembly project, should start from the back-up system. Each gantry has its own steel wheels and hence it can be easily pulled out using the already present railway. Once arrived in the disassembly cavern, each gantry should be disassembled and loaded onto the truck. For BU 7 to 25 there should be no collision problems with the ventilation duct or with the refuge chamber still present in the tunnel. For gantries 3-6, the proposal is to split them due to a possible collision. Regarding the disassembly of the gantry 2, it should be divided into upper and lower parts and then transferred to the disassembly cavern on segment car. The last gantry and the two bridge should be disassembled later, due to the impossibility of pulling them out on the railway.

4.3.2 Shield components disassembly

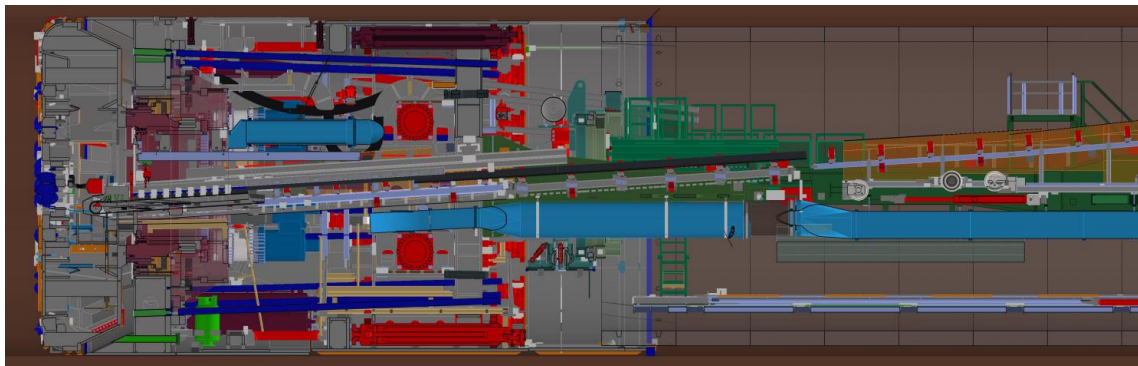


Figure 19 - Starting conditions for the shield disassembly (Herrenknecht, 2022)

Concerning the shield part of the TBM, the first planned operation is to install thrust cylinder extensions at the tailskin level and to extend the thrust cylinders until the thrust cylinders

extension (the blue elements in Figure 20) come into contact with the last concrete ring positioned.

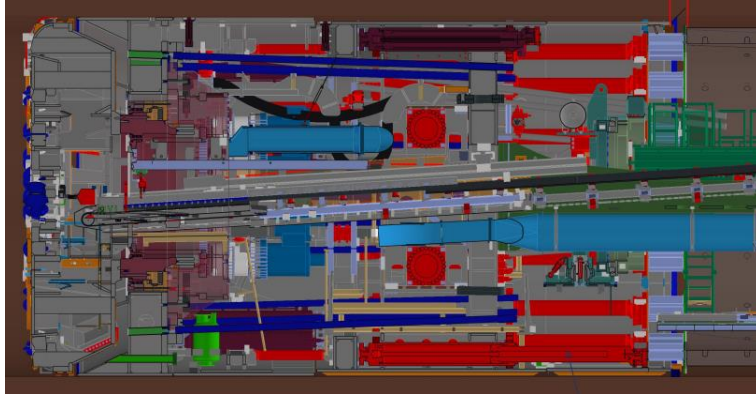


Figure 20 - Installation thrust cylinders extensions ("HK 5102-091-001-01 Shield Disassembly", Herrenknecht, 2022)

After this operation, the front shield should be extended to the maximum position and the cutterhead cut in two portions following the welding line: the bottom portion should be then disconnected from the cutterhead at the level of the flange. Then, the front shield should be retracted and, performing this step, the already disconnected portion of cutterhead will rest on the ground instead of being retracted with the entire machine. At this point it is possible to rotate the cutterhead of 180° and, in this way, the upper portion of the cutterhead will also be in contact with the floor (Figure 21).

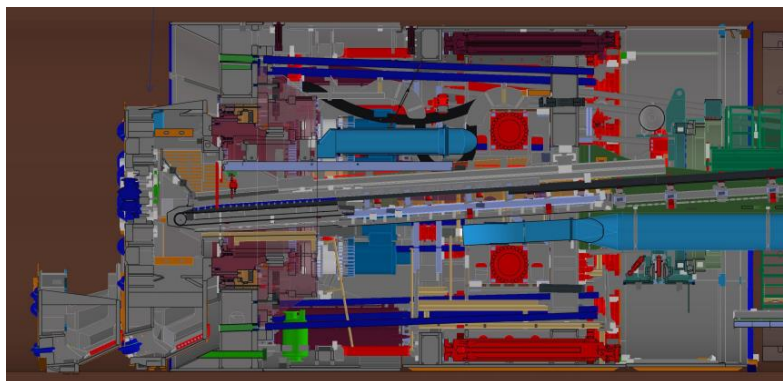


Figure 21 - Cutting and rotation of the cutterhead ("HK 5102-091-001-01 Shield Disassembly", Herrenknecht, 2022)

After the cutting of the cutterhead, the thrust cylinders and the machine conveyor belt present on the TBM shield should be disassembled by using the erector. All the components above mentioned are disassembled, tied to the Erector Telescopic System and lean on the segment car of the train, for the transport to the disassembly cavern.

Once the thrust cylinders and the machine conveyor belt have been removed from the shield area and since the erector is no longer used for the disassembly intention, the suggestion of the disassembly project is to install a crane runway (Figure 22). The crane runway should be installed after the remotion of thrust cylinders and conveyor belt in order to have sufficient space to set up the beam. The number of plates necessary to be used to secure the monorail is dependent on the geology surrounding the TBM in the last tunnelling meters and on the maximum weight to be lifted.



Figure 22 - Crane runway installation ("HK 5102-091-001-01 Shield Disassembly", Herrenknecht, 2022)

At this point, according to the proposed project, the final part of the back-up system should be disassembled.

4.3.3 Disassembly bridges and gantry 1

The disassembly of the last gantry and of the two bridge requires the use of the monorail; it should be installed up to above the segment car position. The first operations should be the installation of six bridge supports, in order to make it possible the disconnection of the gantry

No. 1 and to push it approximately 2 meters backwards. Subsequently, after the installation of four chain hoists, two placed on the crane runway and two on the concrete segment of the tunnel, the disassembly of the first gantry should be started. Initially, two slide beams are welded on the gantry to allow the slide and lift of the upper components in a perpendicular position with respect to the crane runway. Next, the left side of the platform should be also pulled under the monorail, lifted and placed on the segment car. The same operation should be performed concerning the right side, including the deduster placed on it. At this point, also the bottom part of the gantry 1 could be placed on the segment car and hauled out.

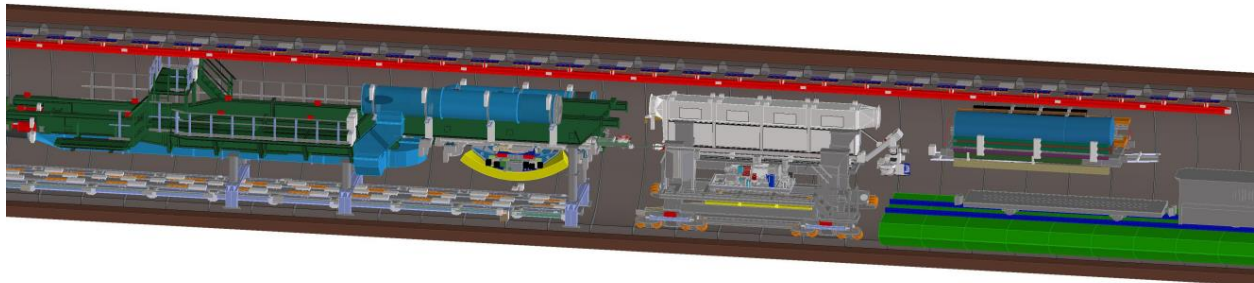


Figure 23 - Disassembly gantry 1 ("HK 5102-091-001-01 Shield Disassembly", Herrenknecht, 2022)

Regarding the bridge 1, first of all it is planned to retract it and to disassemble the segment feeder, followed by the disassembly of the ventilation system and the runway, always by using the monorail previously installed. Once only the bridge frame is still present, it is possible to disassemble the bridge rear part and the bridge front part, including the cylinders used for the bridge support.

At the end, the entire back-up system should be completely disassembled.

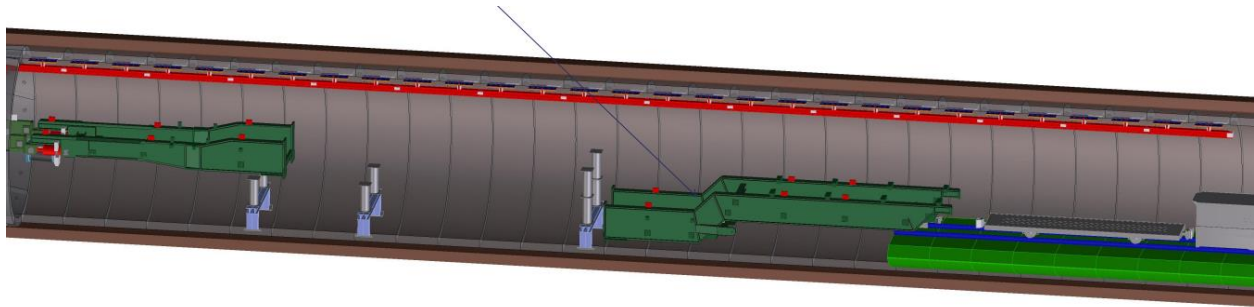


Figure 24 - Bridge 1 dismantling ("HK 5102-091-001-01 Shield Disassembly", Herrenknecht, 2022)

4.3.4 Erector disassembly

The next step is to disassemble the segments Erector System. This operation should be performed using two chain hoists installed on the crane runway previously mounted. After the disconnection of the whole Erector System, it is secured by means of chains to the chain hoist, then it is disconnected from the frame, it is lifted, and it is slid towards the segment car in vertical position. Once it is placed on the segment car, the Erector System should be tilted using the chain hoists. Afterwards, the erector beam should be also disassembled in the same way previously described for the erector system.

After the removal of the erector and of the erector beam, the following step is to lengthen the crane runway towards the tunnel face, as shown in the figure below (Figure 25). For this goal some parts of the top of the shield must be cut by fire cutting in order to allow the installation of the beam.

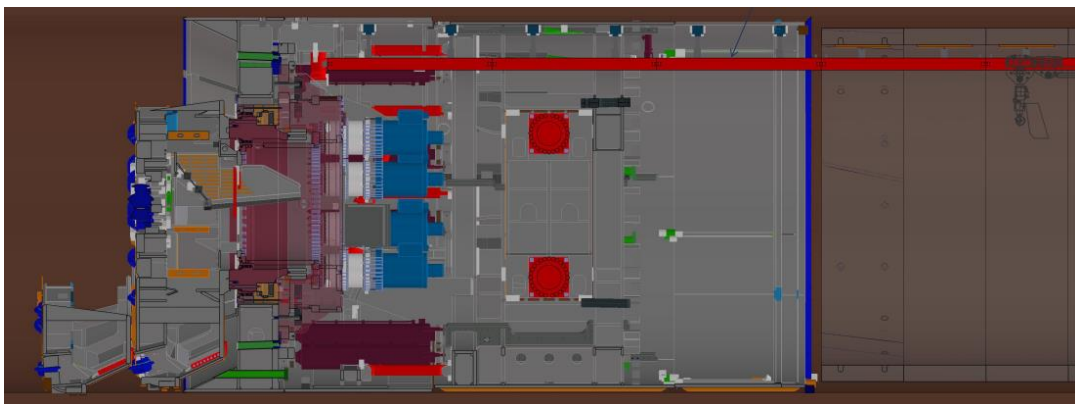


Figure 25 - Lengthen of the crane runway ("HK 5102-091-001-01 Shield Disassembly", Herrenknecht, 2022)

Subsequently, it is possible to proceed with the dismantling of the other components. The first one is the erector support cross, lifted and conveyed towards the segment car in same way as above described for the Erector System. Afterwards, it is planned to disconnect and pull-out the gripper cylinders, then the gripper shoes: even in this case by means of the chain hoists arranged on the crane runway.

It is now possible to disconnect and disassemble the 8 electromotors and their respective gearboxes thanks to the space left by the operations before mentioned. Once disconnected, each motor is loaded on the train and conveyed outside.

Afterwards, it is planned to disassemble and to pull out the two torque cylinders. When the disassembly of the torque cylinders is complete, the shield area behind the main drive is totally empty.

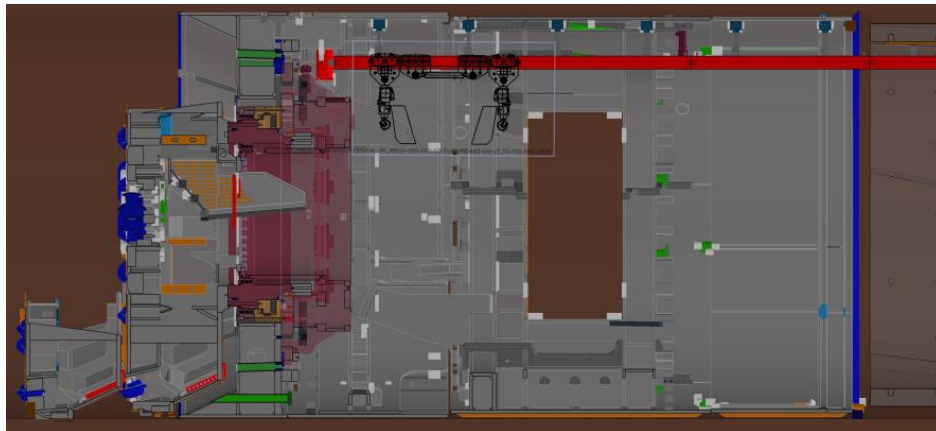


Figure 26 - Gripper shoes and advance cylinders disassembly ("HK 5102-091-001-01 Shield Disassembly", Herrenknecht, 2022)

4.3.5 Main Drive disassembly

Due to the heavy weight of the main drive, the disassembly operation for this component requires some additional disassembly equipment. In particular, the design proposal is to install two beams at the height of the main drive base, to allow the main drive to slide on them. The main drive should be then pulled back by means of specific trolley devices and two pulling cylinders. In addition, should be installed four fixed air chain hoists, two for each side, as shown in the figure below (Figure 27).

Then, the main drive should be pulled backwards of approximately 6 m, dismantled the upper part of the main drive by fire cutting and connected the air chain hoists and the main drive. Once these maneuvers are finished, the last segment of the crane runway should be dismantled to provide more space for the next operation.

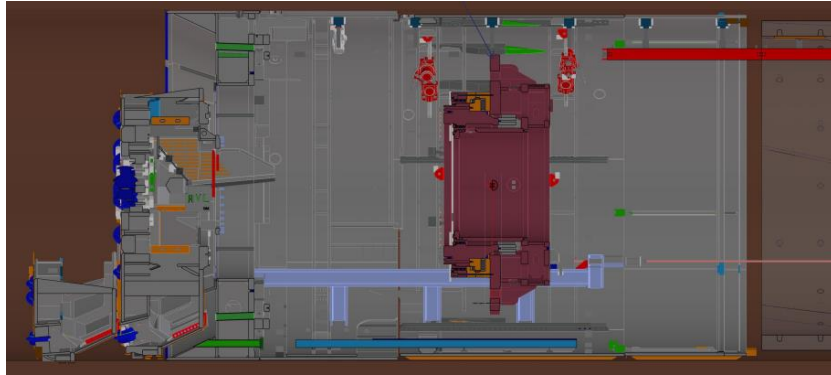


Figure 27 - Main drive pulled backwards by means of pushing cylinders ("HK 5102-091-001-01 Shield Disassembly", Herrenknecht, 2022)

In fact, the main drive should be then lifted of about 0.7 m and the so-called "swivel lug" device should be installed under the main drive. The primary aim of this device is to allow the main drive to be tilted from the vertical position to the horizontal position. Once the swivel lug device is positioned under the main drive, the project proposes the lowering of the main drive, and consequently of the beam, in order to connect the main drive with the swivel lug.

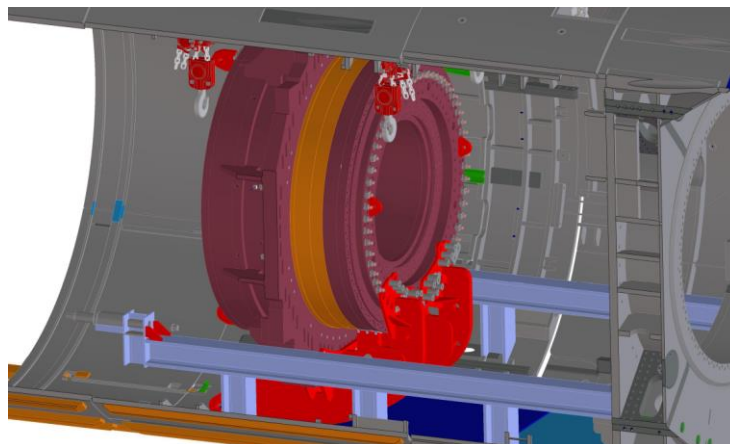


Figure 28 - Swivel Lug device connected to the main drive (Herrenknecht, 2022)

Subsequently, it is possible to dismantle the beam and the trolley system and install an ad-hoc built stopper to prevent the swivel lug from sliding backwards.

The tilting maneuver should be controlled by using the air chain hoists and allowing the sliding of the swivel lug along the vertical beam of the stopper. When the main drive is completely tilted and laid on the steel shield floor, the previously dismantled crane runway can be reassembled and the main drive cut in smaller parts by fire cutting and loaded on the segment car by using the chain hoists.

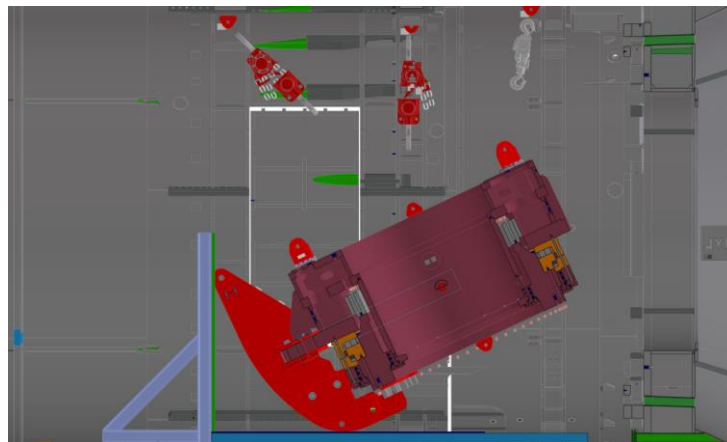


Figure 29 - Tilt maneuver for the main drive ("Investigation Main Drive Disassembly", Herrenknecht, 2022)

At this point the project suggests dismantling the steel structure shield by fire cutting in order to complete the installation of the crane runway to above the smaller cutterhead portion cut before. Then, the cutterhead can be reduced to smaller parts by using the fire cutting and, as done with the main drive, loaded on the segment cars and pulled out by train.

At this point the shield should be completely empty and the next step in the disassembly project is to examine the dismantle of the shield.



Figure 30 - Shield components completely disassembled ("HK 5102-091-001-01 Shield Disassembly", Herrenknecht, 2022)

4.3.6 Shield dismantling

Regarding the shield dismantling, the disassembly project suggests the steps described below.

First, the crane runway assembled in the shield must be dismantled. Then, for the tilting purpose, three air chain hoists should be installed as visible in the next figure (Figure 31).

Afterwards, a double "t" beam should be welded to the shield and the portion of shield to be cut is secured to the chain hoists as shown in the figure (Figure 31); the cut should be made at the level of the upper side of the gripper shoes opening. The entire structure composed by the cut portion of shield roof and the double "t" beam should be subsequently tilted on one side, until the shield wall comes into contact with the beam.

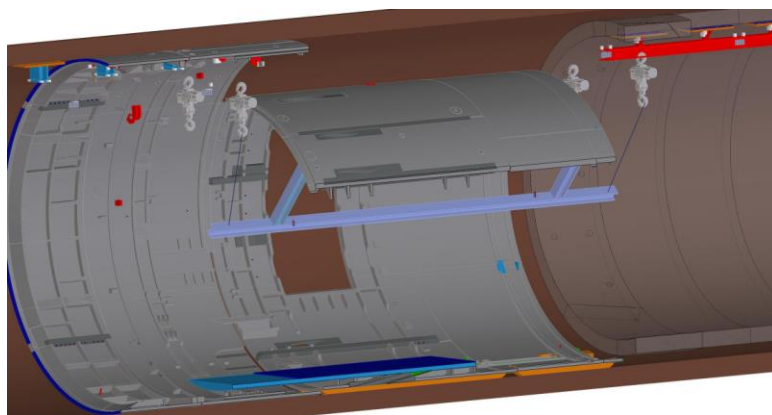


Figure 31 - Installation of "double T beam" on the shield (Herrenknecht, 2022)

At this point the double “t” beam should be uninstalled and the steel roof should be divided into smaller and much more manageable parts.

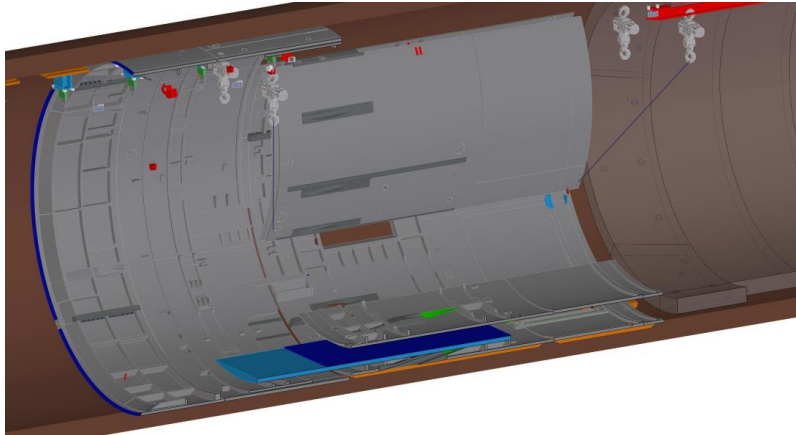


Figure 32 - Cut of shield roof ("Shield disassembly concept", Herrenknecht, 2022)

The front shield roof is then dismantled in the same way above described. In this case it is necessary to install an additional air chain hoist on the rock. Since the shield has been removed and workers have to operate under the unsecured rock, for safety reasons the tunnel rock profile must be secured by means of bolts, wire net and shotcrete, depending on the rock stability. Once the steel roof has been completely removed, the remaining part of the shield can be dismantled by fire cutting, lifting and loading all the components on the segment cars. At the end of these last operations, the TBM is completely dismantled.

4.4 DISASSEMBLY ACTUALLY DONE

4.4.1 Dismantle of the cutterhead

The disassembly of the TBM started from the dismantle of the cutterhead. The first operation performed was the remotion of all the cutter tools and bucket nails from the cutterhead in the last maintenance shift. In this project, the cutterhead was no longer used and therefore it was possible to divide it in three portions, by using the fire cutting. The portion cut was always the bottom part of the cutterhead in order to avoid the lift of heavy parts inside the tunnel. Once the bottom part of the cutter head was divided and disconnected at the flange level, the whole

machine was pulled back, as it is usually done before the maintenance shift, and the cutterhead was rotated at the same time. Afterwards, the same operation was done for the second and the third portion of the cutterhead. The result of the divided cutterhead is shown in the picture below (Figure 33); this photo was taken after the complete disassembly of the shield area but the partition of the cutterhead was the starting disassembly operation.



Figure 33 - Cutterhead divided into three portions. The photo was taken after the main drive disassembly

4.4.2 Dismantle of tunnel and TBM services

At the end of the dismantling of the cutterhead, all the elements present in the tunnel and no longer useful for the disassembly purpose, such as for example the tunnel conveyor belt, have been disassembled. The only components that have been left inside the tunnel are the refuge chambers, the safety devices (ex: fire extinguishers), the ventilation duct and the lights. Even the services, included the high voltage electric current and the water circuit, have been disconnected. For this reason, all the electrical devices present on the TBM were no more usable. In particular, at the beginning of the TBM disassembly, also the erector and the segment transport crane were already out of service because of the lack of electrical current on the TBM.

4.4.3 Pull out of the Back-Up system (from gantries 25 to gantry 3)

The starting operation for the gantry 25 disassembly was the remotion of the duct air storage cassette, secondary ventilation and air cooler, because their positions interfered with the air duct of the tunnel and therefore was not possible to carry them with their relative gantry.



Figure 34 - example of gantry transportation (gantry 24)

Afterwards, they started to pull back all the gantries, until the BU 3. Each gantry has been previously disconnected from the preceding gantry and the upper floor was firstly separated from bottom part of the gantry and then loaded on the segment car of the train by using a train crane (Figure 35).



Figure 35 - train crane used during the disassembly

This operation was necessary to avoid the collision between the gantry itself and the air duct of the tunnel.

Once arrived at the disassembly cavern by railway, each gantry was loaded on the truck and was brought out in the storage area. In this place, the buy-back components were divided, cleaned, and delivered by truck. Instead, the complete steel frames of the gantries and the no more usable parts have been scrapped and then delivered to the steel deposits in Verona.

4.4.4 Disassembly of bridges and gantries 1-2

4.4.4.1 Bridge 2

Regarding the bridge 2, it was firstly stripped of the ventilation deduster by using the crane train. Later, the bridge has been cut into two portions and was loaded on the train trailer; it was possible to perform these operations by using the train crane because the railway was installed almost until the end of the bridge 2 and hence it was allowable to use the crane until this stage without lengthening the railroad. Furthermore, to guarantee the stability of the bridge 2, before the disconnection from the gantry 2 have been installed two wooden supports acting as feet. Once the bridge 2 has been dismantled and removed, three floor segments have been placed where the bridge 2 was positioned by using the train crane, in order to create a flat surface as a safe workplace for the proceed of the disassembly and to allow the use of the train crane also for the next disassembly steps. Indeed, for the second purpose, have been installed the rail on the floor segment.

4.4.4.2 Segment transport crane

After the complete dismantle of the bridge 2, they focused on the remotion of the segment transport crane. Initially, the brakes were opened, and the crane was pushed back to the train crane; the first part that was disconnected and that was loaded on the train trailer was the transport crane drive unit, and subsequently the transport segment plate.

4.4.4.3 Gantry 1

Subsequently, it was possible to remove all the components present on the gantry 1, in particular the deduster. Then, the central floor of this gantry has been cut by fire cutting and brought out of the tunnel.

Then, some wooden supports were installed, as previously done with the bridge 2, to let the disconnection of the bridge from the gantry 1. At the end of this process, the gantry 1 was dismantled, loaded on the train trailer, and brought out of the tunnel. The segment feeder was left inside the tunnel and the invert segments placed on it. This element will be removed at the end of the disassembly of the shield, by remotion of the segment invert, unscrew of the platform in order to divide it into two parts and they will take it out of the tunnel as the last part.

4.4.4.4 Bridge 1

The dismantle of the bridge 1 was performed step by step: after the dismantle by fire cutting of one slice of bridge of almost 2 m length, the wooden supports were moved forward towards the tunnel face and the floor segment placed on the concrete ring. At the same time the bridge was unloaded of the heaviest components mounted on it. The most challenging operation was to uninstall and to bring out the drilling unit: due to the confined space, for this purpose was necessary to cut the drilling unit bearing into two portions in order to permit the lifting and the loading of the drilling unit by means of the train crane.

4.4.5 Disassembly of the Erector

Concerning the erector disassembly, it is important to mention that the only components to be reused, and hence that was not possible to divide in pieces, were the drive unit, the telescopic system, the travel cylinders, and the cross beam included of the erector head.

Each component removed from the erector structure was managed with the train crane. These components are listed below, following the chronological order of remotion.

- 1) Crossbeam and erector head
- 2) Telescopic system

These two first elements were the heaviest components of the whole erector system: the former element had a total weight of 2.5 tons while the latter had a total weight of 3.4 tons; it was however possible to make these maneuvers by means of the train crane.

- 3) Travel cylinders
- 4) Motors and gearboxes of the erector
- 5) Erector bearing

The erector bearing was previously divided into four parts by using the fire cutting in order to reduce the weight and thus to manage it easily.

4.4.6 Disassembly of the shield area

The disassembly of the shield area started with the disconnection and the pull out of auxiliary thrust cylinders. It was not possible to perform this operation for the two bottom auxiliary thrust cylinders because the space occupied by the floor segment did not allow that, as understandable from the Figure 36. The removal of the cylinders was again executed by using the crane.



Figure 36 - disassembly of the shield area: removal of thrust cylinders

The second step, after the removal of the thrust cylinders, was to clean the whole shield area and to remove all the cables and pipes still present inside the shield, in order to get a better and safer workplace.

Subsequently, the gripper cylinders have been removed. As visible in the picture above (Figure 36Figure 35), the gripper cylinders have a huge dimension and hence was not sufficient the only use of the train crane. Indeed, for safety reasons, the cylinders were safe with two additional air chain hoists welded on the shield roof and then, once disconnected, they were loaded on the train trailer and brought out to the storage area.

After the removal of the gripper cylinders, the electromotors and the gearboxes have been disconnected and pulled out. The same type of procedures has been implemented for the removal of the main thrust cylinders and of the torque cylinders; for the last type of cylinder was necessary to use the fire cutting to disconnect the cylinder from the TBM shield.

At that point the machine showed as in the picture below (Figure 37).



Figure 37 - disassembly of the shield area: removal of main thrust cylinders, gripper cylinders, torque cylinders and electromotors with gearboxes

The last step performed during the disassembly of this area was the dismantling of the gripper shoes from the shield. For safety reasons, before the disassembling of the gripper cylinders, the gripper shoes were safe to the shield by means of two steel beams welded on the shield itself, in order to avoid the fall of the shoes towards the center of the shield (Figure 38).



Figure 38 - gripper shoe safe to the TBM shield by means of a steel beam

Then, concerning the dismantling of the gripper shoes, both the crane and the air chain hoist were used, these elements have been pulled out of the aperture and they have been lied on the shield floor before to be divided into two portions and loaded on the segment car of the train.



Figure 39 - gripper shoes dismantling

4.4.7 Main drive disassembly

The disassembly of the main drive has been performed in the following steps:

- 1) Removal of the inner bearings in order to lighten the whole main drive.
- 2) Assembly of a steel platform at the base of the main drive, which allowed the rolling of trolley device installed on the bottom side of the main drive (Figure 40 & Figure 41).

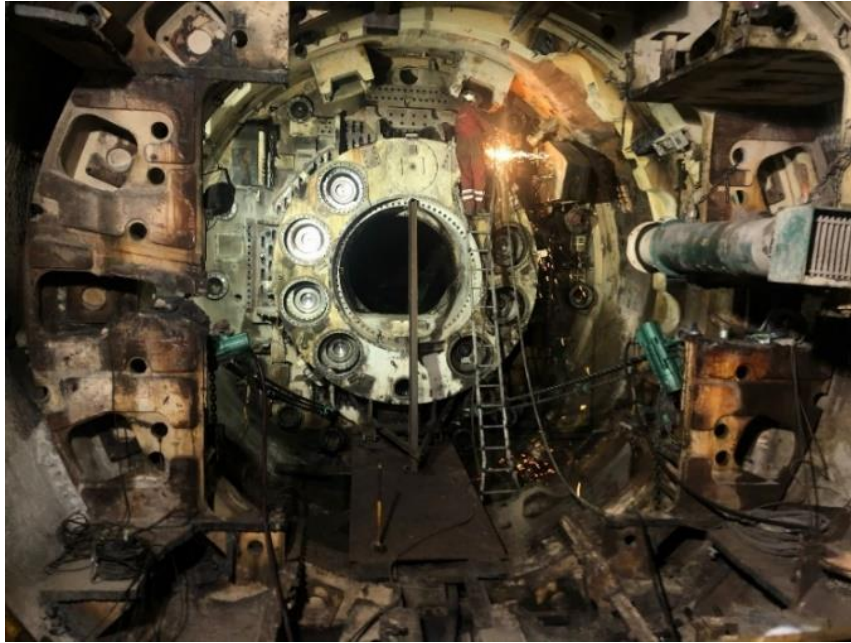


Figure 40 - separation of the main drive from the cutterhead flange

- 3) Installation of a safety device to avoid the back tilting of the main drive (Figure 40). This expedient is a set of five steel beams merged to create a kind of safety easel for the main drive itself.
- 4) Separation of the main drive from the cutterhead flange by means of the fire cutting.
- 5) Pulling back and rotation of the main drive thanks to the steel platform and to the two sets of trolley devices mounted on the bottom of the bearing. This operation was performed by means of two air chain hoists with a capacity of 15 tons each one.



Figure 41- main drive lying on the shield floor, trolley and easel devices

- 6) Once the main drive was rotated on the floor, it was possible to take out all the oil from the inside and to cut it in smaller portions to allow the loading with the train crane and the transportation on the railway.

4.4.8 Dismantling of the shield

Once all the elements present in the shield area have been disassembled and taken out, it was possible to perform the shield dismantling. They started from the tailskin and then proceeded towards the front shield performing the same operations. At the beginning of the dismantling, the portion of the roof shield to be cut has been secured by means of two steel rods and two chain hoists welded on the roof. Then it was possible to start to cut the steel by means of the fire cutting and to rotate the cut portion on one side, as shown in the Figure 31. Afterward, the steel segment of the shield has been laid down on the invert segment and loaded on the segment car by means of the train crane. Once all the upper parts of the shield have been cut and taken out, it

was possible to remove easily also the remaining bottom portion of the shield, using the fire cutting and the train crane in order to load them on the segment car.

4.5 COMPARISON BETWEEN THE DISASSEMBLY PROJECT AND THE WORK ACTUALLY DONE

In this paragraph are highlighted the main differences between the steps proposed by the project and the operations executed during the disassembly.

Firstly, starting from the cutterhead dismantling, which is the first operation proposed in the project and really carried out during the disassembly, the main difference is related to the number of portions in which the cutterhead has been divided. In the project was proposed to slice the cutterhead into two parts while it has been divided into three parts. However, the projected plan regarding how to proceed has been respected.

Concerning the dismantling of the tunnel services and of the back-up system, from gantry 25 to gantry 2, are not recognizable remarkable changes, even because the project is not very specific on how to work since the operations forecasted were quite easy to be done and the did not required specific recommendations.

For the last two gantries and the bridges, the main differences are related to the project suggestion to use the monorail and the actual use of the train crane. Indeed, the use of the train crane has been evaluated more multipurpose, quicker, and cheaper with respect to the installation of the beam on the concrete rings. Thus, in the project explanation, it is not requested to install the invert segments because it doesn't require the use of any machine with wheel for the disassembly of the components in the front part of the TBM.

Another difference is on the type of supports used for the bridge stability. The actual choice is fell on the use of more adjustable wooden supports instead of the steel cylinders proposed.

Concerning the erector, in the disassembly project it was suggested, after the disconnection from the erector beam, to remove the whole erector at the same time by means of the monorail beam. In the real work done, instead, the complete erector system has been divided in more parts and it was used the train crane instead of the monorail beam.

Regarding the shield area, also in this case the main differences are related to the use of train crane instead of the proposed use of the monorail. Indeed, the gripper cylinders, the auxiliary and main thrust cylinders, the torque cylinders, and the electromotors with their relative gearboxes have been disconnected and then actually removed by means of the train crane.

For the main drive disassembly, the project suggested the installation of the trolley devices at almost half height of the main drive, to let the slide of the steel wheel on the two beams previously installed (Figure 28). Instead, for the disassembly of this component, the trolley devices have been welded on the bottom part of the main drive and hence, the installation of the two beams was no longer useful since the slide of the main drive was carried out on the steel platform lying on the floor. Another important difference regards the tilting operation; in the project it was suggested the use of the swivel lug device, while in the real case the overturning has been performed only using the two air chain hoists. This decision has been made to avoid the lifting of the heavy main drive for the installation of the swivel lug device under the main drive itself.

Regarding the shield dismantling, it has been followed the suggestions given by the disassembly project. The most remarkable difference between the project and the work actually performed is the that they did not weld the double t beam on the cut portion of the shield before the tilting operation.

5 PART TWO: BACK ANALYSIS ON CUTTER DISCS WEAR

5.1 INTRODUCTION PART ONE

In this first section of the thesis will be carried out a back analysis on the cutter ring wear depending on the geology. The final aim of this research is the understanding of the best machine parameters to be adopted during the tunnelling, in order to prevent as much as possible the cutter ring wear. Furthermore, the reduction of wear leads to a consequent reduction in tools change in the cutterhead for each shift and this amount of changes is related to a final overall cost saving for the project. In fact, the lowered of the changes means a general decrease in refurbished cost for the cutter rings and a reduction of the maintenance time shift in favor of higher production. Furthermore, for the specific case of this project, the results obtained can be used for the remaining excavation of TBMs S-1071 and S-1072, forecasting in advance the number of cutters tools necessary for each different geological section and suggesting to the operator the machine parameter to be kept during the excavation.

The data used are the absolute wear for each production shift, given by the difference between the cutter ring radius at the end of the maintenance shift and the cutter ring radius after the following production shift. The data were gathered in the most geologically homogeneous areas between the May 23, 2018, which represents the start of the excavation by the TBM S-1054, and the April 10, 2022.

5.2 GEOLOGICAL AREAS ANALYZED

The geological areas in which the analysis has been performed were chosen on the basis of the rock properties and the general rock mass properties.

The main rock properties considered are listed here:

- Specific weight of the rocks analyzed
- Uniaxial compressive strength (UCS)

- Young Modulus (E)
- Cerchar abrasiveness index (CAI)

While the rock mass classification taken into account are:

- Rock Mass Rating (RMR)
- Geological Strength Index (GSI)

5.2.1.1 Specific weight

This parameter indicates the weight per unit volume of rock material. It is usually expressed with the symbol “ γ ” and the unit is weight per unit volume [kg/m^3].

5.2.1.2 Uniaxial compressive strength

This test is performed in a laboratory with a rock core sample with a regular geometry. The rock core specimen is cut to length so that the length to diameter ratio is 2.5 to 3.0. The specimen is then placed in a loading frame and an axial load is continuously applied to the specimen until peak load and failure are obtained. The Uniaxial Compressive Test of a specimen is calculated by dividing the maximum load carried by the specimen during the test by the initial cross-sectional area of the specimen. The unit is expressed in MPa.

5.2.1.3 Young Modulus (E)

The test to obtain the Elastic Moduli of the Intact Rock Core is performed similar to the Uniaxial Compressive Test described above, except that the deformation is monitored as a function of load. Using this test is also possible to estimate the Poisson’s ratio of the intact rock core, measuring both axial and lateral strain during compression. It is generally preferable to use strain gauges glued directly to the rock surface. The unit is expressed in GPa.

5.2.1.4 Cerchar Abrasiveness Index (CAI)

The Cerchar Abrasiveness Index is the most widely known test method for identification of rock abrasiveness. The CAI value is related directly to cutter life in the field. It can be used for evaluating the wear of excavation equipment in different application such as, in this case, the wear of disc cutters.

The testing principle is based on a steel pin with defined geometry and hardness that is scratched on the surface of a rough rock sample over a distance of 10 mm under static load on 70 N. In the original Cerchar equipment setup, the pin and the dead load are moved across the rock surface. The pin is made of a standard steel and has a 90° conical tip. It should have a diameter of at least 6 mm and the length should be such at the visible part of the pin at least 15 mm.

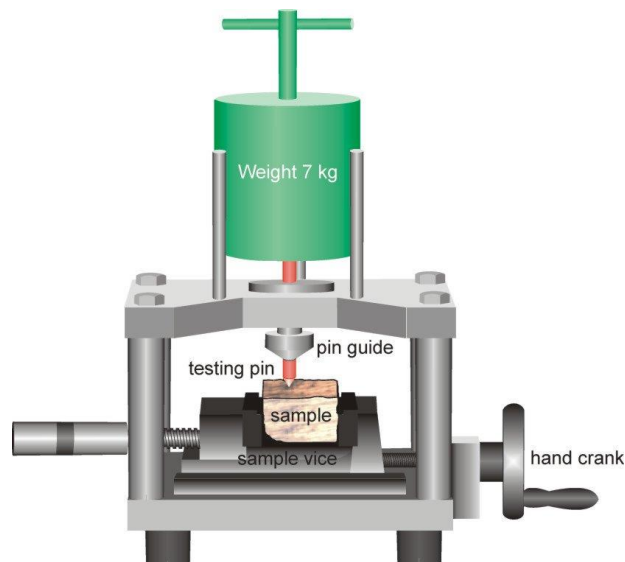


Figure 42 - CAI test equipment (Thuro, 2010)

The rock sample is placed in the equipment and firmly clamped using a rigid vice. The device is rigid and also fixed to avoid any lateral movement. The dead load is then placed on the top of the pin and the pin is carefully lowered to the rock surface. The test is then carried out by relative displacement of the pin on the rock surface across 10 mm at given time intervals. After the test, the pin is removed and the tip flat wear is measured.

The CAI is then calculated from the measured diameter of the resulting wear flat on the pin.

$$CAI = 10 \cdot d$$

where d is the diameter of wear flat measured in mm.

5.2.1.5 Rock Mass Rating (RMR)

The Rock Mass Rating is a geo-mechanical classification system for rock mass, developed by Z. T. Beniawski. This system assigns points to the rock mass based on the analysis of some rock mass parameters. The parameters analyzed are:

- Uniaxial compressive strength of the rock material
- Rock quality designation (RQD)
- Spacing of discontinuities
- Condition of discontinuities
- Groundwater conditions
- Orientation of discontinuities

To each of the six parameters is assigned a value corresponding to the characteristics of the rock. These values are derived from field surveys and laboratory test. The sum of the six parameters is the RMR value, which lies between 0 and 100.

The classification based on the total grade is:

- 0-20 Very Poor
- 21-40 Poor
- 41-60 Fair
- 61-80 Good
- 81-100 Very Good

5.2.1.6 Mixed face conditions

Mixed face conditions (MFC) are characterized by a tunnel face composed by materials with a different boreability, e.g. difference in strength, fracturing grade, voids created by local instabilities ecc.

MFC in generally lead to increasing cutter wear caused by impact forces that create damages of cutter rings and internal parts, as the cutter bearings.

Such conditions have been encountered along the entire tunnel drives. MFC and their impact on the actual cutter wear have not been analyzed within this thesis.

5.2.1.7 Geological Strength Index (GSI)

The Geological Strength Index system was proposed by Hoek in 1994. The GSI concentrates on the description of two factors: rock structure and block surface conditions. It is based on visual inspection and, for this reason, it is possible for different persons to estimate different GSI values from the chart for the same rock mass. The table used for the estimation of GSI value is below reported (Figure 43)






Geological Strength Index (GSI)		Surface conditions				
<p>From the description of structure and surface conditions of the rock mass, pick an appropriate box in this chart. Estimate the average value of GSI from the contours. Do not attempt to be too precise. Quoting a range of GSI from 36 to 42 is more realistic than stating that GSI = 38.</p>		Very good Very rough and fresh unweathered surfaces	Good Rough, maybe slightly weathered or iron stained surfaces	Fair Smooth and/or moderately weathered and altered surfaces	Poor Slackensided or highly weathered surfaces or compact coatings with fillings of angular fragments	Very poor Slackensided and highly weathered surfaces with soft clay coatings or fillings
Structure		Decreasing surface quality				
 Intact/Massive – intact rock specimens or massive in-situ rock masses with very few widely spaced discontinuities	Decreasing interlocking of rock pieces	90			N/A	N/A
 Blocky – very well interlocked undisturbed rock mass consisting of cubical blocks formed by three orthogonal discontinuity sets		80				
 Very Blocky – interlocked, partially disturbed rock mass with multifaceted angular blocks formed by four or more discontinuity sets		70				
 Blocky/Disturbed – folded and/or faulted with angular blocks formed by many intersecting discontinuity sets		60				
 Disintegrated – poorly interlocked, heavily broken rock mass with a mixture of angular and rounded rock pieces		50				
		40				
		30				
		20				
		10				

Figure 43 - Geological Strength Index table (Hoek, 1997)

Generally, the rock mass properties are not directly related to the cutter wear but must be considered for the complete analysis of the machine parameters. For example, the thrust required to excavate a rock mass characterized by a RMR very low should be lower than the thrust required for a rock mass with a high RMR value, considering the same productivity (m^3 excavated per hour) and the same rock type.

5.2.2 Lithologies analyzed

On the basis of the above-described parameters, the different lithologies on which the study about the cutter ring wear is carried out and their properties are below listed:

	Rock Properties				Rockmass Properties	
	gamma [kN/m ³]	UCS [MPa]	E [GPa]	CAI [-]	RMR	GSI
Paragneiss	28	72	50	4	60	50
Amphibolite	28	140	53	4.3	65	55
Metabasalts	26	150	51	4	50	40
Calchshists	27	100	50	2	55	55
Granitic Gneiss	25	220	50	5	75	70

The chainage relative to each geology analyzed are reported in the following table (Figure 44).

		Chainage TBMS-1071		Chainage TBMS-1072		Chainage TBMS-1054		Tot [m]
		Start	End	Start	End	Start	End	
1	Paragneiss	46250	45800	46250	45800	13180	13480	1200
2	Amphibolite	45500	45400	45500	45400	13800	13900	300
3	Metabasalts	40750	40450	40750	40450	18540	18840	1500
		40000	39800	40000	39800	19300	19500	
4	Calcschists	39600	39000	39600	39000	19700	20130	3390
		38700	38120	38700	38100	20460	20940	
5	Gneiss	-	-	35400	34500	24000	27220	4120

Figure 44 - chainage relative to each geology

5.3 CUTTERHEAD DESIGN

The cutterhead is the portion of TBM which is contact with the tunnel face. On the cutterhead are placed the cutter tools, which aim is to break chips of rock from the tunnel face by rotating and applying high contact pressure.

Concerning the cutterheads of the analyzed TBMs, they are divided into three zones, which are, starting from the center towards the contour: the center, the face and the gauge. The distance between cutters is not always the same but it changes with the position of cutters. In particular, for those machines, this distance is 100 mm for the central cutters, ranging between 75 mm and 90 mm for face cutters and shorter between gauge cutters.

For each cutter track has been evaluated the circumference traveled per cutterhead rotation [m] and the area of influence [m²]. In particular, the area of influence represents the area which is theoretically cut by each cutter: it is the ring area representative of the space between the half distance between a cutter and its previous one plus the half distance between the same disc and its next.

In the successive graphs are reported the circumference and the area of influence for each track, for the TBM S-1054 and TBM S-1071/TBM S-1072 respectively.

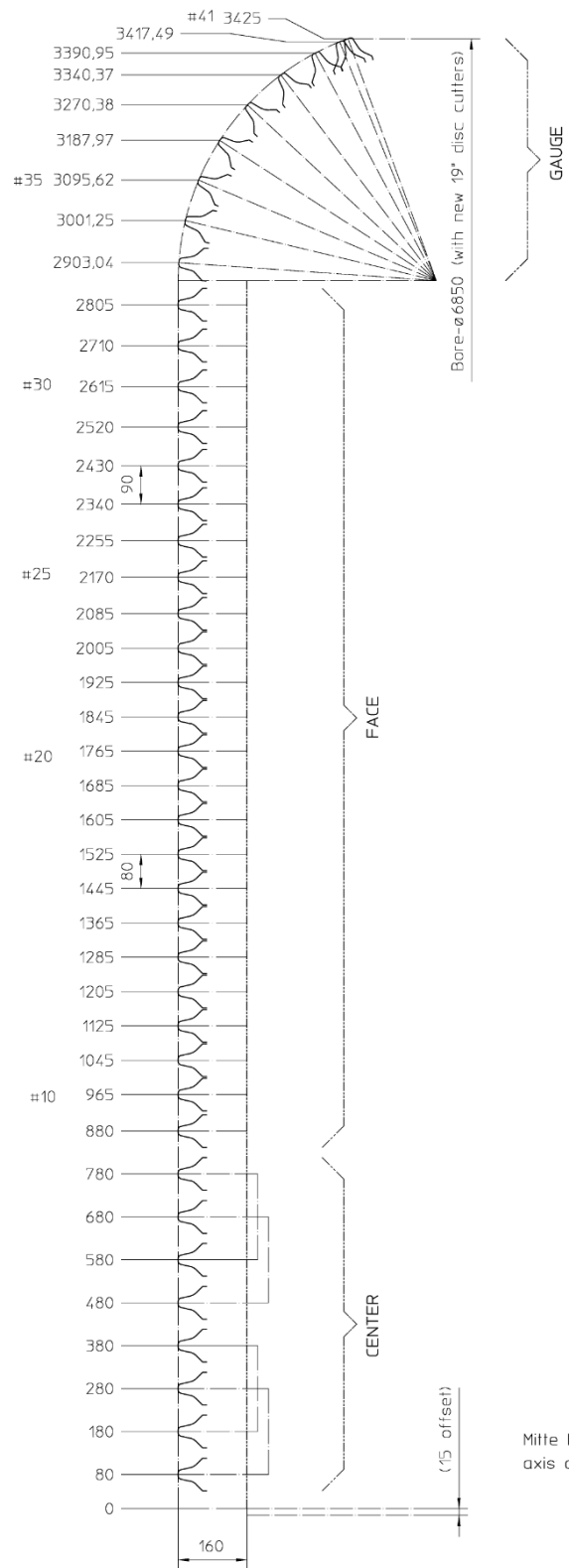


Figure 45 - Cutterhead lateral view TBM S-1054 – cutter position (Herrenknecht , 2017)

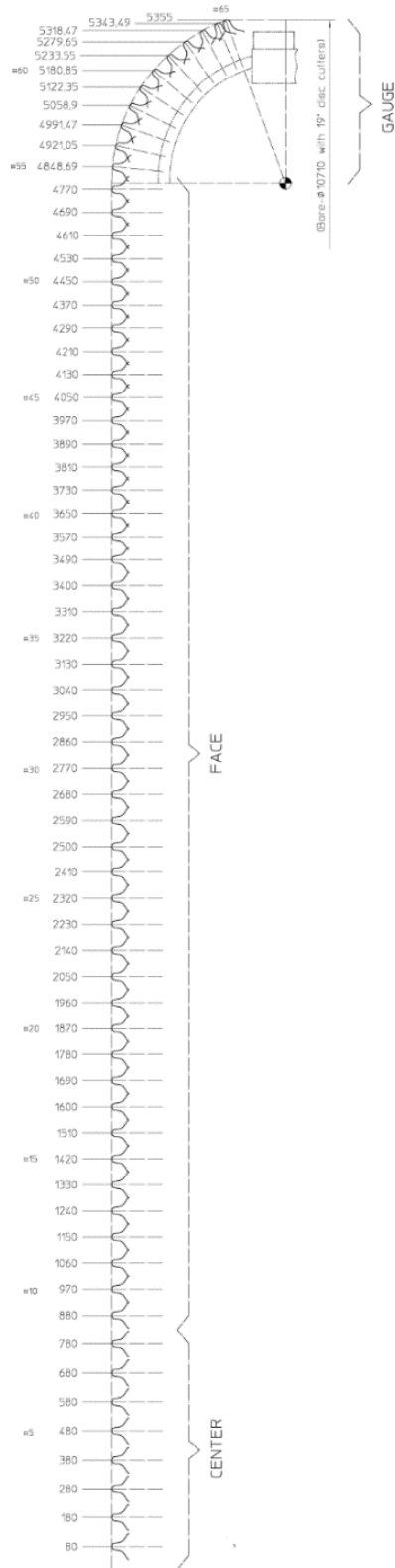


Figure 46 - Cutterhead lateral view TBM S-1071 & TBM S-1072 – cutter position (Herrenknecht, 2017)

5.3.1 Design analysis TBM S-1054

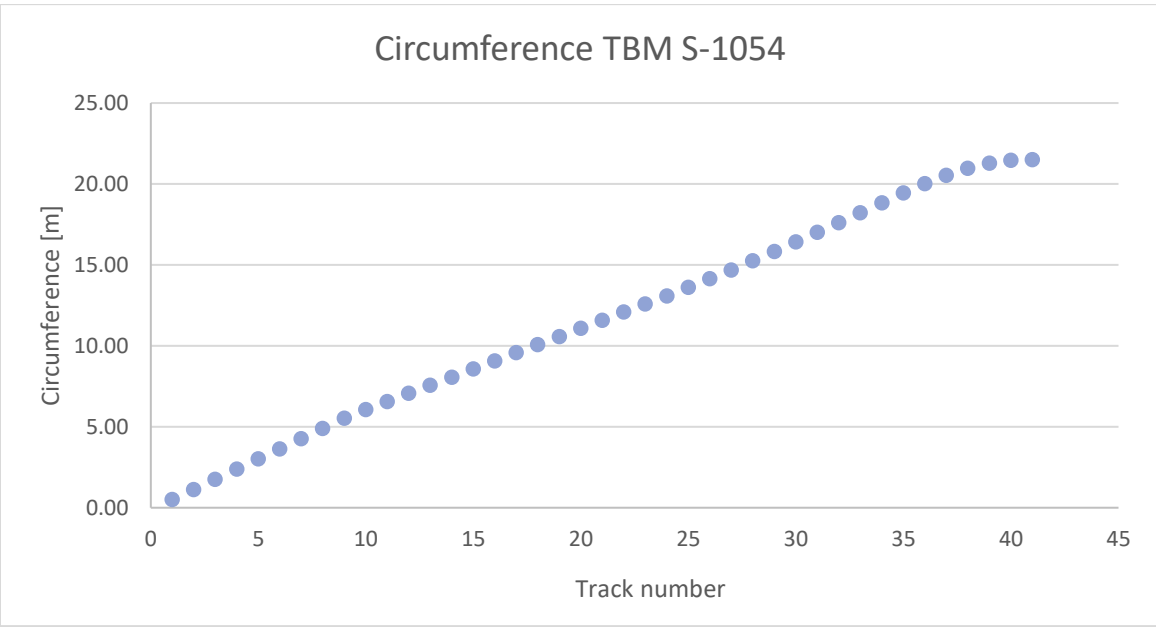


Figure 47 - Circumference per each track number (TBM S-1054)

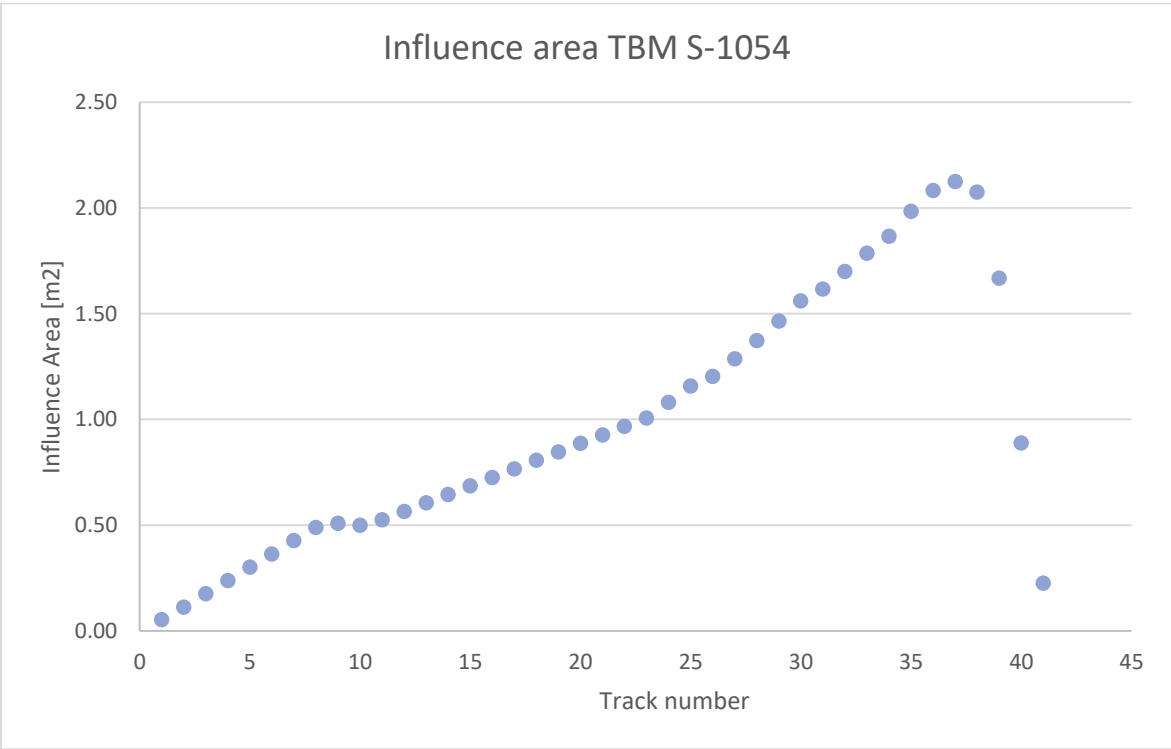


Figure 48 - Influence area per each track number (TBM S-1054)

5.3.2 Design analysis TBM S-1071 and TBM S-1072

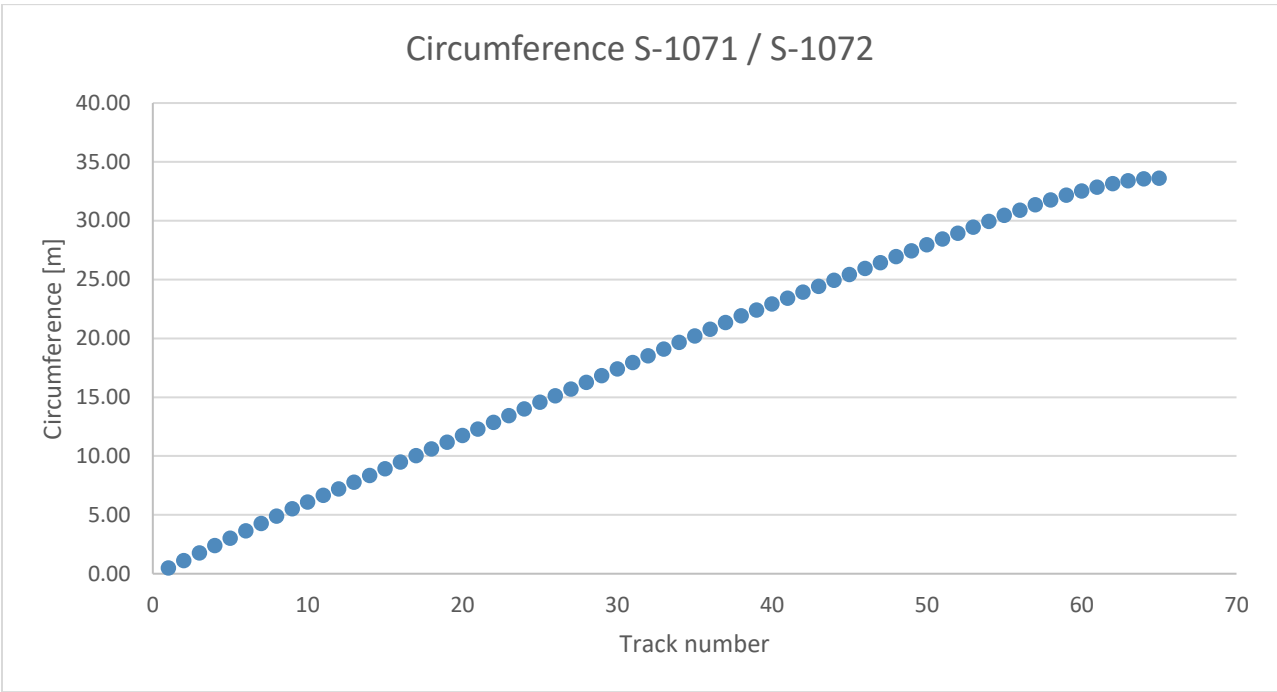


Figure 49 - Circumference per each track number (TBM S-1071 & TBM S-1072)

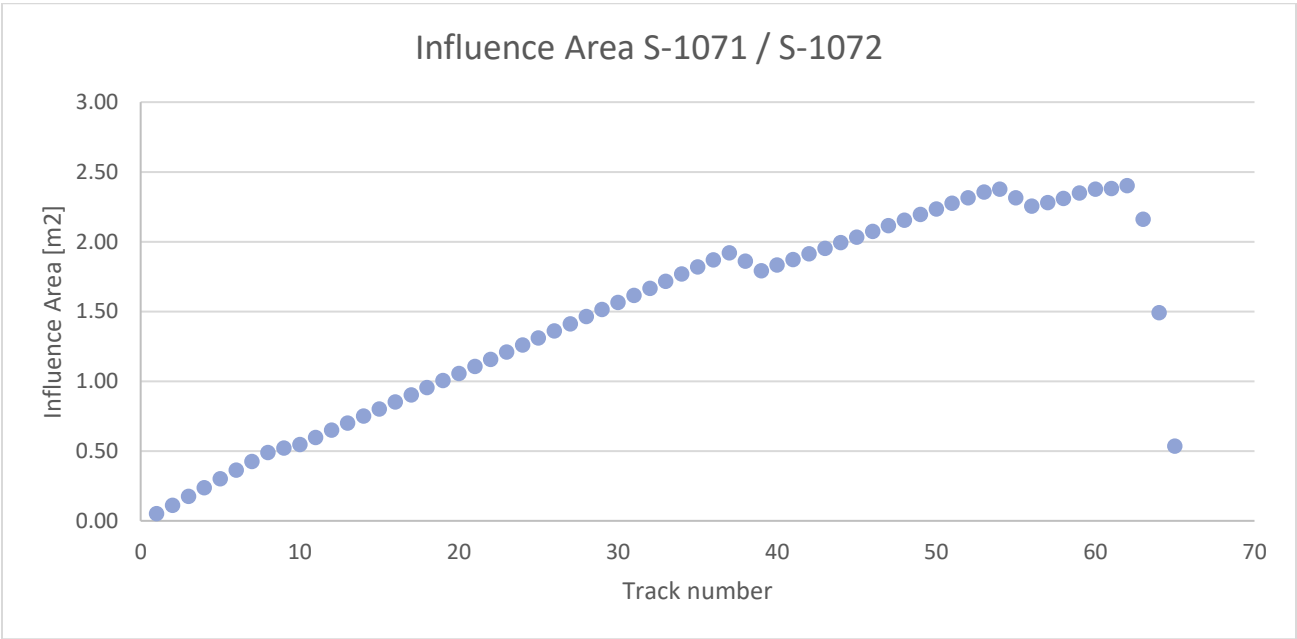


Figure 50 - Circumference per each track number (TBM S-1071 & TBM S-1072)

Due to the non-constant distance between cutters, the circumference doesn't increase linearly and, at the same time, as is clearly visible from the area of influence plot for TBM S-1071 & TBM S-1072, it shows a stairs behavior. Furthermore, in the gauges zone, where the distance between two cutters is very low, even if the diameter of the tracks is the highest, the influence area is very small.

5.4 MACHINE PARAMETERS

The TBM parameters on which the investigation is performed are:

- Cutterhead rotation speed [rpm]
- Thrust force advance cylinders [kN]
- Advance speed [mm/min]
- Penetration rate [mm/rot]
- Cutterhead torque [MN·m]

All these parameters are measured during the tunnelling by means of sensors placed on the TBM.

5.4.1.1 Cutterhead rotation speed:

The cutterhead rotation speed represents the number of revolutions performed by the cutterhead during the tunnelling per unit of time. The unit is 1/min (rpm).

For the TBM S-1054 it can range between 0 rpm and 9 rpm, while for the TBM S-1071 and S-1072 it varies between 0 rpm and 5.1 rpm.

5.4.1.2 Thrust Force Advance of main cylinders

The Thrust Force Advance of cylinders is the total force applied by the advance cylinders to push the cutterhead against the rock. Generally, higher is the force and higher is the productivity, but also increases the wear of cutter tools. The thrust limit is controlled by the cutter type, maximum thrust capacity of the machine and TBM head design. (Villeneuve, 2017)

The maximum thrust force that can be applied by the advance cylinders of the TBM S-1054 is 57000 kN, while the other two machines analyzed have a maximum thrust force of 95000 kN. In

this research is considered the net total thrust, which is the only component of the total force that is used to push the cutterhead against the rock. Hence it is not considered the shear force component which is related with the shear between the shield and the rock mass.

5.4.1.3 Advance Speed

The Advance Speed is not a parameter strictly related to the TBM. Indeed, it depends on the mutual correlation between the thrust force imposed and the geologic characteristics found during the excavation. It measures the horizontal displacement per unit of time. The unit is mm/min.

The evaluation of the maximum advance speed is related to the maximum capacity of the buckets and to maximum capacity of the machine conveyor belt: if the productivity is too high with respect to the conveyor belt maximum capacity the entire system will be stopped.

The conveyance rate for TBM S-1054 is 800 t/h while the conveyance rate for TBM S-1071 and TBM S-1072 is 1200 t/h.

5.4.1.4 Penetration rate

The Penetration Rate expresses the horizontal displacement of the cutterhead per revolution of the cutterhead. It is not usually a parameter measured by the machine, but it can be easily calculated with the ratio between the Advance Speed and the Cutterhead Rotational Speed (equation below). The penetration limit is consequently a function of bucket design, cutter wear and the maximum cutterhead speed [rpm].

$$Penetration\ rate\ [\frac{mm}{revolution}] = \frac{Advance\ Speed\ [\frac{mm}{min}]}{Cutterhead\ Rotational\ Speed\ [\frac{revolutions}{min}]}$$

5.4.1.5 Cutterhead torque [MN·m]

The rotational power is generated by electric motors. The motors drive the common ring gear which in turn transmits the torque through the drive shaft, located in the center of the torque tube, to the cutterhead. (Askilsrud)

The cutterhead nominal Torque for the TBM S-1054 is 8597 kN·m, while for the TBM S-1071 and S-1072 the nominal Torque is 23934 kN·m.

5.5 CUTTER DISCS DESCRIPTION

This paragraph concerns a brief explanation about the general features of cutting tools used on hard rock TBM.

5.5.1 Failure mechanism

By the rolling of cutters on the tunnel face, if the thrust force is large enough the cutter disc edges can penetrate into the rock.

As the cutterhead rotates, the force on the individual cutter varies continuously: the peak load of individual cutters can be several times the average load. Therefore, the action of the cutter includes a percussive effect.

As the cutter rolls, three major failure mechanisms occur:

- Cracks are formed, penetrating radially into the rock from the cutter edge.
- Material under the cutter is crushed to a fine powder, of which some is compacted and left in the groove.
- Chipping of pieces takes place between the grooves.

The chipping between the grooves does not necessarily take place for each pass of the cutter. Depending on the rock, the thrust per cutter and the cutter spacing, it may take several cutterhead revolutions before the ridge between the groove's chips away. If the spacing between the grooves are too large, the stress pattern created may not reach the influence zone caused by adjacent cutters and this behavior will cause inefficient boring and low rate of penetration. On the other hand, if the spacing is too close or the cutter tip is too blunt, only small chips will form,

generally meaning inefficient boring and low overall rate of penetration. Furthermore, local weaknesses in the rock mass will influence the cutting, by allowing easier cracking or chipping, or by increasing the size of the pieces that break loose. The crack formation takes place radially from the cutter edge, into the rock or to the next groove, parallel to the high compressive stresses from the cutter edge. (Bruland & Blindheim)

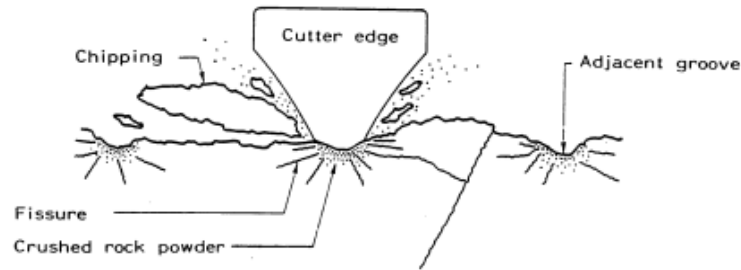


Figure 51 - Failure mechanism for disc cutters ("Boreability Testing", Blindeheim and Bruland)

5.5.2 Main parts of cutter discs

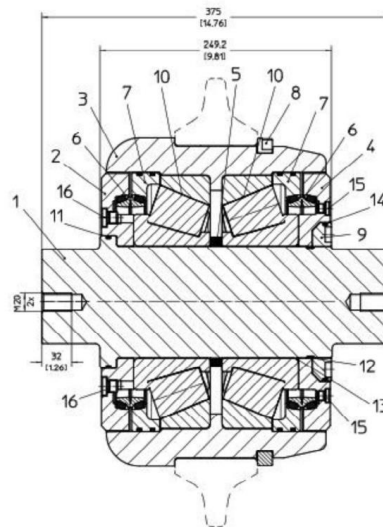


Figure 52 - Section of a cutter disc (Herrenknecht, 2021)

In the sketch above (Figure 52) is showed a section of the cutter used in this project. For the tracks 1-3, 2-4, 5-7 and 6-8 are used double rings cutters (Figure 53), while in the other tracks

are used single ring cutters. The main components that make up the cutter, with reference to the Figure 52 are:

- 1) Cutter Shaft
- 2) Cutter Retainer
- 3) Cutter Hub
- 8) Cutter Split Ring
- 10) Cutter Bearing
-) Cutter Ring (project dependent)



Figure 53 - Double ring cutter

5.5.3 Theoretical overview on wear mechanism of cutter ring and HRC influence:

One of the most important parameters to be considered during the cutter analysis is the hardness of the cutter ring; indeed, it generally influences the mechanical properties of the cutter ring.

According to a study carried out by Zhang et Al. based on laboratory tests on different cutter discs and lithologies, the wear mechanism of the cutter ring is mainly abrasive wear caused by hard particles sliding on the wear surface. The abrasive wear includes three typical wear mechanisms, namely micro cutting, furrow deformation and brittle fracture:

- Micro cutting: the material is cut away from the worn surface by abrasive particle
- Furrow deformation: the material is ploughed on both sides of the groove
- Brittle fracture: the material is detached from the worn surface due to micro cracks propagation and instant peeling.

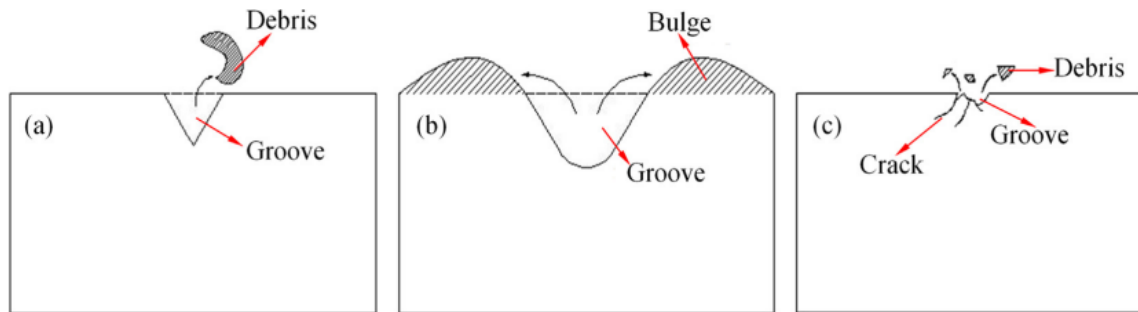


Figure 54 - Abrasive wear mechanism: a) Micro cutting; b) Furrow deformation; c) Brittle fracture. ("Experimental study on wear of TBM disc cutter rings with different kinds of hardness", Zhang et al., 2018)

According to study on the cutter wear carried on by Zhang (2018), in which are tested three cutter rings with different hardness (55.5 HRC, 56.5 HRC and 57.5 HRC) on hard rock (gneiss), shown:

- 55.5 HRC cutter ring: mechanism of wear is furrow deformation and severe micro cutting.
- 56.5 HRC mechanism of wear is mainly related to furrow deformation and micro cutting.
- 57.5 HRC phenomenon of micro cutting becomes very infrequent, and a large number of brittle fractures begin to appear.

Furthermore, always taking into account this experiment, in the following graph (Figure 55) is shown the wear loss for cutter ring tested on different geology. What is important for the Brenner project is the comparison between the hardness of cutter ring and the wear loss in the gneiss material. The hardness and the toughness of a cutter ring are related to the presence of carbon atom in the steel. The former, gives to the material the ability to resist mechanical indentation and it increases when the percentage of carbon atom raises up. The latter, indeed, is the ability of a material to absorb energy and plastically deform without fracturing: the toughness increases with the decrease of the carbon atom present in the steel. As it is visible in the Figure 55, for gneiss, the wear loss of the cutter ring first decreases and then increases with the increase of

hardness. This type of behavior can be explained because when the hardness is increased to 58.0 HRC, the impact toughness of the cutter ring decreases, leading to poor fracture resistance. Then, the wear mechanism of the cutter ring shows slight micro cutting and severe brittle fracturing due to the high vibration and drastic load caused by gneiss, which has high mechanical strength and large CAI of the rock types studied in this research, resulting in an increase in wear loss. Due to the presence of hard rock to be excavated, in particular for the last area excavated by the TBM S-1054 and partially by the S-1072 and will be excavated by the TBM S-1072, this behavior can be similar to what actually happens in the last part of the tunnelling. (Zhang, 2018)

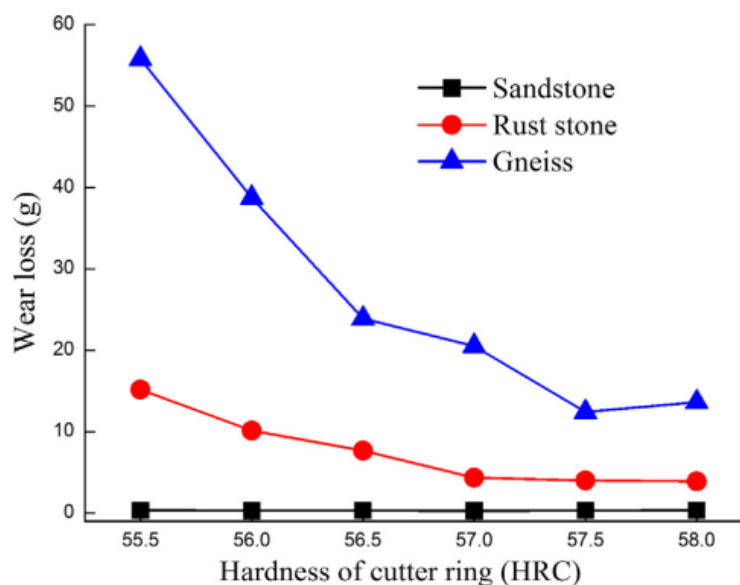


Figure 55 - Hardness of cutter ring ("Experimental study on wear of TBM disc cutter rings with different kinds of hardness", Zhang et al., 2018)

The type of discs which are/were used in this project are:

- HD-Standard: Toolsteel; HRC 55 - 57
- W15: X40 Material; HRC 55 - 57
- W19: X50 Material; HRC 56 – 59

Geometrically they are the same with 19" diameter and 16 mm of tip.

5.6 WEAR AND DAMAGE OF DISC CUTTERS

The cutter disc wear must be verified daily during the maintenance shift. The measurement of the wear is performed with a wear gauge (Figure 56)



Figure 56 - Wear gauge template for cutter ring wear measurement

The maximum wear for the center and face tracks is 30 mm while for the gauge tracks is ranging between 25 mm and 15 mm. In general, center cutters are subjected to a higher side force and skid force due to their low radius of rotation. Hence, the center cutter wear is allowed to be a bit more. Instead, the gauge cutters wear play an important role because if the gauge tools have a high absolute wear, the diameter of excavation will be reduced; indeed, to avoid this problem, they are subjected to more preventive substitutions.

The time needed for the disc replace is about 30 minutes to which must be added the time required for measurements of all discs wear and the decisions, hence are usually changed 10 discs per shift. However, the number of discs replaced and the possibility to change the disc is also related to the geology of the tunnel face for the crew safety work conditions.

In the following part are listed the main cutter wear types.

1) Normal wear



Figure 57 - Cutter normal wear (Herrenknecht, S-1054 TBM GL Brenner Basis Tunnel Lot 2-3 Mauls/Mules, 2017)

The normal wear of a disc refers to an even cutting ring wear with a specified wear degree along all the cutting ring. The wear degree can be measure with a template.

2) Clogging bearing



Figure 58 - Cutter clogging bearing (Herrenknecht, S-1054 TBM GL Brenner Basis Tunnel Lot 2-3 Mauls/Mules, 2017)

When the disc cutter is not rolling with the cutterhead rotation, the cutting ring is subjected to a unilateral wear due to the relative movement between the tunnel face and the cutting ring. In this case we can recognize a flat part in the cutting ring. It can be verified when the rock in the tunnel face has a too weak geo-mechanical properties.

3) Fissures or breakage at the cutting ring



Figure 59 - Cutting ring breakage

This type of wear is related to an excessive contact force between the tools and the tunnel face. It can be caused by rolling over too hard objects or a too high imposed thrust. If the cutting ring breaks at two positions, the complete cutting ring or some parts can get lost in the excavation chamber and the tunnelling will be suspended.

4) Chipping – parts of cutting ring broken



Figure 60 - Cutting ring chipping

The so called “chipping wear” is verified when individual pieces come off in fragments while the cutting ring as whole does not break, as shown in the picture. This typology of wear is usually related to a too high hardness of the cutter ring steel and, in general, it is related to the geology encountered during the tunnelling.

5) Mushrooming – severe deformation of the cutting ring



Figure 61 - Cutting ring mushrooming

If the working surface of the cutting wheel applied to the tunnel face broadens and is deformed to the outside in the form of a mushroom, as depicted in the figure (Figure 61), this is referred to a mushroom cutting ring. This wear usually happens when the steel hardness of the cutting ring is lower than the rock hardness.

6) Defective roller casing



Figure 62 - Defective roller casing

By over rolling metal, such as loss of cutting ring parts or screws, the casing can be destroyed or roller base body a lateral cover can get jammed and the disc cutter can no longer rotate about its own axis. This type of wear is shown by an uneven wear of the cutter ring more pronounced on one side of the cutting ring.

7) Circlipping - Lost or worn-out circlip



Figure 63 - Circlipping

The circlip is the part of the cutter which aim is to prevent the cutting ring from moving in parallel with the disc axis. When the circlip is heavy wear or lost, the disc cutter must be replaced.

8) Leaky disc cutter

The disc cutter can leak oil due to a defective sealing. The damage to the lateral cover or roller base body cannot be detected.

9) Preventive replacement

When a certain value of wear is reached, in particular for the gauge discs, the cutter disc must be replaced with a new one. It is very important to verify the wear of the gauge disc because if the wear is too high the tunnel diameter will decrease and could arise problems for the following tunnelling.

5.7 CUTTER DISCS REFURBISHMENT

The worn cutters are sent to the workshop for refurbishment. Upon arrival in the workshop, the cutters are thoroughly checked for further damages which are not detected on the job site, where only the cutter ring wear is measured. In the workshop, apart from the cutter ring, all worn out and damaged parts are replaced by new

parts.

The cutter refurbishment is not object of this thesis, thus the wear analysis presented in chapter 5.8.4 does not contain the information about additional damages detected during cutter refurbishment.

5.8 BACK ANALYSIS: GENERAL FEATURES

For each single portion of excavation with a length relative to one stroke, which is the width of a concrete segment (1.5 m for the TBM S-1054 and 1.75 m for the TBM S-1071 and S-1072), have the recorded average parameters that are interested in this research been downloaded from the TBM database: Cutting wheel Torque, Cutting wheel Rotation Speed, Total Thrust Force and Penetration. The last parameter involved in this study, the Advance speed [mm/min], is instead a parameter derived from the mathematical division between the Penetration and the Cutting wheel Rotation Speed. It was then evaluated the average value of the machine parameters for each single production shift analyzed in this research.

Subsequently, each average machine parameter has been correlated with the wear measured for the relative portion of excavation and it was computed an average cutter ring wear value for each excavation shift.

In this thesis the specific wear is expressed in mm of wear per meter of circumference traveled by the cutter tool on the excavation face. The specific wear value can also be expressed in other different ways, such as, for example, the mm of wear relating to a cubic meter of material excavated or the milligrams of weight lost by the cutter relative to the unit of volume excavated. However, these different ways express the same wear value, and they can be calculated later, arranging the results obtained in this research according to the use requested.

5.8.1 Mechanical Parameters analysis

In this paragraph are analyzed the machine parameters used in each geology. For each different geology are reported the graphs regarding the average machine parameter regarding each excavation shift, with reference to the tunnelmeter achieved. The red line is mean of the parameters reported in each graph.

5.8.1.1 *Paragneiss*

This geology is relative to the first type of rock crossed by the TBMs. From a geo-mechanical point of view, the Paragneiss lithology is characterized by a high specific weight and a low Uniaxial Compressive Strength of 72 MPa; while, regarding the rock mass properties, it can be classified as a fair rock mass, blocky and with an altered and weathered surface, according to the RMR and GSI rate selected during the excavation.

For this geology are analyzed the data relative to the chainage from 13200 m to 13500 m for the TBM S-1054 and from 46200 m to 45800 m for TMB S-1071 and S-1072, for a total of 1100 meters examined.

In the following figure (Figure 64) are shown the machine parameters chosen during the excavation. The torque is in general lower for the TBM S-1054 with respect to the TBM S-1071 and S-1072 due to the smaller diameter of the cutterhead. It is ranging in between 0.3 MNm and 1 MNm for the S-1054 and 1 MNm and 4 for the other two TBM. The cutting wheel rotation speed is almost independent on the TBM and the values are ranging between 1.5 rpm and 5 rpm. The thrust force is another parameter strongly dependent on the TBM diameter, and as we can see on the third row of the graph below (Figure 64), it is almost the double for the two larger machines with respect to the smaller one, reaching some peaks of more than 16000 kN. Concerning the penetration and the advance speed, due to the lack of data recorded, it is not possible to perform an analysis on the two twin TBM but only on the S-1054. The Penetration is thus ranging between 4 and 10 mm for each cutterhead rotation while the advance speed reaches some peak values over 40 mm/min. It is interesting to mention that in this geology not always a high value of penetration means a high advance speed, which is, at the end, the excavation production.

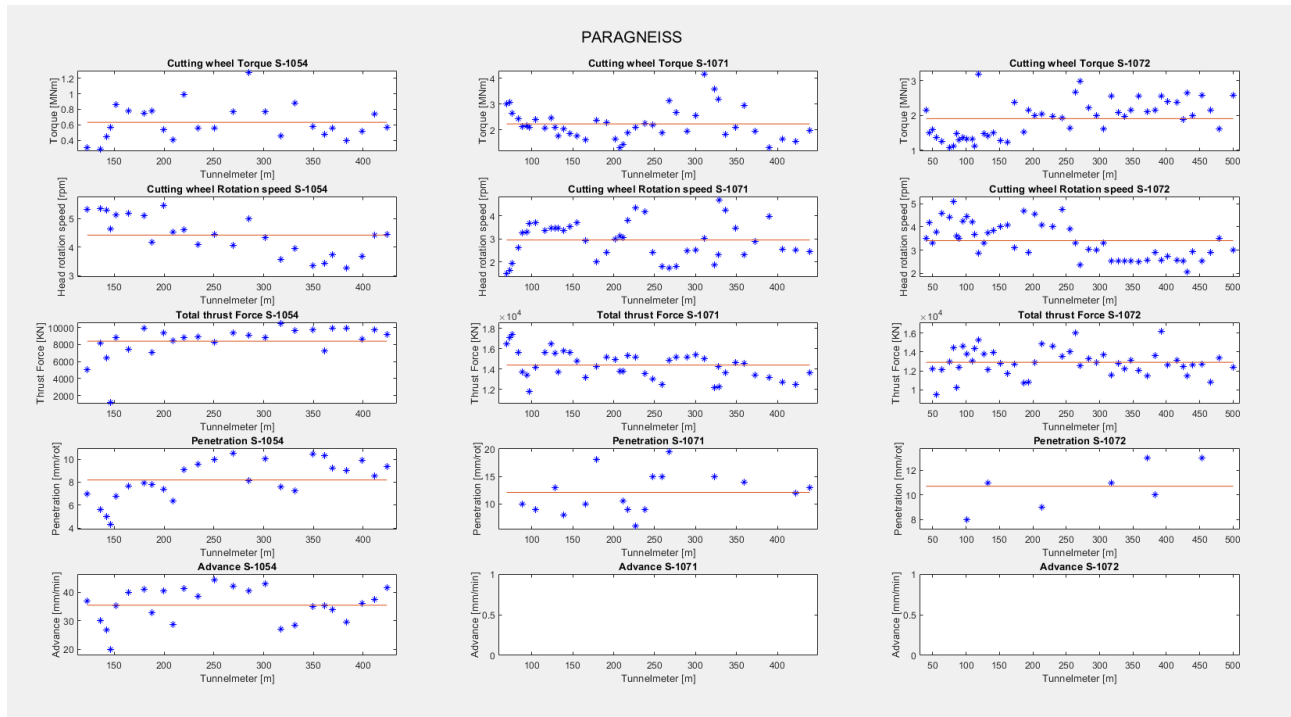


Figure 64 - Machine parameter recorded during the tunnelling in Paragneiss

5.8.1.2 Amphibolite

The second geology analyzed is the Amphibolite. It is represented by a high specific weight of 28 kN/m³, a quite high UCS of 140 MPa and a CAI index of 4.3. The rock mass properties are slightly better than the geology previously described with a RMR value of 65 and a GSI value of 55. The problems on the analysis of this section are related to the small amount of data; in fact, the total length analyzed is almost 300 and hence the total amount of data is relative to less than 30 production shifts. However, the Amphibolite has been also selected in this analysis due to the homogeneous and interesting geo-mechanical characteristics.

Also in this case the torque and the total thrust force are dependent on the machine diameter while cutting wheel rotation speed, the penetration and the advance speed are not strongly correlated to the TBM dimension. Additionally, as previously described for the Paragneiss geology, due to the lack of recorded data for the penetration in the TBM S-1071 and S-1072 is not possible to perform a statistical analysis based on these two parameters. The values are reported on the graphs collected below (Figure 65)

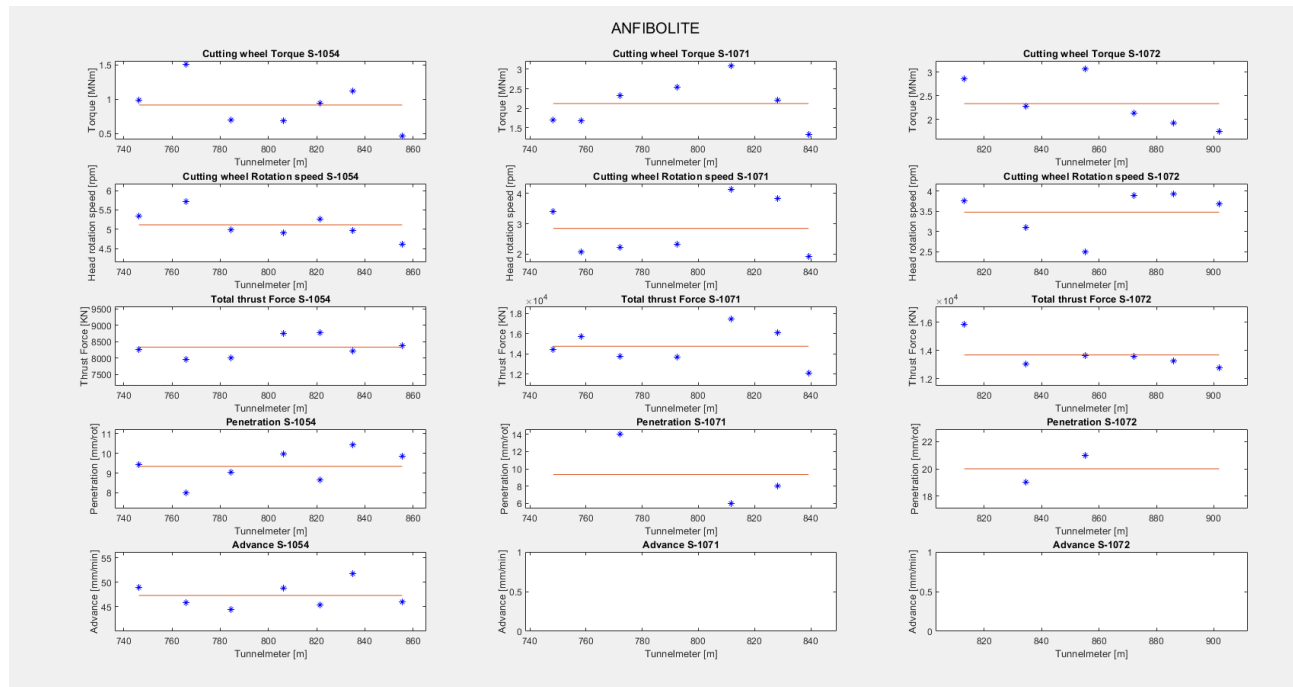


Figure 65 - Machine parameter recorded during the tunnelling in Amphibolite

5.8.1.3 Metabasalts

The Metabasalts encountered in this project is characterized by a high CAI value and a very low rate regarding the rock mass properties: 50 for the Rock Mass Rating and 40 for the Geological Strength Index, which represent a rock mass with many intersecting discontinuities sets and fair surface quality.

The total length analyzed for this type of geology is subdivide into three sectors for the TBM S-1054, between the project chainage 18500 and the project chainage 19600, and two sectors for the S-1071 and S-1072 tunnel in the range of 40750 and 35800 with reference to the project chainage. The overall length examined is almost 1800 m.

In this lithology all the data are available, and it was thus possible to perform a complete analysis even for the penetration and the advance speed parameters for the S-1071 and S-1072.

The torque and the total thrust are also in this case dependent on the TBM diameter and similarly the cutting wheel rotation speed is higher for the S-1054 with respect to the other two machines: the former has an average rotation speed of almost 6 rpm while the latter shows an average rotation speed of almost 5 rpm.

Regarding the penetration and advance speed, they look like independent on the TBM and they range between 2 mm/rot and 10 mm/rot in the case of the penetration and 20 mm/min and 40 mm/min for the case of the advance speed. Furthermore, these two parameters are generally correlated, which means that, for this lithology, a low penetration value matches, in general, with a low value in advance speed.

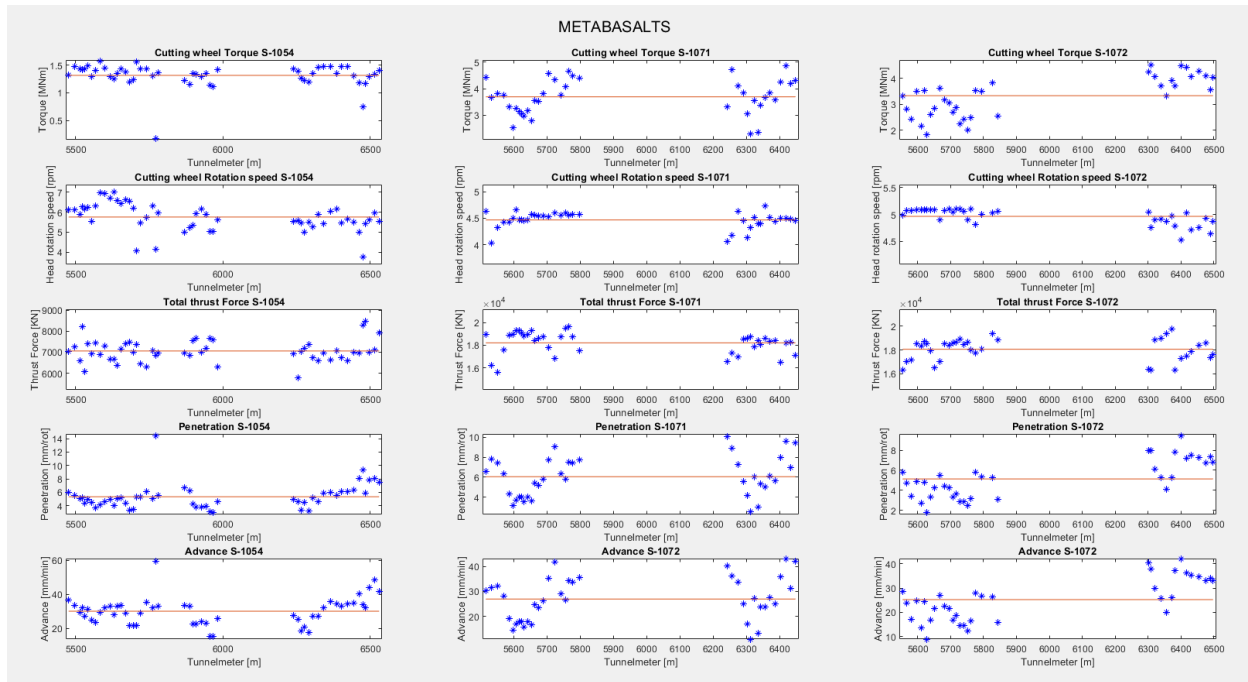


Figure 66 - Machine parameter recorded during the tunnelling in Metabasalts

5.8.1.4 Calcschists

The tunnelling in this section is characterized by very long advances per shift, reaching also more than 30 m per shift. This performance is thanks to the good rock properties for the excavation purpose. The UCS and the CAI are respectively 100 MPa and 2, which are low values with respect to the other geologies before analyzed. Regarding the rock mass properties, this lithology has been evaluated with 55 for both the RMR and the GSI classification. That means a fair quality rock mass with a fracturing grade that helped to improve the excavation in this area.

Also in this case the back analysis has been carried out in the most homogeneous sectors: are analyzed 3150 m of total excavation, ranging between the project chainage 19700 m and 20850

for the exploratory tunnel and between the project chainage 39600 and 38000 for the two twin tubes.

For the parameters analysis it is recognizable the dependance of the torque and the thrust force on the TBM diameter. The former parameter is higher than the other geology analyzed, while the latter is lower; in the figure below are shown the values depending on the excavation shift (Figure 67). The cutting wheel rotation speed is almost constant and the mean value is nearly 5 rpm. There is then a good correlation between the penetration and the advance speed and, as explained before, the values are relatively high.

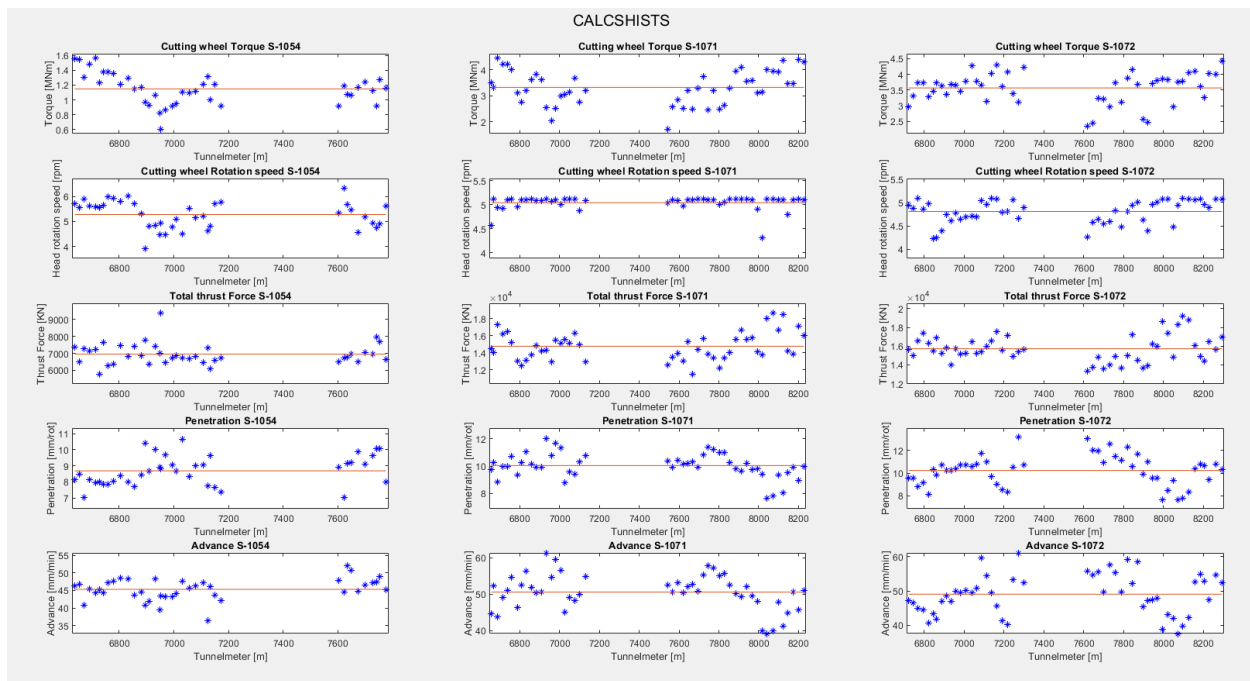


Figure 67 - Machine parameter recorded during the tunnelling in Calcschist

5.8.1.5 *Gneiss*

The last geology examined in this thesis is the Gneiss. At this moment, it has been excavated for the whole length by the TBM S-1054 and for a partial length by the TBM S-1072. According to the geology forecast, the TBM S-1071 should encounter this geology in the next period. Due to this issue, the only data recorded are provided by the TBM S-1054 and S-1072. However, this geology is related to the nucleus of the Tauri window and therefore it is very persistent. In fact, it has been possible to analyze the last 3200 m of excavation for the TBM S-1054 and around 850 m of excavation for the TBM S-1072. Furthermore, due to the high value of UCS (220 MPa) and CAI (5.0), and due to the very good rock mass quality, the advances per shift are very short and hence there are many data collected on which is possible to carry out the analysis.

Regarding the machine parameters recorded during the tunnelling, the torque has a relative low value with respect to the other geology: the mean is almost 1 MNm for the TBM S-1054 and 2.8 MNm for the S-1072. On the contrary, the thrust force applied is the highest among the geologies analyzed, due to the high Uniaxial Compressive Strength and the rock mass quality: the average values are 8000 kN for the small diameter TBM and 16000 kN for the big diameter TBM. The cutting wheel rotation speed is, also in this case, as happened for the other lithologies examined previously, almost constant and with an average value of 6 rpm and 4.7 rpm respectively for the S-1054 and S-1072. Furthermore, due to the good geo-mechanical properties, the penetration and the advance speed are quite low, with an average value of respectively 4 mm/rot and 23 mm/min, not dependent on the TBM dimension.

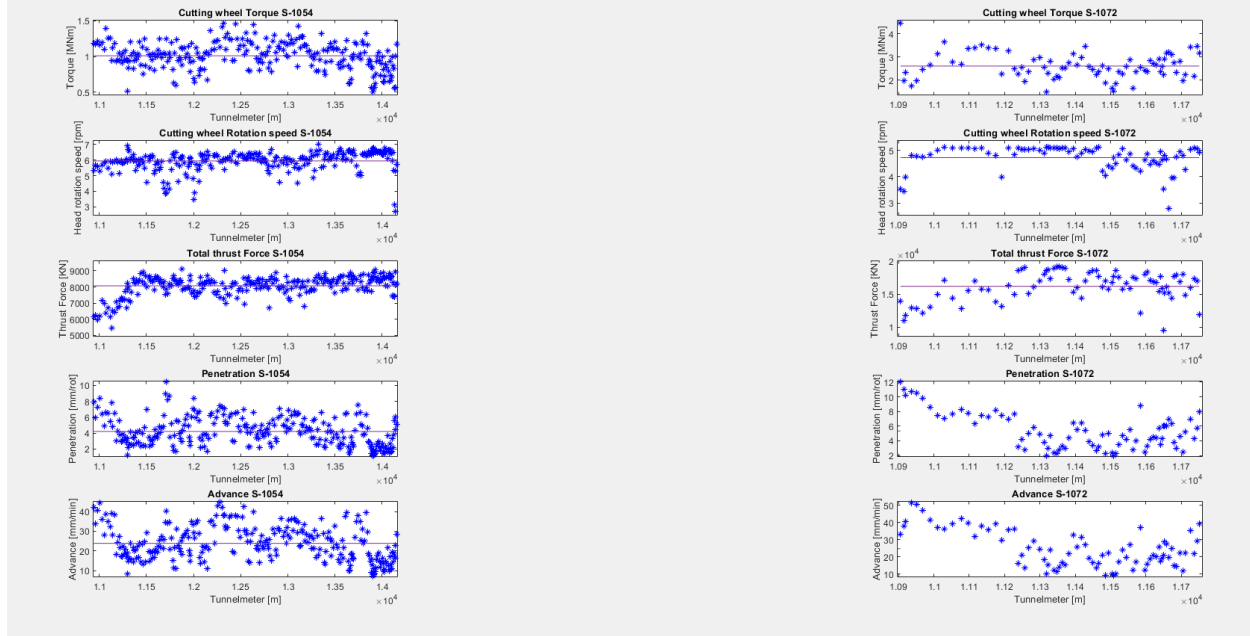


Figure 68 - machine parameter recorded during the tunnelling in Gneiss

5.8.2 Wear analysis – dependance on the machine parameters

In this part are shown the graphs representing the dependance of the cutter ring wear on the machine parameters.

The wear is always expresses in millimeters of cutter ring worn per meter traveled by the tool on the tunnel face [mm/m].

5.8.2.1 Torque vs Specific Wear

The first parameter examined is the torque. It is not properly a parameter chosen by the TBM driver operator and hence it depends on the mutual correlation of the other parameters chosen.

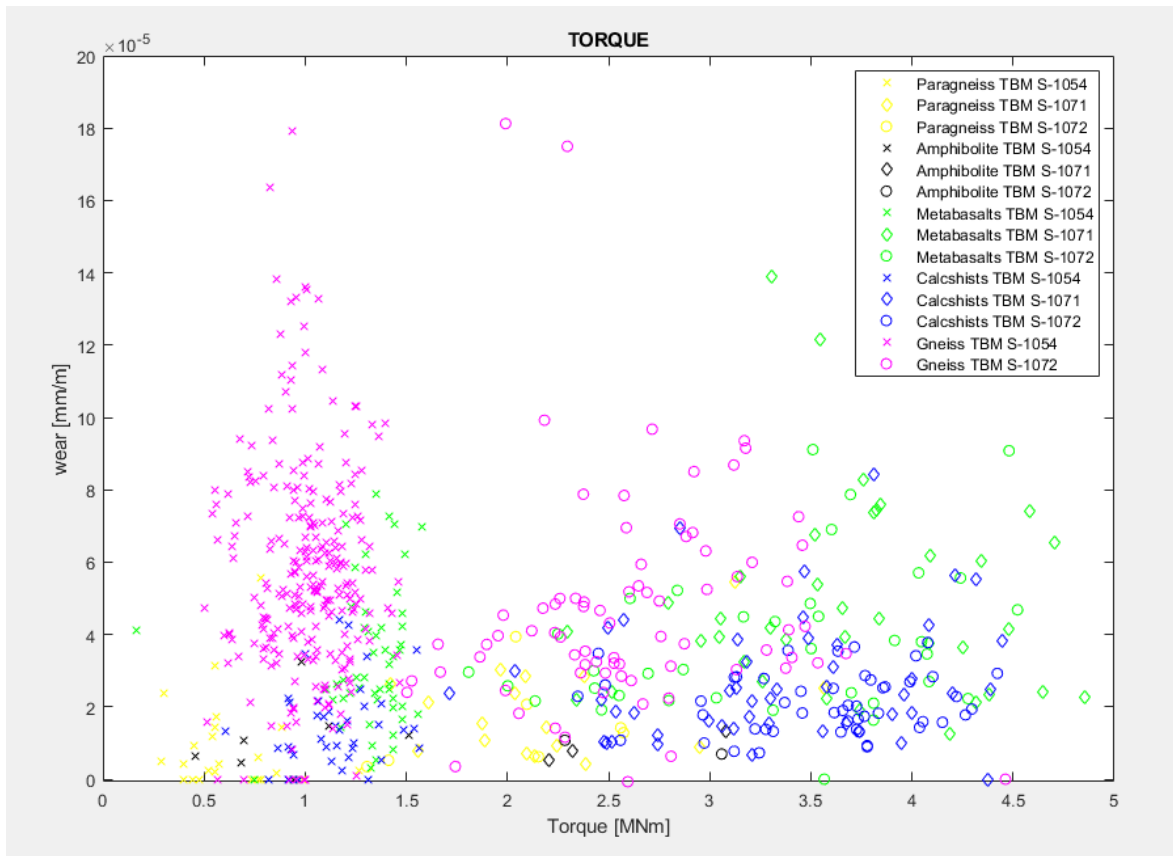


Figure 69 - Cutter ring wear [mm/m] vs torque [MNm] depending on the TBM and the geology

The torque, as already explained previously, depends on the TBM diameter. Therefore, in the figure above (Figure 69), are distinguishable two different clouds of points: the first, closer to the x axis origin, which is formed by the S-1054 data while the second cloud is related to the S-1071 and S-1072 data. In general, considering each different geology, for each value of torque the range of wear is the same and hence it is not clearly visible any correlation between the torque and the cutter discs wear. The different combination between geology analyzed and TBM are described in the legend.

5.8.2.2 Total Net Thrust Force vs Specific Wear

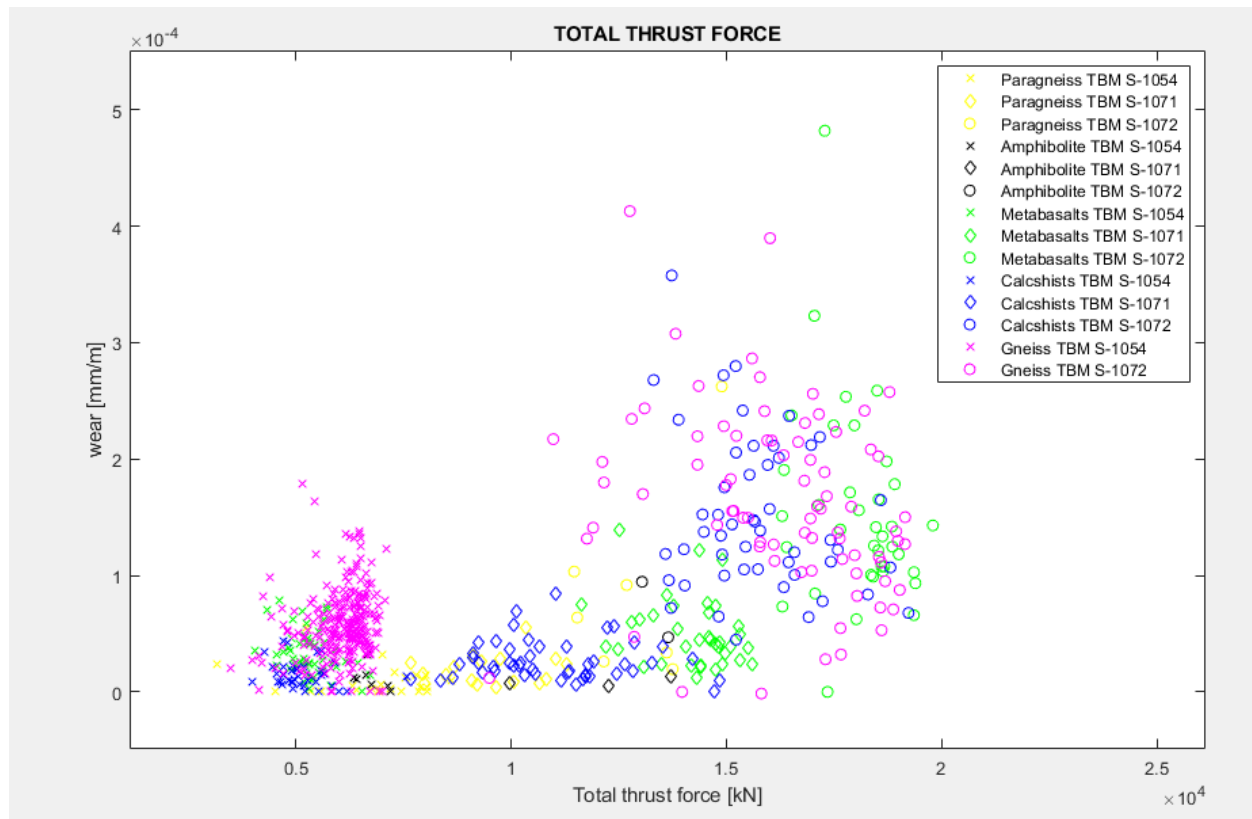


Figure 70 - Cutter ring wear [mm/m] vs total thrust force [kN] depending on the TBM and the geology

The second machine parameter which has been related to the wear is the total thrust force. The total thrust which is used for the computation of this analysis is relative at the net force used to push the cutter tools into the rock, hence not considering the shear force between the shield and the rock. It is the so-called cutterhead contact force. Not having the possibility on this TBM to directly measure the value of the contact force on the cutterhead, the net force has been calculated as the total thrust force applied by the cylinders minus the thrust force needed to bring back the TBM in contact with the tunnel face after the maintenance shift. For each lithologies has been evaluated the correspondent rate of shear force and the values are here reported.

	TBM S-1054	TBM S-1071 / TBM S-1072
Shear force Paragneiss (kN)	2000	4500
Shear force Amphibolite (kN)	1800	3800
Shear force Metabasalts (kN)	1800	4000
Shear force Calcschists (kN)	1600	3500
Shear force Gneiss (kN)	1900	4000

Also in this case, the total thrust force applied during the tunnelling is dependent on the TBM cutterhead surface and thus there are two different clouds of data. The first cloud, which is related to the smaller force applied, is about the TBM S-1054, while the other data, represented by the diamond or circle points, are given by the association between the wear and the thrust force applied on the other two machines. Even in this case, it is not recognizable a very distinct correlation between the wear the machine parameter analyzed. However, regardless to some outlier data related to the excavation in the Gneiss geology, the higher values of specific wear are generally related to a high total thrust force applied: this is mainly valid for the TBM S-1072 and S-1071.

5.8.2.3 Cutting Wheel Rotation Speed vs Specific Wear

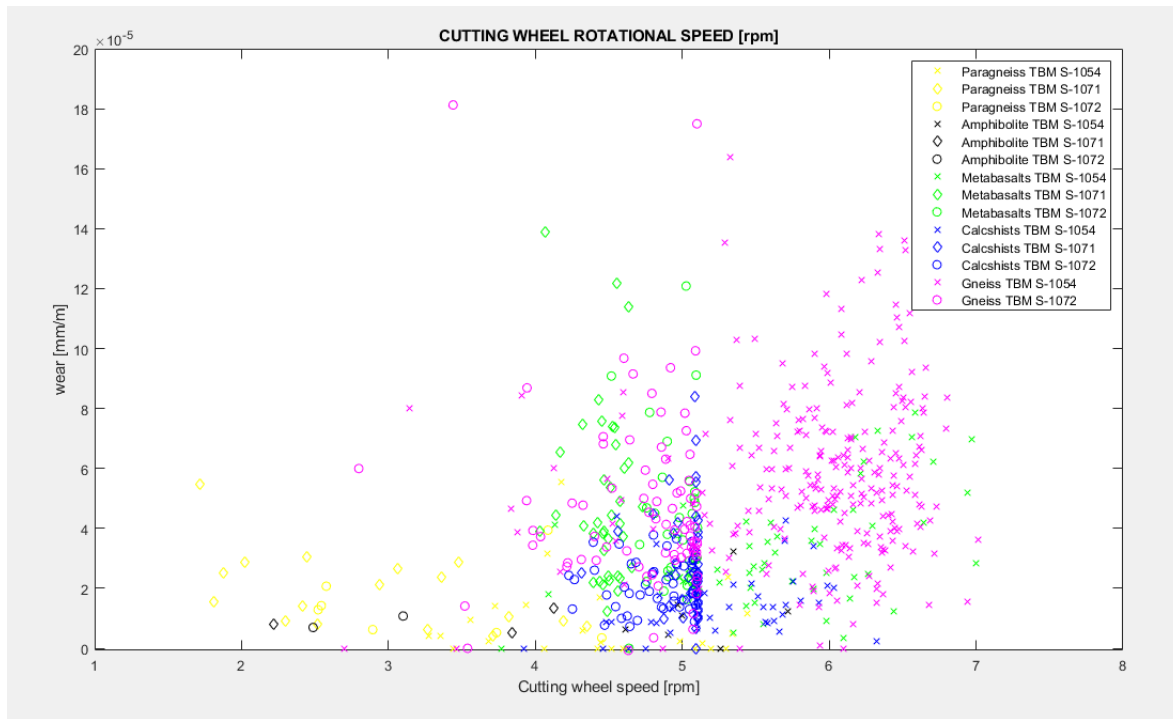


Figure 71 - Cutter ring wear [mm/m] vs cutting wheel rotational speed [rpm] depending on the TBM and the geology

The third parameter plotted is the cutting wheel rotation speed. The graph above (Figure 71) shows higher values of rotation speed [rpm] for the smaller TBM, but they are generally of the same order of magnitude.

During the tunnelling in the Calcschist, the cutting wheel rotational speed was kept almost constant and hence it is not interesting to analyze the dependance of the specific cutter ring deterioration on this parameter for the Calcschist geology.

Instead, regarding the other geology, in particular for the Gneiss and the Metabasalts where there are many data available, it is slightly visible an increase of wear with the increasing of the cutting wheel rotational speed. For example, considering the Gneiss geology, the maximum wear for the TBM S-1054 is almost 5 mm/m for a cutting wheel rotation speed of 5 rpm and it is almost 14 mm/m for a rotation speed of 6.5 rpm. However, also in this graph there are some outliers: for the Gneiss geology, there are some high wear values for slow rotation of the cutterhead and some low small values of specific wear for fast rotation speed.

5.8.2.4 Penetration vs Specific Wear

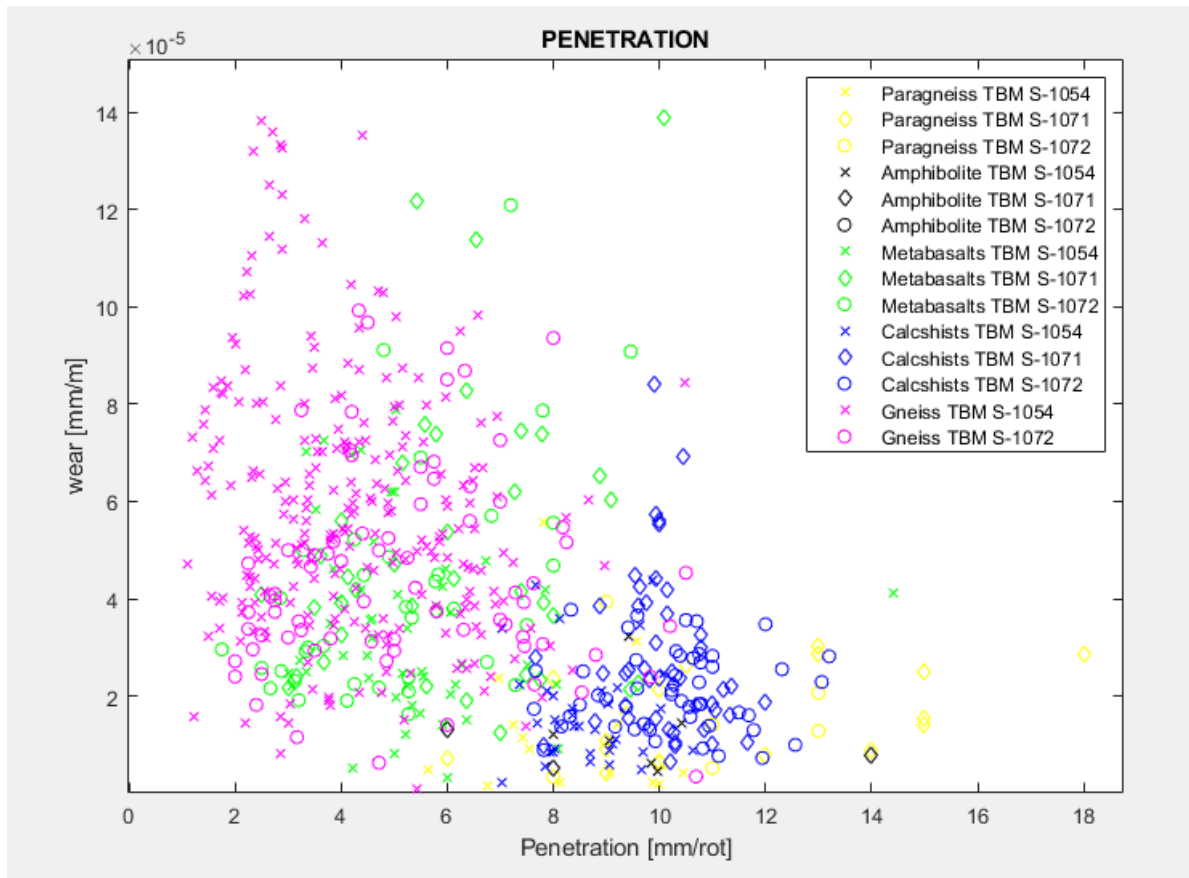


Figure 72 - Cutter ring wear [mm/m] vs penetration [mm/rot] depending on the TBM and the geology

In the figure above (Figure 72) is reported the graph which relates the specific cutter ring wear with the penetration [mm/rot]. Despite some outlier data are present also in this case, there is a general reduction in specific wear when the penetration increases. This behavior can be explained with the fact that the best rock properties for the excavation (low UCS) coincide with a very low Cerchar Abrasiveness Index in the geologies analyzed in this research. Thus, that means that a rock mass which is easily excavated will be also less wearing for the tools. This type of cloud shape is recognizable for the Gneiss and Metabasalts geology group, even if the densest part of the cloud is ranging in the same interval for each different penetration value. On the other hand, a hard, massive and abrasive rock mass, excavated with a high thrust force and low penetration rates, lead to increasing cutter wear due to the fact that the cutters are required to

do more rotations in the abrasive material in order to excavate the same tunnel length compared to a rock mass which is equally abrasive but less compact and which is therefore excavated with higher penetration rates.

5.8.2.5 Advance speed vs Specific Wear

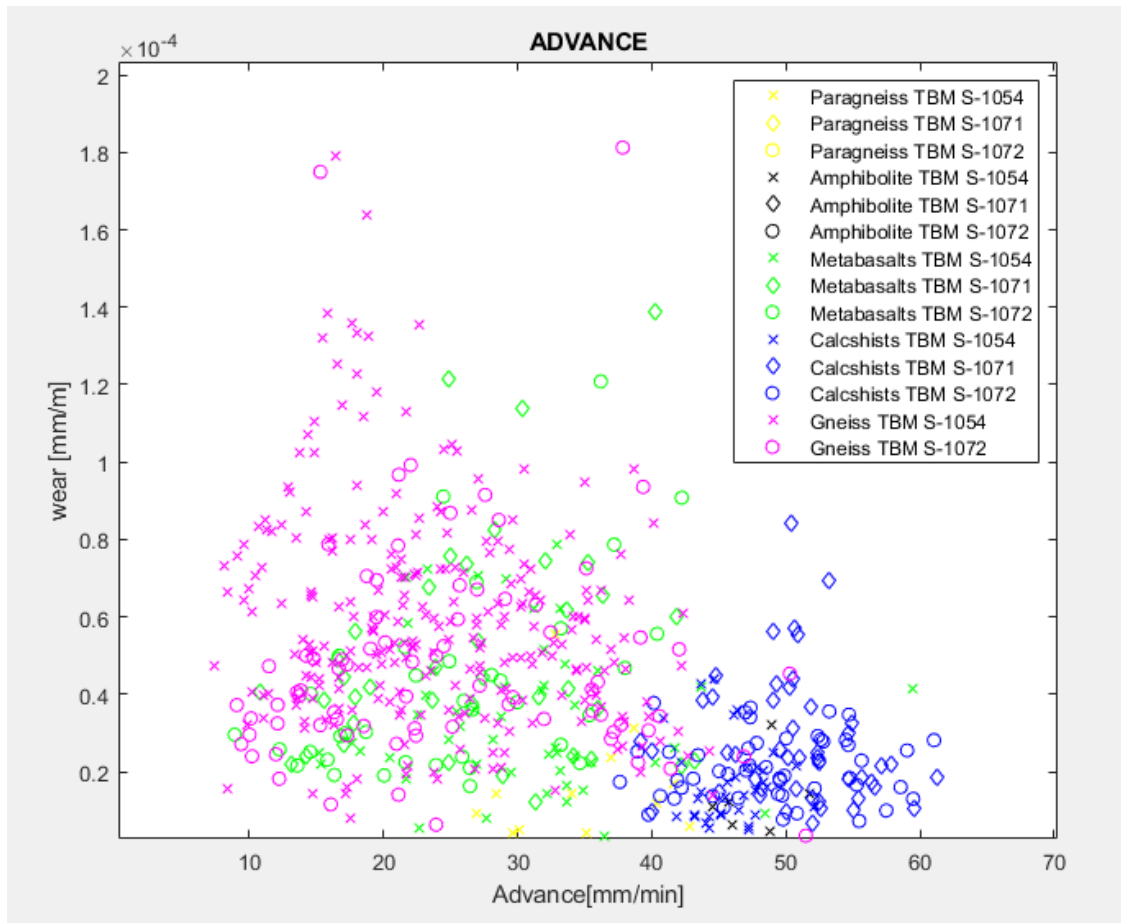


Figure 73 - Cutter ring wear [mm/m] vs advance speed [mm/min] depending on the TBM and the geology

The last parameter correlated with the specific cutter ring wear is the Advance speed [mm/min]. As previously said, the advance speed is given by the correlation between the penetration and the cutterhead rotation speed. Therefore, for the Calcschist, where the cutting wheel rotational speed is almost constant, the cloud shape is the same of what found in the Figure 73 and the

specific wear is quite independent on the advance speed. Then, for the Gneiss, it is recognizable a decrease of specific wear when the advance speed raises up, while for the Metabasalts is visible a opposite behavior, because the specific wear increases when the advance speed became greater.

5.8.3 Analysis on the cutter ring specific wear per each track

In this paragraph is examined the specific wear of the cutter ring, always expressed in mm/m, as a function of the track on which the tool is placed. The data analyzed are, as done before, the difference of the cutter ring diameter measured in two following maintenance shifts. As previously said, due to the lack of recorded data regarding the penetration in the Paragneiss and Amphibolite for the TBM S-1071 and S-1072, it is not possible to get this type of specific wear for these two geologies. In addition, always regarding those two lithologies, from the analysis carried out on the data available from the TBM S-1054 we have an almost constant specific wear. However, those graphs could be not completely reliable because the amount of data is very low and thus some cutter tools could be change after the overcome of the geological section.

The study is much more interesting for the other geologies, because it is appreciable an higher specific cutter ring wear for the external track of the cutterhead with respect to the internal tracks. It is interesting because the way on which the wear is evaluated is completely independent on the position of the cutter tool in the cutterhead (track number) because the millimeters of wear are normalized on the distance travelled by each disc during the production shift. Thus, the increase of cutter wear, which is visible in the Figure 74 for the Metabasalt, the Gneiss and the Calcschist is actually an increase of the specific cutter ring wear. This increase involves in particular the tracks from 31st to 36th in the S-1054 and from 53rd to 58th in the S-1071 and S-1072 TBM. On the contrary, for the gauge tracks there is a further decrease in specific wear until to reach the same wear value of the central cutter for the most external track (41st for the S-1054 and 65th for S-1071/S-1072).

This bell shape behavior could be explained with be the fact that, in order to keep the same cross section during the tunnelling, the external cutters are the most changed and the fresh

refurbished cutter tool generally wears less than an old cutter ring. Furthermore, as visible on the Figure 45 and Figure 46, the discs mounted on the external tracks are not working perpendicular to the tunnel face, but they work with a certain inclination with respect to the advance axis and, therefore, the wear is probably more pronounced on the side of the tip pushed towards the rock. However, being the template used to check the wear able to work only in a vertical position, it is not possible to evaluate properly the cutter ring wear.

In addition, in the 1st track of the three last geologies analyzed there is a peak of specific wear; it is because the circumference travelled per each round of the cutterhead is very short (0.5 meters for each round) and hence, even a small wear detected (1 mm) increases a lot the specific wear of that track. Nevertheless, due to the by hand procedure used to get the diameter, this peak of specific wear can be seen as a “technical error”, due to the sensibility of the template (1mm), the operator accuracy and the diameter of the track.

Moreover, it is interesting to analyze the different order of magnitude of the specific wear related to the different geologies. For the Calcschist, Paragneiss and Amphibolite the wear is in the order of 10^{-5} mm/m while in the case of Metabasalt and Gneiss the wear is higher, in the order of 10^{-4} mm/m. Indeed, the first geological group above mentioned is represented by some type of rocks with better mechanical and petrochemical properties from the excavation point of view, while the second group shows a high Uniaxial Compressive Strength and Cerchar Abrasiveness Index.

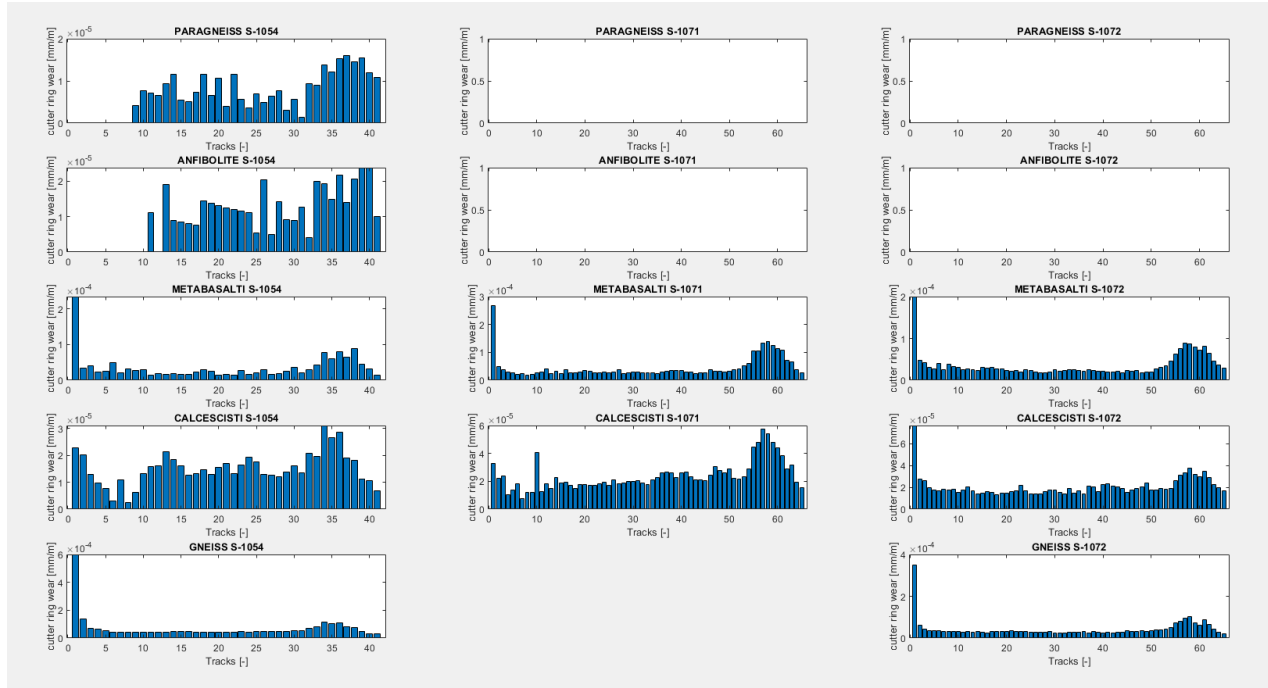


Figure 74 - Cutter ring wear [mm/m] depending on the track for each TBM and each geology

5.8.4 Analysis on the type of wear and damage

From the data collected along the time it is also possible to perform an analysis on the type of wear that interested the cutter tools in each different geology crossed. This analysis is related to the reason of the tool change and to the frequency of changes; the frequency is expressed in number of changes per unit volume of excavated rock [substitutions/m³]. Due to the very small values obtained, in the graph are reported the values related to the number of tool substitutions per 1000 m³ excavated.

For each different geology are reported two graphs: the pie chart which displays the percentage of the typology of disc replace and the bar graph which is indeed related to the frequency of changes. One thousand cubic meter excavated means a tunnelling length of 27.5 m for the S-1054 and a tunnelling length of 11.3 m for the S-1071 and S-1072.

5.8.4.1 Type of wear and damage – Paragneiss

In the Paragneiss geology, most of the disc are replaced due to the preventive substitution (86%) and the normal wear of the cutter ring (11%). The other types of replacement are irrelevant

because the amount of change is very small. However, these data are provided by the operator inspection, and in the case of the first geology overcome, the workers' knowledge about the cutter ring wear was possibly not enough to collect this type of data successfully. For this reason, some preventive replaces, or some normal wear damage could be belonged to some other damage classes.

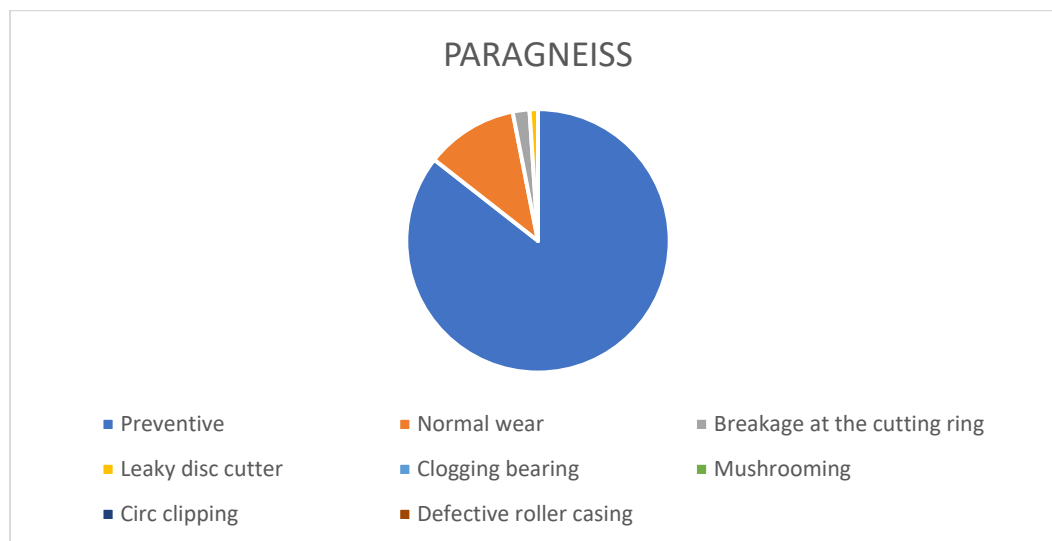


Figure 75 – Disc replacement causes during the tunnelling in the Paragneiss

The total amount of replacements is 1.78 substitutions/1000 m³. It is subdivide as shown in the following graph (Figure 76). The preventive replacements are in the order of 1.5 substitutions/1000 m³ and the remaining substitutions are mainly related to the normal wear.

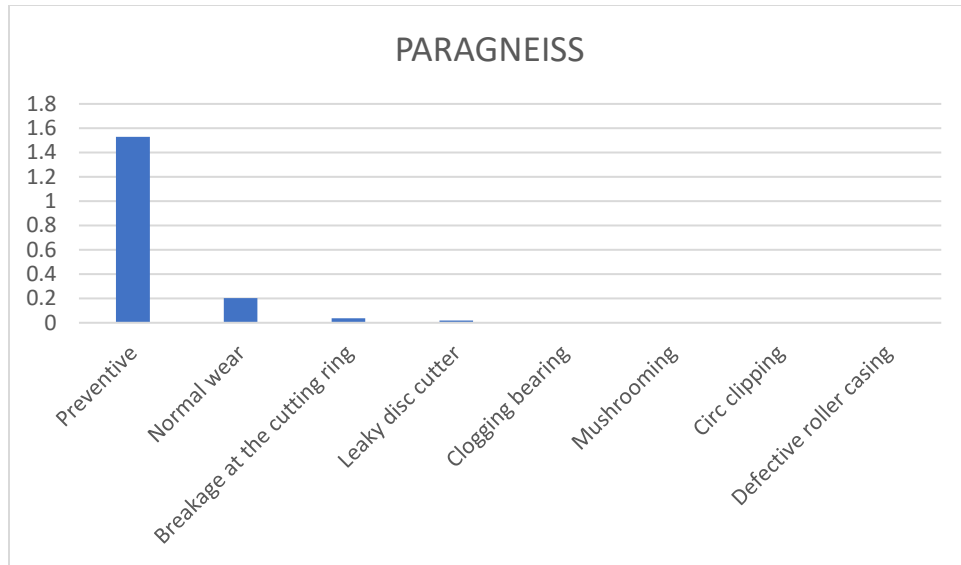


Figure 76 - Different frequencies of cutter tools substitution related to the excavation in Paragneiss

5.8.4.2 Type of wear and damage – Amphibolite

As already explained previously, regarding the second geology analyzed, due to the small quantity of data the analysis could be not very effective. However, most of the replacements are due to preventive interventions (78%), normal wear (17%) and breakage at the cutter ring (5%).

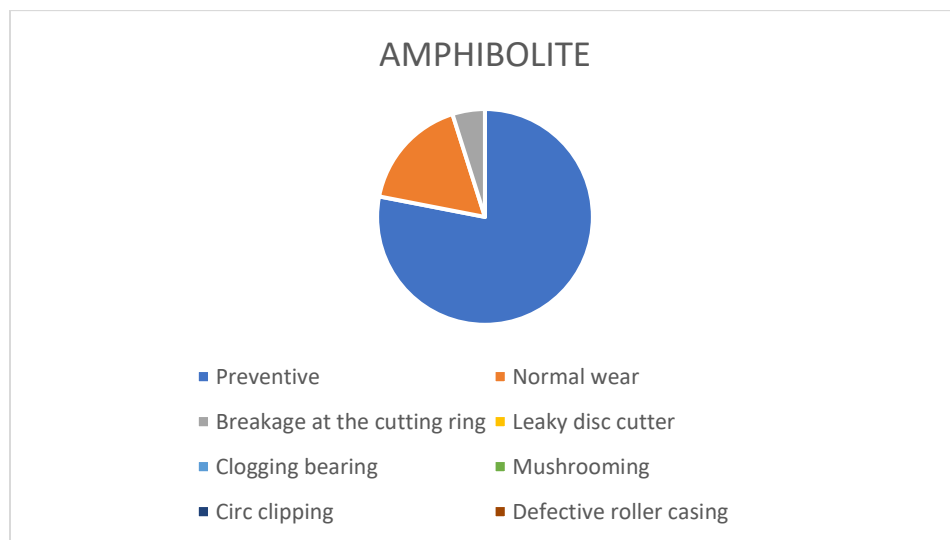


Figure 77 – Disc replacement causes during the tunnelling in the Amphibolite

Concerning the frequencies of changes, it is detectable a total amount of replacements for each 1000 m³ of excavation which is comparable with the Paragneiss (1.77 replaces/1000 m³). In the following graph (Figure 78) is reported the number of changes for each 1000 m³ excavated, depending on the typology of replacement.

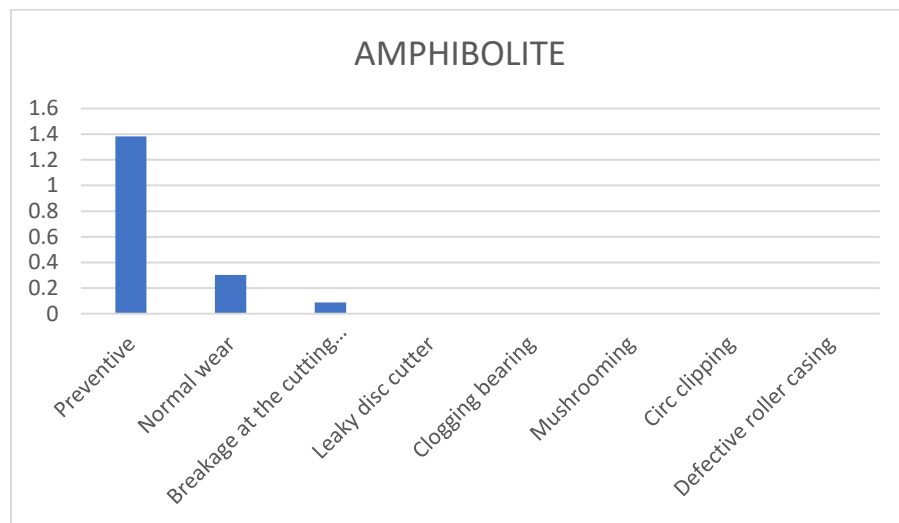


Figure 78 - Different frequencies of cutter tools substitution related to the excavation in Amphibolite

5.8.4.3 Type of wear and damage – Metabasalts

Thanks to the high amount of data available for this geological section and the later period of data collection, giving the necessary time for the workers training for the recognition the different typologies of cutter ring wear, we have a much more diversified type of wear. The preventive replacement and the normal wear are the main reason of cutter tool substitution, but in the Metabasalts, there is a significant number of changes due to clogging bearing (6%), leaky disc cutter (2%) and breakage at the cutter ring (4%).

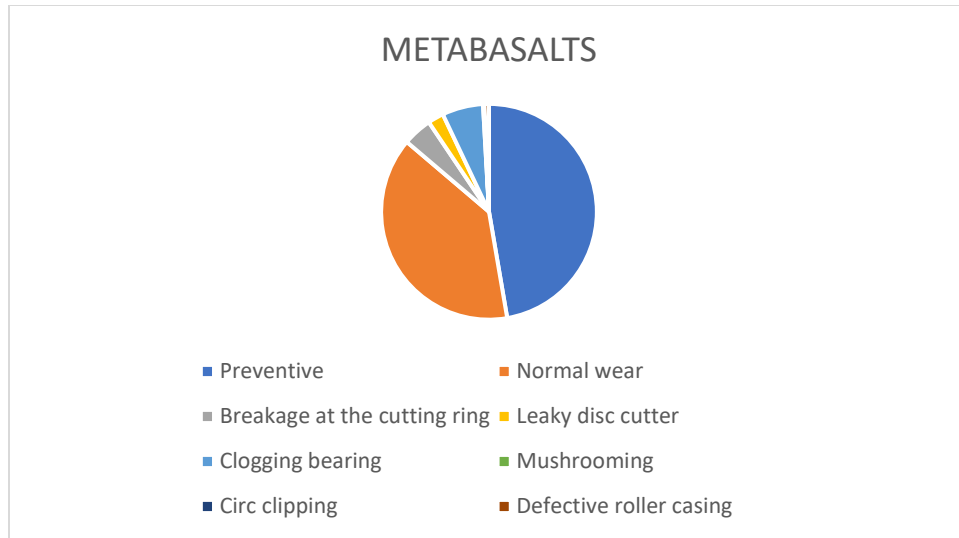


Figure 79 – Disc replacement causes during the tunnelling in the Metabasalts

The overall cutter disc replacement is 11.38 changes/1000 m³ and the different type of changes are reported in the following graph (Figure 80). Due to the higher UCS and CAI with respect to the lithologies previously analyzed, the number of tool replacements is significantly greater.

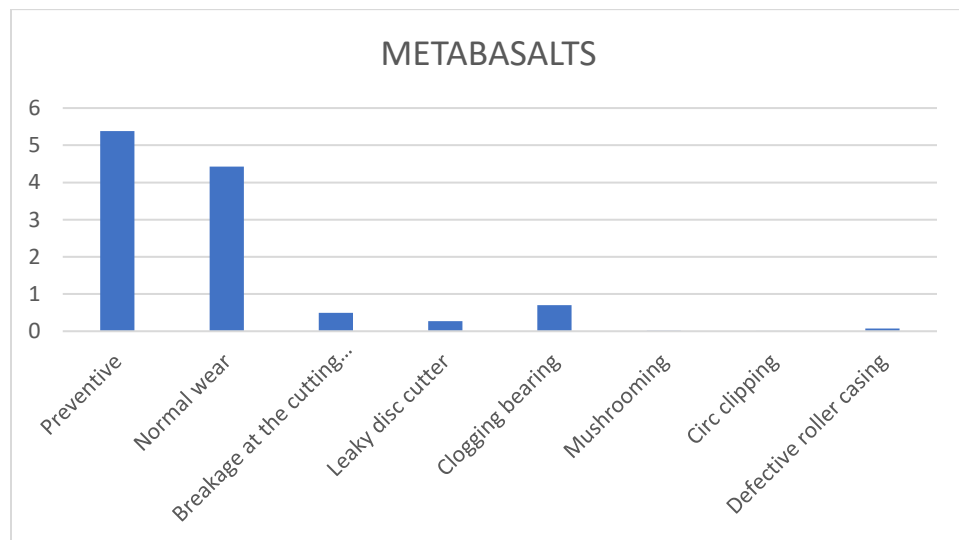


Figure 80 - Different frequencies of cutter tools substitution related to the excavation in Metabasalts

5.8.4.4 Type of wear and damage – Calcschists

In this case the 47% of the total changes are due to preventive replacement, the 43% to a normal wear and the remaining changes are due to other types of damage almost in the same percentage (2/3 %).

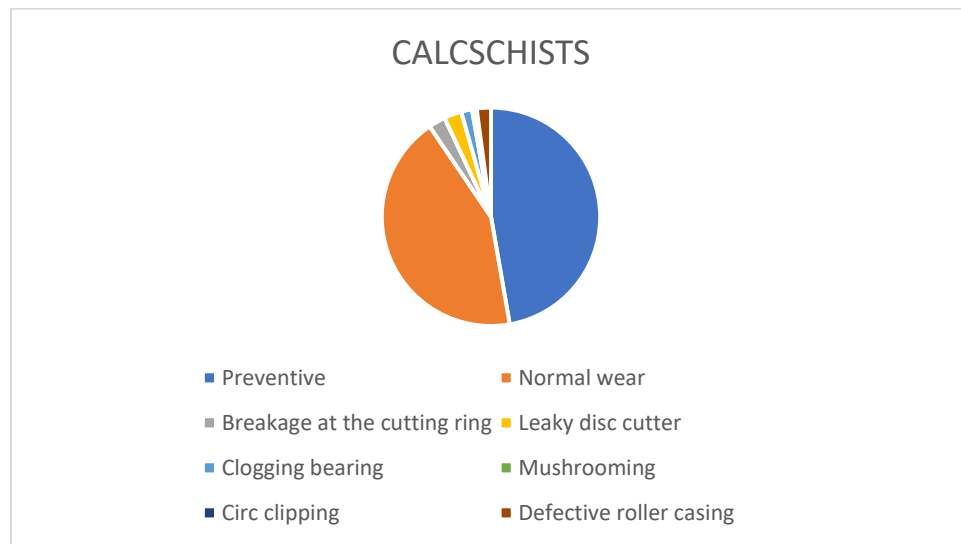


Figure 81 – Disc replacement causes during the tunnelling in the Calcschists

The total disc substitutions are around 4 replacements / 1000 m³ and the number of changes for each type of wear/damage are shown in the figure below (Figure 82). According to these data analyzed the preventive replacements was made 1.8 time for each 1000 m³ excavated and the changes due to preventive substitution and normal wear are respectively 1.9 disc/1000 m³ and 1.7 disc/1000 m³. The other types of changes are approximately 0.1 changes/1000 m³.

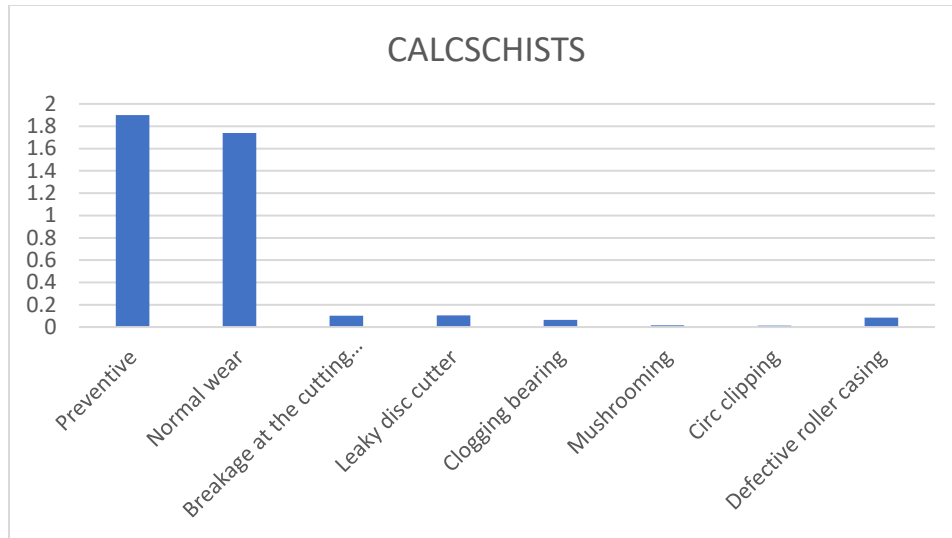


Figure 82 - Different frequencies of cutter tools substitution related to the excavation in Calcschists

5.8.4.5 Type of wear and damage – Gneiss

In the last geology analyzed the main changes have been related with preventive replacement (49%) and the normal wear (45%). The other types of replacement are not very significant in percentage (around 1%) but, due to the high number of discs changed for 1000 m³ of material excavated, they reach some relevant frequencies of damage.

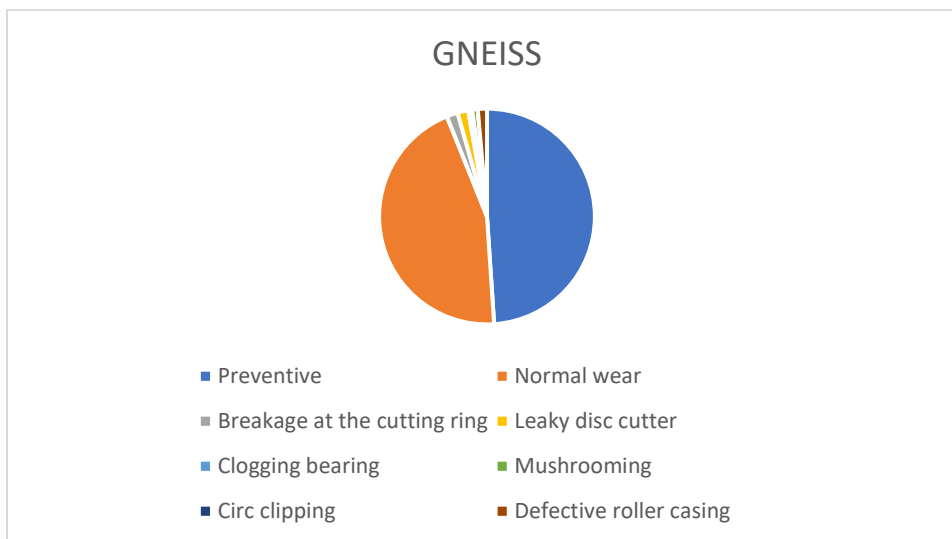


Figure 83 – Disc replacement causes during the tunnelling in the Gneiss

Indeed, the total tool substitution in this geology is around 17.5 discs per 1000 m³ of rock excavated, which are subdivided in 8.5 substitutions/1000 m³ and 8 substitutions/1000 m³ respectively for the preventive replacements and the normal wear and almost 0.3 substitutions /1000 m³ due to the other typologies of damage.

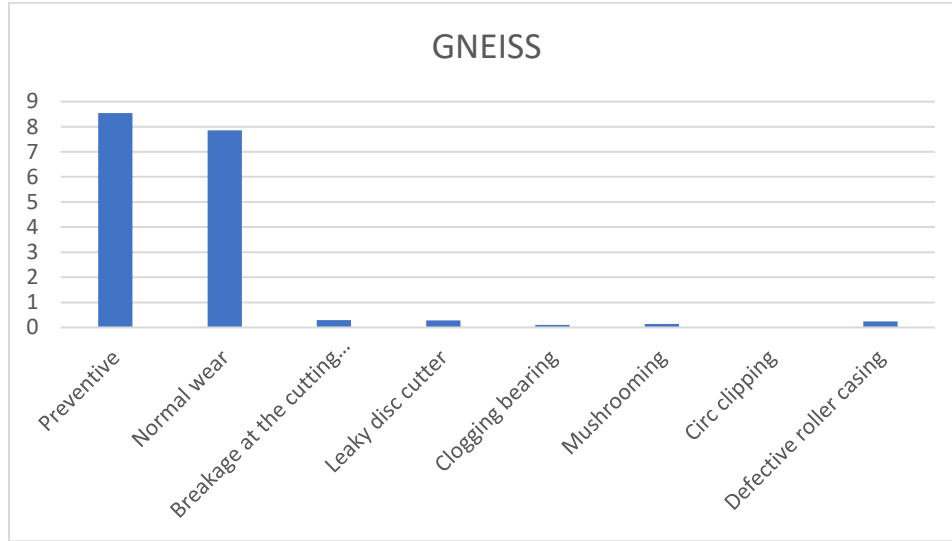


Figure 84 - Different frequencies of cutter tools substitution related to the excavation in Gneiss

5.9 NTNU PREDICTION MODEL FOR THE CUTTER DISCS WEAR ANALYSIS

The NTNU prediction model is an objective and semi-empirical tool that has been developed for estimating the excavation rate and costs, as well as planning and risk assessment of hard rock TBMs project. The NTNU prediction model for hard rock TBMs combines rock boreability properties and TBM parameters, in order to forecast the penetration rate, advance rate and cutter ring wear. This model has had successive development since the first version in 1976 and the last edition is based on data from almost 250 km (Bruland, 1998).

5.9.1 Determination of the penetration rate

The prediction model for the determination of the penetration is based on the following formula:

$$i_0 = \left(\frac{M_B}{M_1} \right)^b$$

Where:

- i_0 = penetration [mm/rev]
- M_B = Maximum thrust per disc cutter [kN]
- M_1 = Critical thrust per disc cutter [kN]
- b = penetration coefficient

The Drilling Rate Index (DRI) expresses the drillability or boreability of the intact rock. DRI is evaluated on the basis of two laboratory tests: the Sievers' J-Value (SJ) miniature drill test and the Brittleness Value (S_{20}). This parameter can be defined as an indirect measure of the required breaking work and hence the ability to be crushed by repeated impacts. Depending on the rock type, the DRI value can be estimated by using this table (Figure 85):

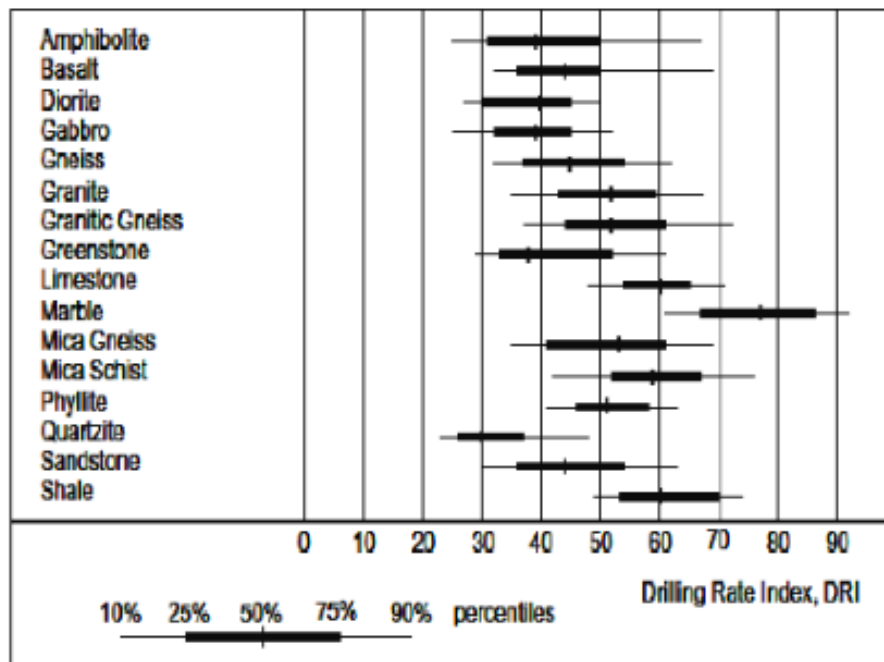


Figure 85 - Recorded Drilling Rate Index (DRI) for some rock types (Bruland, 1998)

Since M_B and b are parameters, they must be obtained following these steps:

1) Determination of the fracture class:

Fracture Class (Joints = Sp / Fissures = St)	Distance between Planes of Weakness [cm]
0	-
0-I	160
I-	80
I	40
II	20
III	10
IV	5

Figure 86 - Determination of fracture class (NTNU Method)

Rock mass fracturing is found to be the rock parameter of largest influence on the net penetration rate in hard rock conditions. (Burland, 1998)

2) Determination of the orientation of discontinuities:

The determination of the α angle is achieved by using this formula:

$$\alpha = \arcsin (\sin \alpha_f \cdot \sin(\alpha_t - \alpha_s))$$

Where:

α_f = dip

α_t =tunnel axis

α_s =strike

This is the angle between the tunnel axis and the planes of weakness.

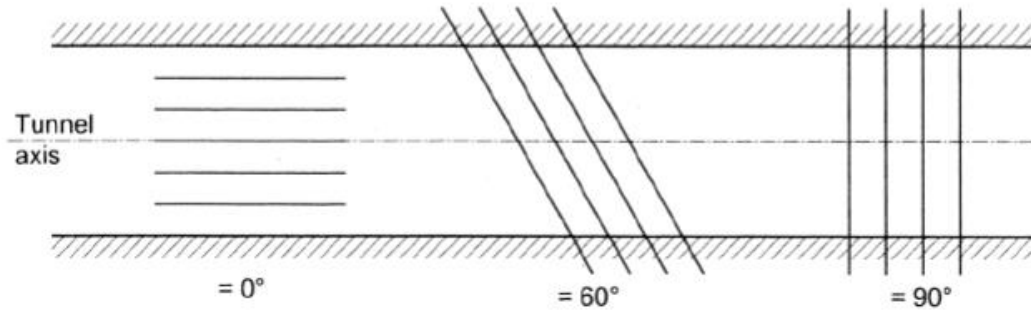


Figure 87 - examples of inclination of weakness planes

3) Evaluation of the K_s (fracturing factor) parameter:

It is dependent on the fracture class and on the α , and it is got by using this chart:

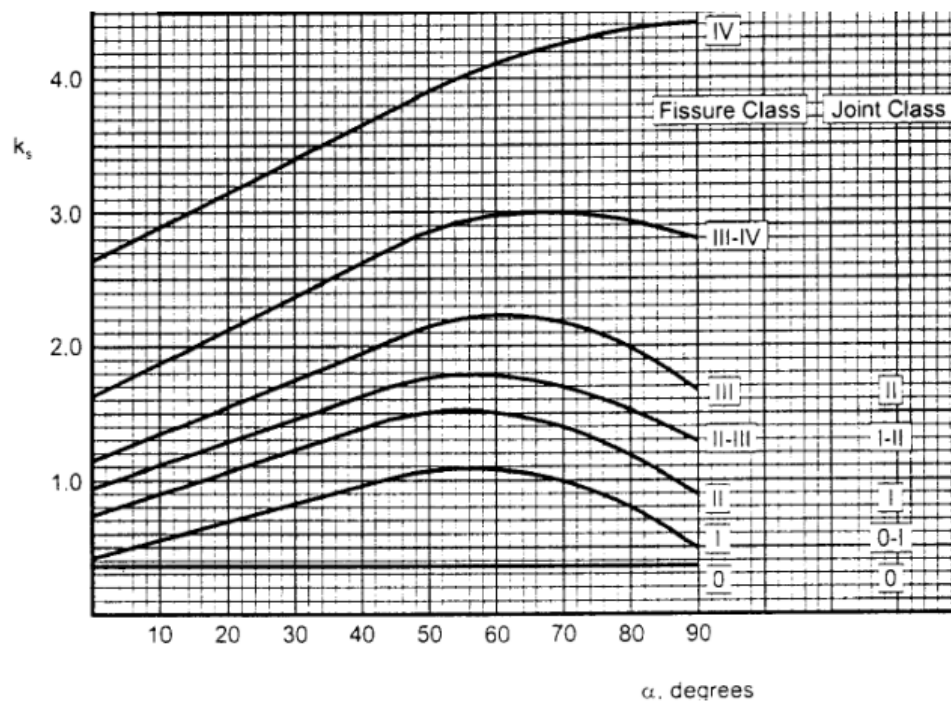


Figure 88 – Chart for the determination of K_s parameter

4) Determination of the general fracturing factor:

It correlates all fracturing factors in case are present more than one set of joints.

$$k_{s-tot} = \sum_{i=1}^n k_{si} - (n - 1) \cdot 0.36$$

5) Determination of K_{DRI} :

This diagram correlates the K_s coefficient with the DRI value in order to get the K_{DRI} coefficient value.

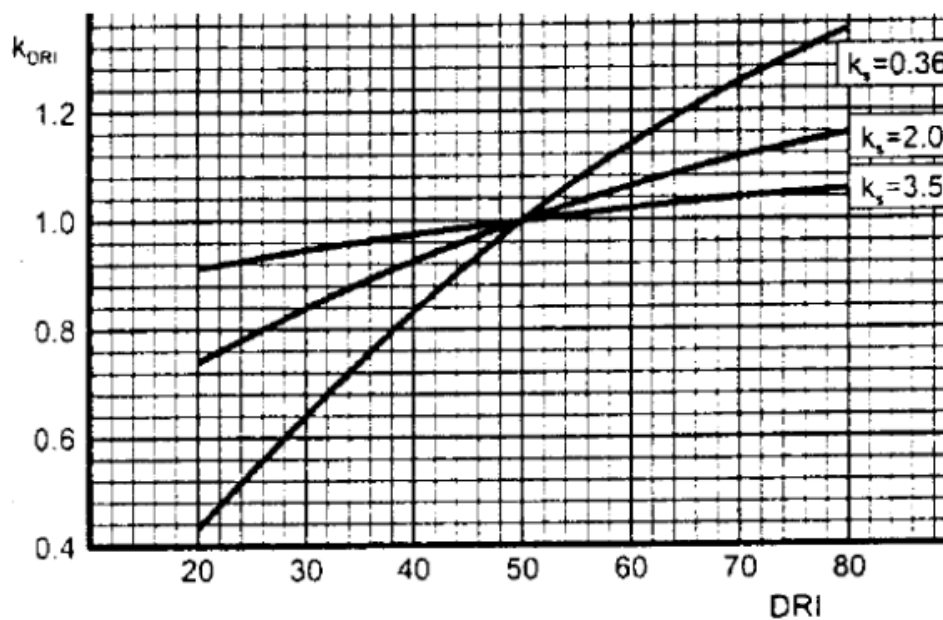


Figure 89 - Determination of the K_{DRI} value

6) Correction for the cutter diameter K_d :

Since the diameter of cutters used in hard rock TBM are not all of the same diameter it is necessary to insert a correction coefficient to perform the calculation depending also on the cutter dimension.

The diameter on the x axis is expressed in mm and hence the usually provided inches diameter must be adapted multiplying by 25.4. In this computation we have a cutter disc diameter of 19" which means 483 mm of diameter.

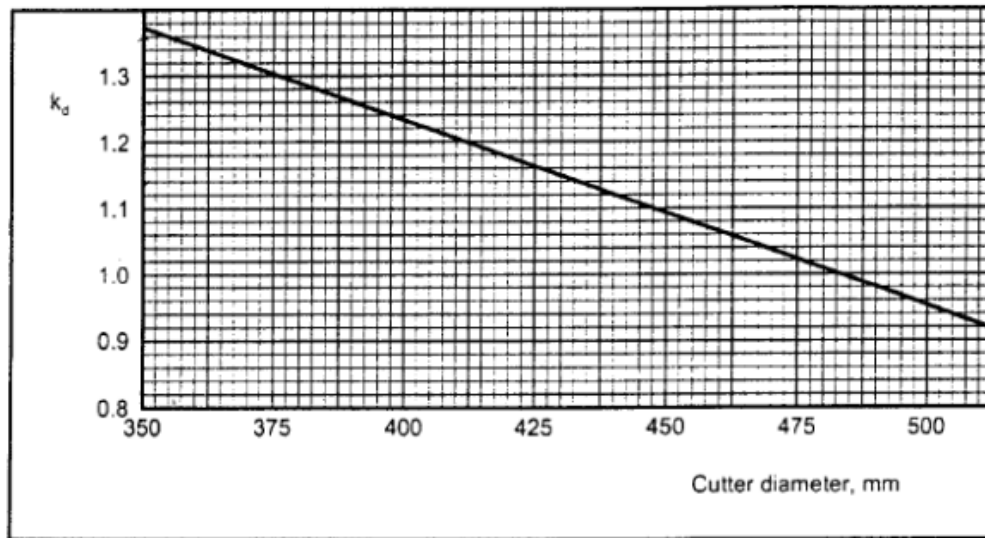


Figure 90 - Determination of K_d coefficient

7) Correction for cutter tools spacing (K_a).

Also in this case, the spacing between cutters on the cutterhead is not constant and it depends on the project. The average distance between cutter paths is 85 mm for the TBMs S-1071 and S-1072, while in the TBM S-1054 the distance between cutters is 87 mm. Since the values are similar in both the TBM type, I will consider only one value for $k_a=0.9$.

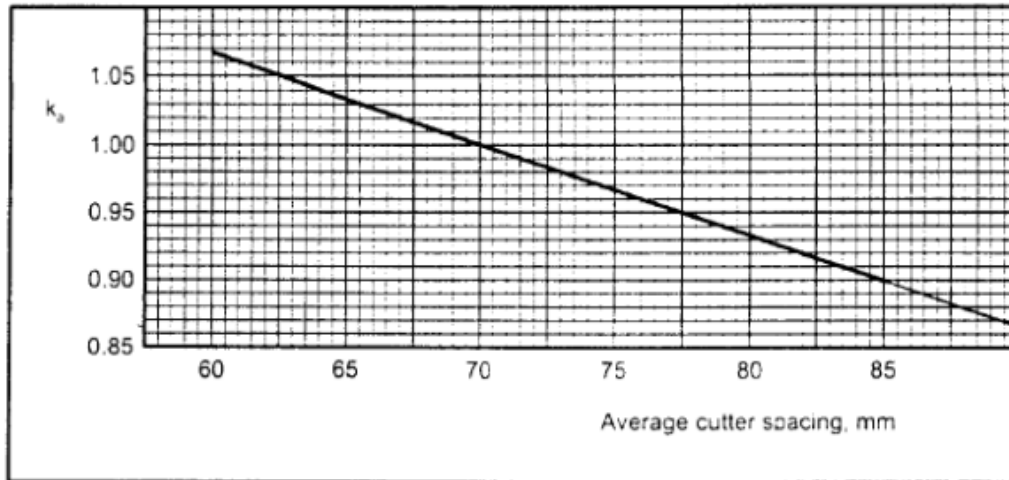


Figure 91 - Determination of cutter spacing coefficient (K_a)

8) Influence of porosity diameter (K_{por})

The influence of porosity can be explained by the poring acting as crack initiators and amplifiers of the crack propagation. It shows a clear influence on the penetration rate.

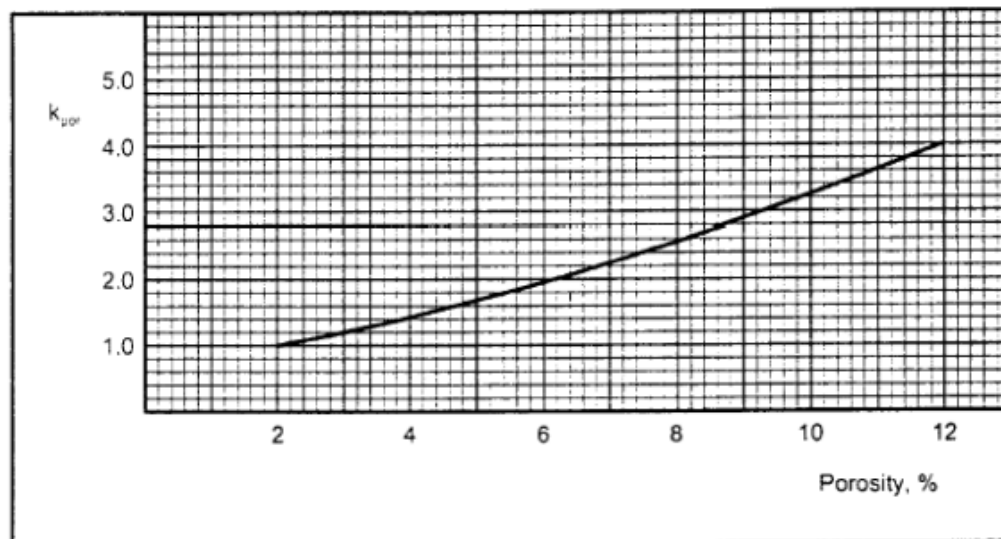


Figure 92 - Determination of the porosity coefficient (K_{por})

9) Equivalent Fracturing Factor (K_{ekv}) and Equivalent thrust per cutter (M_{ekv})

At this point is possible to evaluate the values of the Equivalent Fracturing Factor (K_{ekv}) and Equivalent thrust per cutter (M_{ekv})

$$K_{ekv} = K_s \cdot K_{DRI} \cdot K_{por}$$

$$M_{ekv} = M_B \cdot K_d \cdot K_a$$

Where:

M_B = maximum thrust per cutter

10) Determination of the critical thrust (M_1):

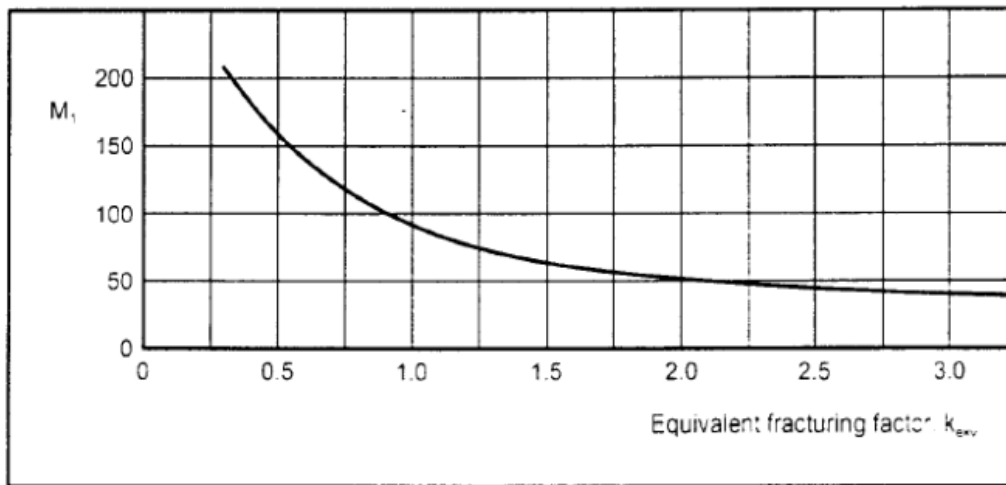
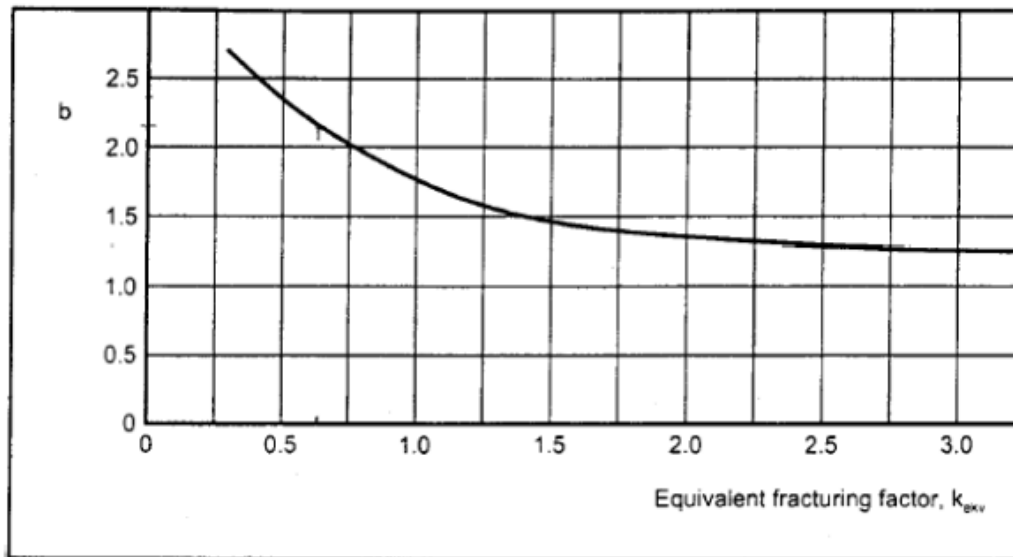


Figure 93 - Determination of the critical thrust M_1

11) Determination of the penetration coefficient b:



12) Evaluation of the base penetration:

Once obtained the values of M_{ekv} , M_1 and b it is possible to evaluate the base penetration with the formula already shown previously:

$$i_0 = \left(\frac{M_B}{M_1} \right)^b$$

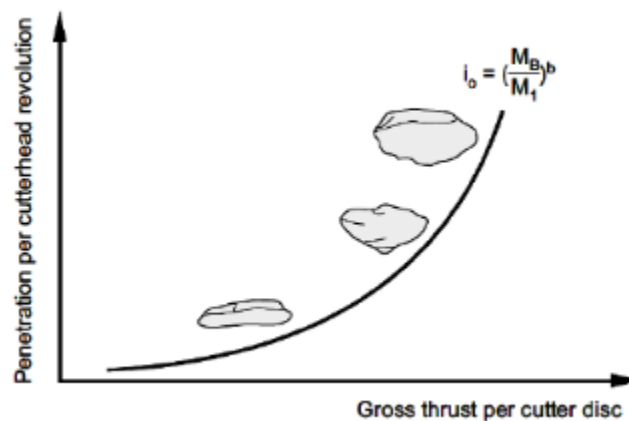


Figure 94 - General progress of a penetration curve (Bruland , 1998)

5.9.2 Wear prognosis

Even the evaluation of the cutter ring wear can be carried out by following the steps here proposed:

1) Determination of the CLI (Cutter Life Index)

The Cutter Life Index is a parameter which depends on the type of rock that is excavated. It is ranging between 0 and 90 and depending on the different geologies it can vary in a certain interval, as shown in the following figure:

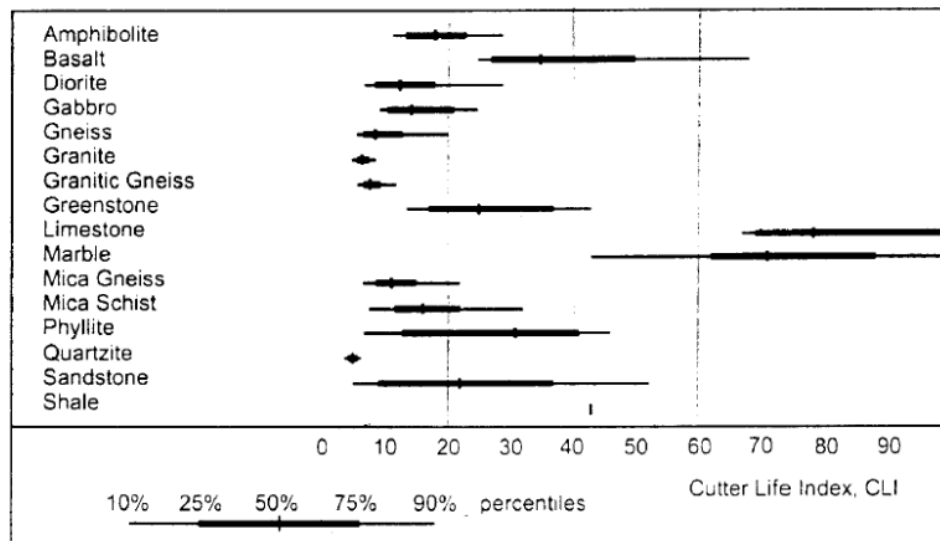


Figure 95 - Correlation between CLI (Cutter Life Index) and geology

2) Calculation of the base cutter life (H_c):

It depends on the diameter of the cutters and on the CLI.

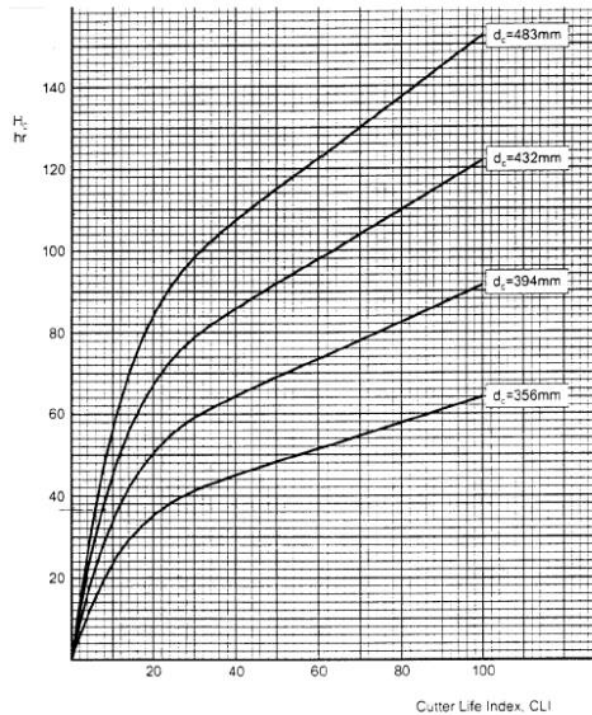


Figure 96 - Determination of the Base cutter life (H_c)

3) Correlation with quartz content (K_Q)

The quartz is the most wearing mineral. For this reason, the content of this mineral must be considered for the evaluation of the cutter disc wear.

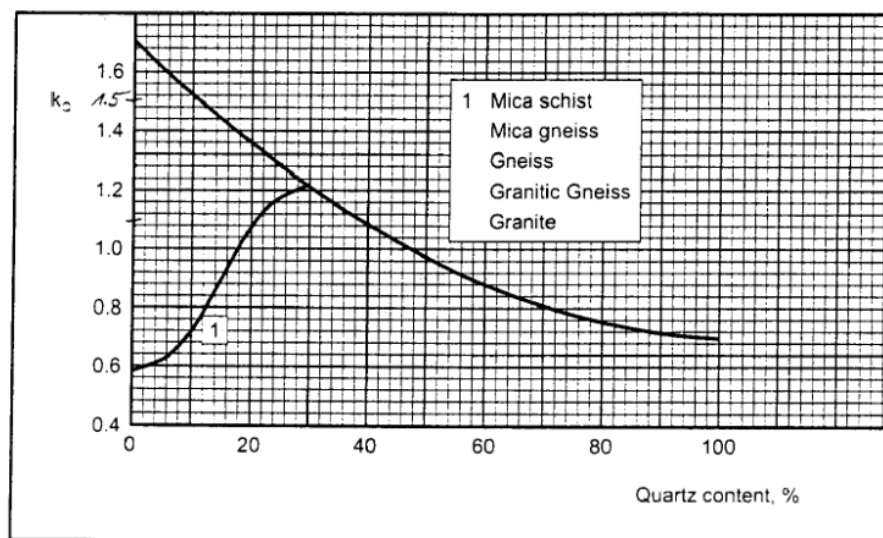


Figure 97 - Correction due to the quartz content

4) Correction due to the rotational speed [rpm] (K_{RPM})

It depends on the diameter of the TBM and on the cutterhead rotational speed and it is obtained by means of this formula:

$$K_{RPM} = \frac{50}{d_{TBM} \cdot RPM}$$

5) Correction for the cutterhead diameter (K_d)

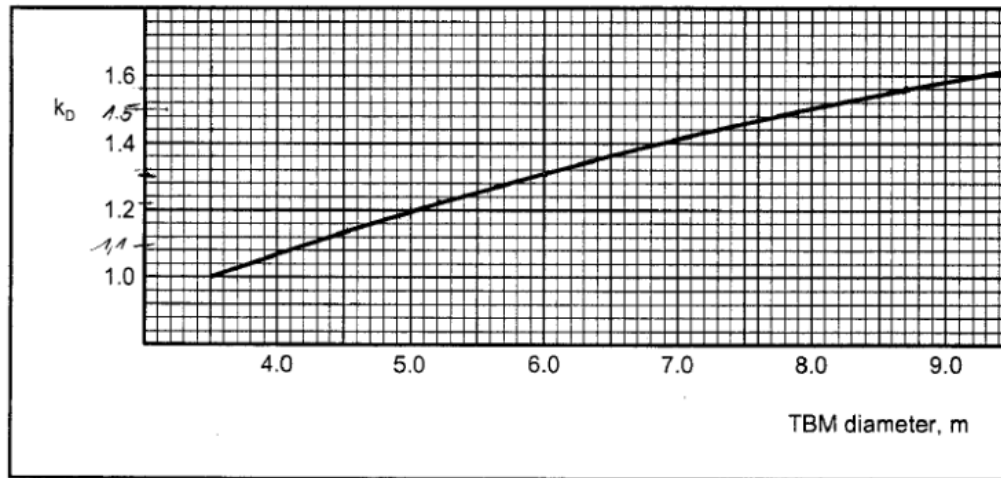


Figure 98 - Correction for cutterhead diameter (K_d)

6) Correction for number of disc cutters:

$$K_N = \frac{N_{TBM}}{N_0}$$

Where N_0 is given by the following chart:

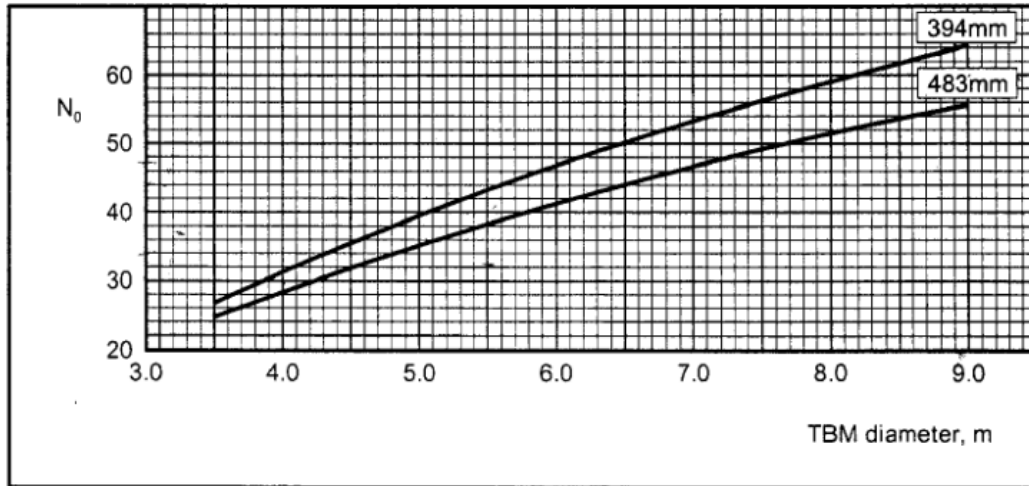


Figure 99 - Determination of the parameter N_0

7) Evaluation of the cutter ring wear:

- Cutter life in [hours/cutter]

$$H_h = \frac{H_0 * K_D * K_Q * K_{RPM} * K_N}{N_{TBM}}$$

- Cutter life in [m³/cutter]

$$CutterRingLife = \frac{D_{cutterhead}^2 * \pi}{4} * i_0 * RPM * \frac{60}{1000} * H_h$$

5.9.3 Model computation for the different geologies analyzed:

By following the above explained steps it is evaluated the penetration [mm/rot], the advance speed [mm/min], the Cutter Ring Life (CLI) [hours/cutter] and the specific theoretical consumption [replacements/1000m³] for each geology analyzed: Paragneiss, Amphibolite, Metabasalts, Calcschist and Gneiss.

5.9.3.1 Paragneiss

Parameter	Value
Drilling Rate Index (DRI)	55
Fracture class	II
$\alpha_f [^\circ]$	30
$\alpha_t - \alpha_s [^\circ]$	40
$\alpha [^\circ]$	19
K_s	1.1
K_{DRI}	1
K_d	1
K_a	0.9
K_{por}	1
K_{ekv}	1.1
Max thrust per cutter tool [kN]	300
M_{ekv} [kN]	270
M_1	80
b	1.65
l_0 [mm/rot]	8.9

The results of this model give us the theoretical values of the penetration [mm/rot] and, consequently, the advance speed [mm/min]. In the paragneiss the penetration should be 8.9 mm/rot and the advance speed, depending on the cutterhead rotation speed, should be 28 mm/min for the TBMs S-1071 & S-1072, while, in the case of the TBM S-1054, the advance speed should be 38.1 mm/min. Instead, from the machine data recorded during the tunnelling, the average penetration and advance speed are 8.2 mm/rot and 35 mm/min, while, for the two twin TBM is only possible to compare the penetration because of lack of data. In this case, the real value registered is 11.1 mm/rot.

Parameter	Value (S-1071/S-1072)	Value (S-1054)
Drilling Rate Index (DRI)	55	55
Cutter Life Index (CLI)	5	5
H_0	25	25
K_Q	0.8	0.8
RPM	3.2	4.3
K_{RPM}	1.47	1.70
K_D	1.6	1.35
N_0	65	45

K_N	1	0.91
Hh [hours/cutter]	0.73	1.02
Cutter Ring Life [m^3 /cutter]	108.8	85.0
Cutter consumption [re places/1000 m^3]	9.1	11.8

The cutter consumption should be 9.1 substitutions/1000 m^3 for the S-1071/S-1072 and 11.8 substitutions /1000 m^3 for the other TBM. Instead, the real amount of cutter discs substitution is less than 2 substitutions/1000 m^3 , also considering the replacements due to the preventive substitutions.

5.9.3.2 Amphibolite

Parameter	Value
Drilling Rate Index (DRI)	40
Fracture class	I
$\alpha_f [^\circ]$	40
$\alpha_t - \alpha_s [^\circ]$	40
$\alpha [^\circ]$	25
K_s	0.8
K_{DRI}	0.9
K_d	1
K_a	0.9
K_{por}	1
K_{ekv}	0.72
Max thrust per cutter tool [kN]	300
M_{ekv} [kN]	270
M_1	120
b	2
l_0 [mm/rot]	6.3

Concerning the Amphibolite geology, as already explained before, there is the problem of absence of data due to a too short length of analysis of this geology and hence it is possible to compare the results obtained with this model only with the data coming from the S-1054 monitoring: in this case the actual penetration and advance speed is respectively 9.3 mm/rot and 48.1 mm/min, while the results obtained from the implementation of this model are 6.3 mm/rot and 32.8 mm/min.

Parameter	Value (S-1071/S-1072)	Value (S-1054)
Drilling Rate Index (DRI)	40	40
Cutter Life Index (CLI)	13	13
H_0	60	60
K_Q	0.85	0.85
RPM	3.2	5
K_{RPM}	1.47	1.47
K_D	1.6	1.35
N_0	65	45
K_N	1	0.91
Hh [hours/cutter]	1.9	2.3
Cutter Ring Life [m ³ /cutter]	195.9	153.1
Cutter consumption [replaces/1000 m ³]	5.1	6.5

The actual value of substitution in this case is 1.77 replacements/1000m³, while the forecast result is 5.1 substitutions/1000m³ and 6.5 substitutions/1000m³ respectively for the TBM S-1054 and TBM S-1071/1072.

5.9.3.3 Metabasalts

Parameter	Value
Drilling Rate Index (DRI)	45
Fracture class	II
$\alpha_f [^\circ]$	70
$\alpha_t - \alpha_s [^\circ]$	40
$\alpha [^\circ]$	37
K_s	1.4
K_{DRI}	0.95
K_d	1
K_a	0.9
K_{por}	1
K_{ekv}	1.33
Max thrust per cutter tool [kN]	300
M_{ekv} [kN]	270
M_1	65
b	1.5
l_0 [mm/rot]	9.9

During the crossing of the Metabasalts geology, the penetration has been had the same value for each TBMs and it was equal to 5.8 mm/rot, while the average advance speed was 33 mm/min for the TBM S-1054 and 27 mm/min for the TBMs S-1071 and S-1072. The result of this model shown a forecast penetration of 9.9 mm/rot which means an advance of 57.1 mm/min and 47.5 mm/min for the S-1054 and S-1071/S-1072.

Parameter	Value (S-1071/S-1072)	Value (S-1054)
Drilling Rate Index (DRI)	15	15
Cutter Life Index (CLI)	35	35
H_0	50	50
K_Q	0.85	0.85
RPM	4.8	5.8
K_{RPM}	0.98	1.27
K_D	1.6	1.35
N_0	65	45
K_N	1	0.91
Hh [hours/cutter]	1.0	1.6
Cutter Ring Life [m ³ /cutter]	258.9	202.4
Cutter consumption [re places/1000 m ³]	3.9	4.9

The actual value of substitution in the Metabasalts is 11.38 replacements/1000m³, while the forecast results is 3.9 substitutions/1000 m³ and 4.9 substitutions/1000m³ respectively for the TBM S-1054 and TBM S-1071/1072. Considering only the replacements due to the complete wear of the cutter ring and not those related to preventive substitutions, the number of changes decreases to 4.8 substitutions/1000m³, which is a value more like the one obtained by using the NTNU method.

5.9.3.4 *Calcschists*

Parameter	Value
Drilling Rate Index (DRI)	50
Fracture class	II
$\alpha_f [^\circ]$	80
$\alpha_t - \alpha_s [^\circ]$	50
$\alpha [^\circ]$	49
K_s	1.5

K_{DRI}	1
K_d	1
K_a	0.9
K_{por}	1
K_{ekv}	1.5
Max thrust per cutter tool [kN]	300
M_{ekv} [kN]	270
M_1	55
b	1.45
l_0 [mm/rot]	11.7

Regarding the Calcschist, the forecast values are 11.7 mm/rot of penetration and 60.9 mm/min of advance speed, while, from the data collected during the tunnelling, the real average penetration is 8.8 mm/rot for the small diameter TBM and 10.1 mm/rot for the other two TBMs. The advance speed is correspondingly 47.2 mm/min and 51.3 mm/rot.

Parameter	Value (S-1071/S-1072)	Value (S-1054)
Drilling Rate Index (DRI)	50	50
Cutter Life Index (CLI)	15	15
H_0	70	70
K_Q	0.95	0.95
RPM	5	5.2
K_{RPM}	0.94	1.41
K_D	1.6	1.35
N_0	65	45
K_N	1	0.91
Hh [hours/cutter]	1.5	2.8
Cutter Ring Life [m ³ /cutter]	478.2	373.9
Cutter consumption [re places/1000 m ³]	2.1	2.7

In the Calcschist geology the prediction of cutter consumption is about 2.1 substitutions/1000 m³ and 2.7 substitutions/1000m³. Instead, the total amount of substitutions performed during the tunnelling is 4 replacements/1000m³ and 1.8 replacements/1000m³ are related to the preventive substitutions, while the remaining part of replacements is related to the normal wear or to the damage of the cutter discs.

5.9.3.5 Gneiss

Parameter	Value
Drilling Rate Index (DRI)	45
Fracture class	I
$\alpha_f [^\circ]$	75
$\alpha_t - \alpha_s [^\circ]$	80
$\alpha [^\circ]$	72
K_s	1
K_{DRI}	0.95
K_d	1
K_a	0.9
K_{por}	1
K_{ekv}	0.95
Max thrust per cutter tool [kN]	300
M_{ekv} [kN]	270
M_1	100
b	1.7
l_0 [mm/rot]	6.5

For the last geology analyzed, the Gneiss, from the actual data we have a penetration of 4.2 mm/rot and 5.2 mm/rot, while the advance speed are 25.2 mm/min and 20.2 mm/min, respectively for the TBM S-1054 and TBM S-1072. On the other hand, the forecast penetration and advance speed are 6.5 mm/rot and 27.3 mm/min for the TBM S-1054 and 31.2 mm/min for the TBM S-1072.

Parameter	Value (S-1071/S-1072)	Value (S-1054)
Drilling Rate Index (DRI)	45	45
Cutter Life Index (CLI)	5	5
H_0	25	25
K_Q	0.8	0.8
RPM	4.8	6
K_{RPM}	0.98	1.22
K_D	1.6	1.35
N_0	65	45
K_N	1	0.91
Hh [hours/cutter]	0.5	0.7
Cutter Ring Life [m ³ /cutter]	79.5	62.2

Cutter consumption [replaces/1000 m ³]	12.6	16.0
--	------	------

In the Gneiss, the forecast values for the cutter consumption are 12.6 replacements/1000 m³ for the S-1071/S-1072 and 16.0 replacements/1000 m³ for the S-1054. The effective data obtained during the analysis in the previous chapter of the thesis are: 17.5 discs per 1000 m³ of rock excavated, which are subdivided in 8.5 substitutions/1000m³ and 8 substitutions/1000m³ respectively for the preventive replacement and the normal wear and almost 0.3 substitutions /1000m³ due to the other typologies of damage.

5.9.4 Summary of the results obtained by the NTNU prediction model

In the table below is reported the forecast penetration obtained by means of the NTNU prediction model and the actual penetration obtained from the back analysis performed in the previous part of this thesis.

Geology	Predicted penetration [mm/rot]	Actual penetration S-1054 [mm/rot]	Actual penetration S-1071/1072 [mm/rot]
Paragneiss	8.9	8.2	11.1
Amphibolite	6.3	9.3	-
Metabasalts	9.9	5.8	5.8
Calcschist	11.7	10.1	8.8
Gneiss	6.5	5.2	4.2

In the following table are summed up the results of the NTNU prediction model for the cutter consumption and the actual values found during the analysis on the cutter discs consumption. In brackets are shown the value relative to the cutter rings consumption without considering the preventive replacements.

Geology	Predicted cutter consumption S-1054 [subst./1000m³]	Predicted cutter consumption S-1071/S-1072 [subst./1000m³]	Actual cutter consumption [subst./1000m³]
Paragneiss	11.8	9.1	1.78 (0.3)
Amphibolite	6.5	5.1	1.77 (0.25)
Metabasalts	4.9	3.9	11.38 (4.8)
Calcschist	2.7	2.1	4.00 (1.7)
Gneiss	16	12.6	17.5 (8.3)

Being the NTNU method an empirical prediction model, the results obtained should be only qualitative and hence to give an idea of the conditions that should be found during the excavation.

For the first two geologies analyzed (Paragneiss and Amphibolite), due to the small amount of data, the actual results achieved with the back analysis are not consistent, and therefore they are almost different from the predicted values. On the other hand, regarding the other geologies, the results obtained from the back analysis fit better the NTNU model. However, also in this case there are some outliers since the parameters used in the NTNU prediction model are punctual and therefore they can not describe perfectly all the zone crossed in the same geology. However, the order of magnitude is correct for the three different lithologies.

6 CONCLUSIONS

From the comparison between the proposed disassembly project and the work actually done, it is possible to point out the main differences between the two. Those differences are mostly related to the use of the train crane instead of the use of the monorail proposed in the disassembly project. For this reason, proceeding with the disassembly, it was required the installation of the invert segments in order to go on with the disassembly of the next elements. Additionally, the most challenging component to be removed from the tunnel, due to its weight, has been the main drive. In this case, the trolley devices have been welded on the bottom of the main drive and hence, the installation of the two beams was no longer useful since the slide of the main drive was carried out on the steel platform lying on the floor. Furthermore, for the tilting operation, it was not used the swivel lug as deemed too dangerous to lift up the main drive and install the device. Thus, the overturning has been performed only by using two chain hoists.

In general, the main difficulties related to the execution of works and to the description of the work done have been associated to the confined space, to the long train travel time (almost one hour) and limited number of rides per day from the disassembly chamber to the TBM, and to the bad internet connection that didn't allow the communication by using pictures from the TBM to outside the tunnel.

However, thanks to the synergy between the companies involved in this project, it was possible to complete the disassembly operations of the TBM S-1054 within the established time and thus, although not always following the guidelines provided by the project, to reach the goal.

In the second part of the thesis has been carried out the analysis of the cutter rings wear with respect to five machine parameters: wheel torque, cutting wheel contact force, cutting wheel rotational speed, penetration and advance speed. For each parameter has been made a graph to correlate the actual wear [mm/m travelled on the tunnel face] and the machine parameter value. Regarding the wheel torque, it was not detected any correlation with the cutter disc wear.

For the cutting wheel contact force, evaluated as the difference between the total force applied by the thrust and the shear force between the shield and the rock mass, it doesn't show a very clear dependence of the wear by the net force, but, generally, the specific wear rises with the

increase of the force applied. Furthermore, regarding the next machine parameter analyzed, it is slightly visible an increase of the cutter ring wear with the increasing of the cutting wheel rotational speed.

Concerning the penetration, it affects the cutter tools wear with a decreasing of the wear corresponding to an increase of the penetration rate. This behavior be explained with the fact that the rock masses with better mechanical properties for an excavation point of view, which means a low value of Uniaxial Compressive Strength, have also a low value of Cerchar Abrasiveness Index and hence, the rock mass which is easily excavated is also less wearing for the cutter tools.

For the last parameter analyzed, the Advance speed, from the graph it is visible a double opposite behavior: in the case of the Gneiss, it is recognizable a decrease of specific wear when the advance speed raises up, while, for the Metabasalts, the specific wear increases with the raise up of the advance speed. Furthermore, as it is visible in the Figure 74, most of the wear is related with the cutter placed in the pre-gauge area, while the cutter discs placed on the central and gauge zone have almost the same rate of specific wear. Moreover, from the bar chart is also visible a peak of wear related to the first track for each TBM, due to the fact that the circumference travelled per each round of the cutterhead is very short (0.5 meters for each round) and hence, even a small wear detected (1 mm) increases a lot the specific wear of that track.

After that, from the analysis on the type of wear and damage, there is a good correlation between the CAI value of the geology analyzed and the number of cutter discs substitution performed during the tunnelling. Indeed, in the case of the Calcschist, which has a low CAI of 2, the amount of cutter changes is less than 2 substitutions/1000m³, while, for the Gneiss, having a CAI of 5, the total tool substitution in this geology is around 17.5 discs per 1000 m³ of rock excavated. Those number of substitutions are inclusive of the preventive replacements.

Then, these values obtained related to the cutter changes have been compared with the NTNU empirical prediction model. For the Paragneiss and the Amphibolite the results are not very satisfactory, probably due to the short length crossed during the excavation (450m/TBM for the Paragneiss and 100m/TBM for the Amphibolite). On the other hand, regarding the Metabasalts,

Calcschists and Gneiss, the results obtained are more similar to the values obtained by the analysis of the actual data. Generally, the number of substitutions obtained from the NTNU prediction model are slightly higher than the substitutions actually performed, and it could be related to a good management of the excavation that allow to limit the cutter discs consumption and save on time and costs. However, the NTNU empirical prediction method can give only qualitative results because the input data are punctual while the geological characteristics are not constant along all the length crossed during the tunnelling.

In general, from an overview of all the analyzes carried out on the cutter rings wear and damage, it is possible to assert that the length of the geology analyzed must be at least greater than 500 m per TBM and that it is better to avoid the first hundreds of meters of TBM excavation because the workers must be trained on how to evaluate the type of damage.

7 BIBLIOGRAPHY

- Askilsrud, O. (n.d.). Development of TBM technology for Hard Rock TBM conditions. *Atlas Copco Robbins*, 40.
- BBT SE . (2015). *Relazione geomeccanica generale* . Bolzano.
- BBT SE . (2022). *2022 - Brenner Basistunnel BBT SE*. Retrieved from Construction Progress: <https://www.bbt-se.com/en/tunnel/construction-progress/>
- BBT SE - Brenner Basis Tunnel Società Economica. (2008). *Final Project - Technical Drafting of the Project - General Report - Summary*. Bolzano.
- Bruland, A., & Blindheim, O. (n.d.). Boreability Testing. 21-22.
- Gwildis U. & Aguilar J. (2018). Tool wear analysis for the cutterhead configuration and resource planning in glacial geology
- Herrenknecht . (2017). *S-1054 Double Shield TBM Galleria del Brennero - Lotto costruttivo Mules 2-3*. Schwanau / Germany.
- Herrenknecht . (2022). *Single Shield TBM - Herrenknecht AG*. Retrieved from Herrenknecht : <https://www.herrenknecht.com/en/products/productdetail/single-shield-tbm/>
- Herrenknecht. (2017). *S-1071/S-1072 TBM GL Brenner Basis Tunnel Lot 2-3 Mails/Mules* . Schwanau.
- Herrenknecht. (2021). *Disc Cutter Assembly Instruction*. Schwanau.
- Herrenknecht. (2022). *Double Shield TBM - Herrenknecht AG*. Retrieved from Herrenknecht : <https://www.herrenknecht.com/en/products/productdetail/double-shield-tbm/>
- Herrenknecht. (2022). *EPB Shield - Herrenknecht AG*. Retrieved from Herrenknecht: <https://www.herrenknecht.com/en/products/productdetail/epb-shield/>
- Herrenknecht. (2022). *Gripper TBM - Herrenknecht AG*. Retrieved from Herrenknecht: <https://www.herrenknecht.com/en/products/productdetail/gripper-tbm/>
- Herrenknecht. (2022). *HK 5102-091-001-01 Shield Disassembly*. Schwanau.
- Herrenknecht. (2022). *Investigation Main Drive Disassembly*. Schwanau.
- Herrenknecht. (2022). *Shield Disassembly Concept*. Schwanau .
- Hoek, E. B. (1997). Practical estimates of rock mass strength . In *Rock Mech. Min. Sci.* (pp. 1165-1186).
- Li et al. (2016). Analysis and prediction of TBM disc cutter wear when tunnelling in hard rock strata: a case study of a metro tunnel excavation in Shenzhen, China.

- Mancktelow, B. a. (1980). General Geological Order of Brenner Area.
- mineARC systems. (2020, December). Hard Rock Mine Refuge Chamber. Perth.
- Thuro, H. K. (2010). Determining rock abrasivity in te laboratory. *EUROCK*.
- Transport, D. G. (n.d.). *European Commission website*. Retrieved from Transport Europa:
https://transport.ec.europa.eu/transport-themes/infrastructure-and-investment/trans-european-transport-network-ten-t/scandinavian-mediterranean-corridor_en
- Villeneuve, M. (2017). Hard rock tunnel boring machine penetration test as an indicator of chipping process efficiency. *Journal of Rock Mechanics and Geotechnical Enigineering* , 612-622.
- WeBuild. (2022). *WeBuild*. Retrieved from Brenner Base Tunnel - Mules 2-3:
<https://www.webuildgroup.com/en/projects/railways-underground/brenner-base-tunnel-mules-2-3-lot>
- Zhang. (2018). Experimental study on wear of TBM disc cutter rings with different kinds of hardness.
- Bruland. (2014). The NTNU Prediction Model: A Tool for Planning and Risk Management in Hard Rock TBM Tunnelling
- Rostami et Al. (2013). Study of dominant factors affecting Cerchar abrasitivity index